# UNIVERSITY OF SOUTHAMPTON

FACULTY OF MEDICINE

Bone and Joint Research Group

Volume 1 of 1

**Examination of MicroRNAs in Skeletal Stem Cell Differentiation**

by

**Kelvin Sin Chi Cheung**

Thesis for the degree of Doctor of Philosophy

September 2015

**UNIVERSITY OF SOUTHAMPTON**

# ABSTRACT

FACULTY OF MEDICINE

Bone and Joint Research Group

Thesis for the degree of Doctor of Philosophy

**EXAMINATION OF MICRORNAS IN SKELETAL STEM CELL DIFFERENTIATION**

Kelvin Sin Chi Cheung

MicroRNAs (miRNA/miRs) play a crucial role in a variety of biological processes including stem cell differentiation and function. Foetal femur-derived skeletal stem cells (SSCs) display enhanced proliferation and multipotential capacity, indicating excellent potential as candidates for tissue engineering applications. This thesis has identified and characterised subpopulations of skeletal stem cells found within the foetal femur. Cells isolated from the epiphyseal region of the foetal femur expressed higher levels of genes associated with chondrogenesis while cells from the diaphyseal region expressed higher levels of genes associated with osteogenic differentiation. In addition to the difference in osteogenic and chondrogenic gene expression, epiphyseal and diaphyseal cell populations displayed distinct miRs expression profiles. To examine the role of miRNA during skeletogenesis, a robust cell culture model containing differentiating SSCs and an effective transfection protocol was developed. Spermine-pullulan complex, a potential delivery system for miRNA-based gene therapy, was shown to be able to transfect SSCs with miRNA mimics and inhibitors but with lower efficacy compared to liposome base transfection reagent. Through miRNA gene expression profiling and *mRNA* targets analysis, miR-146a was found to be expressed by diaphyseal cell populations at a significantly enhanced level compared to epiphyseal populations and was predicted to target various components of the TGF-β pathway. Examination of miR-146a function in foetal femur cells confirmed regulation of protein translation of *SMAD2* and *SMAD3* following transient overexpression in epiphyseal cells. The down-regulation of *SMAD2* and *SMAD3* following overexpression of miR-146a resulted in an up-regulation of the osteogenesis-related gene *RUNX2* and down-regulation of the chondrogenesis-related gene *SOX9*. In conclusion, this thesis has identified subpopulations of skeletal stem cells with enhanced osteogenic and chondrogenic potential and has explored new miRNA targets involved in skeletogenesis in the attempt to develop novel treatments for patients requiring reparation of the skeletal system.

# Table of Contents

# List of Tables

# List of Figures

# DECLARATION OF AUTHORSHIP

I, Kelvin Sin Chi Cheung

declare that this thesis and the work presented in it are my own and have been generated by me as the result of my own original research.

Examination of MicroRNAs in Skeletal Stem Cell Differentiation

I confirm that:

1. This work was done wholly or mainly while in candidature for a research degree at this University;
2. Where any part of this thesis has previously been submitted for a degree or any other qualification at this University or any other institution, this has been clearly stated;
3. Where I have consulted the published work of others, this is always clearly attributed;
4. Where I have quoted from the work of others, the source is always given. With the exception of such quotations, this thesis is entirely my own work;
5. I have acknowledged all main sources of help;
6. Where the thesis is based on work done by myself jointly with others, I have made clear exactly what was done by others and what I have contributed myself;
7. Parts of this work have been published as:

Cheung, K.S.C. et al., 2014. MicroRNA-146a Regulates Human Foetal Femur Derived Skeletal Stem Cell Differentiation by Down-Regulating SMAD2 and SMAD3. *PloS one*, 9(6), p.e98063.

Gothard, D. et al., 2015. Regionally-derived cell populations and skeletal stem cells from human foetal femora exhibit specific osteochondral and multi-lineage differentiation capacity in vitro and ex vivo. *Stem cell research & therapy*, 6(1), p.251.

Signed:……..Kelvin Sin Chi Cheung.....

Date:……..29th September 2015

# Acknowledgements

This work was conducted at the Bone and Joint Research Group, Institute of Developmental Sciences, Southampton General Hospital, University of Southampton, United Kingdom. The work was supported by a Strategic Longer and Larger grant (sLOLA) from the Biotechnology and Biological Sciences Research Council, United Kingdom.

I would like to dedicate this thesis to the memory of Dr. Trudy Roach, who sparked my interest in research and encouraged me to embark on a PhD degree.

First and foremost, I would like to thank my supervisors Professor Richard Oreffo and Dr. Tillmen Sanchez-Elsner for their support and guidance throughout my PhD study. I would like to thank my collaborators, Professor Yasuhiko Tabata and Dr. Masaya Yamamoto at Kyoto University, Japan, for the development of spermine-pullulan complex as a transfection reagent for microRNA in skeletal stem cells and their hospitality during my stay Japan, making my attachment at Kyoto University a memorable experience. I would like to thank Dr. Tamas Dalmay and Dr. Guy Wheeler at the University of East Anglia for their help with microRNA *in situ* hybridisation and Dr. David Gothard for his help with 3D pellet culture and Stro-1 expression in foetal skeletal stem cells. I would like to thank all my colleagues at the bone and joint research group at the University of Southampton for their friendship and help with various experimental tasks throughout my PhD research. I would like to thank Mr. Byron Fericks for his help with proofreading this thesis.

Finally, I would like to thank my mother for her unconditional love and support throughout my medical career.

# Definitions and Abbreviations

| | |
|---|---|
| 2D | Two dimensional |
| 3'UTR | 3’ untranslated region |
| 3D | Three dimensional |
| A/S | Alcian blue/Sirius red |
| ALP | Alkaline phosphatase |
| APC | Adenomatous Polyposis Coli |
| Asc | Ascorbate-2-phosphate |
| BFGF-R | Basic fibroblast growth factor receptors |
| bHLH | Basic helix-loop-helix |
| BMP | Bone morphogenic protein |
| BSA | Bovine serum albumin |
| BSP | Bone sialoprotein |
| Cbfa-1/Pebp2αA/ AML3 | Core binding factor a1 |
| CDI | N,N’-carbonyldiimidazole |
| *Cdk4* | Cyclin-dependent kinase 4 |
| CFU-F | Colony forming units-fibroblasts |
| CKlα | casein kinase lα |
| Co-SMAD | common mediator SMAD |
| CSF-1 | Colony stimulating factor |
| DAPI | 4',6-diamidino-2-phenylindole |
| Dex | Dexamethasone |
| Dkk | Dickkopf-related protein |
| Dlx | Homeodomain transcription factors |
| DNA | Deoxyribonucleic acid |
| DNMT | DNA methyltransferase |
| DY547 | DyLight Phosphoramidite |
| ECM | Extracellular matrix |
| EDTA | Ethylenediaminetetraacetic acid |
| FACS | Fluorescence-activated cell sorting |
| FCS | Foetal calf serum |
| FHL | Four and a half LIM domains protein |
| FZD | Frizzled |
| GSK3β | Glycogen synthase kinase-3 beta |

| | |
|---|---|
| HA-PLA | Hydroxyapatite-poly lactic acid |
| HBMSC | Human bone marrow stromal cell |
| HDAC5 | Histone deacetylase 5 |
| HMG | High motility group |
| I-SMADs | inhibitory *SMADs* |
| IBMX | Isobutyl-1-methylxanthine |
| ICAM-1 | Intercellular Adhesion Molecule 1 |
| IFNGR1 | Interferon gamma receptor 1 |
| Ihh | Indian hedgehog |
| IL-1R | Interleukin-1 receptor |
| INF-Ɣ | Interferon gamma |
| ISH | In Situ Hybridisation |
| ITS | Insulin/transferrin/sodium selenite |
| JNK | c-Jun N-terminal kinases |
| Klf4 | Kruppel-like factor 4 |
| LPL | lipoprotein lipase |
| LRP5 | Low-density lipoprotein receptor |
| MACS | Magnetic activated cell sorting |
| MHC | Major histocompatibility complex |
| miR/ miRNA | MicroRNA |
| miRISC | RNA-induced silencing complex |
| miRNP | microRNA-containing ribonucleoprotein complex |
| MSC | Mesenchymal stem cell |
| Msx | Msh homeobox |
| N/P | Nitrogen/Phosphate ratio |
| NK cell | Natural killer cell |
| Nkx3-2/Bapx1 | Bagpipe homeobox homolog 1 |
| NLK | Nemo-Like Kinase |
| OCN | Osteocalcin |
| Oct4 | Octamer-binding transcription factor 4 |
| ON | Osteonectin |
| OSX | Osterix |
| P1/P2/P6 | Passage 1/2/6 |
| PBS | Phosphate buffered saline |
| PCR | Polymerase chain reaction |
| PDGF-R | Platelet-derived growth factor receptor |

| | |
|---|---|
| PFA | Paraformaldehyde |
| PKC | Protein kinase C |
| PPAR-γ | proliferation-activated receptor γ |
| PTFE | Polytetrafluoroethylene |
| R-SMADs | receptor-activated *SMADs* |
| RANKL | Receptor activator of NG-κB ligand |
| Rb | Retinoblastoma protein |
| RNA | Ribonucleic acid |
| RT-qPCR | Real Time quantitative PCR |
| RUNX2 | Runt-related transcription factor 2 |
| S-P | Spermine-Pullulan |
| SD | Standard deviation |
| sFRP | Secreted frizzled-related protein |
| SOX2 | Sex determining region Y-box 2 |
| SOX9 | Sex determining region Y-box 9 |
| SSC | Skeletal stem cell |
| Tcf3 | Transcription Factor 3 |
| TGF-β | Transforming Growth Factor beta |
| TGFBR | transforming growth factor beta receptor I |
| THY1 | Thy-1 Cell Surface Antigen |
| TNF-R | Tumor necrosis factor receptor |
| Twist-1 | Twist family bHLH transcription factor 1 |
| U.V. | Ultraviolet |
| Vitamin $D_3$ | 1,25-dihydroxyvitamin $D_3$ |
| WIF | Wnt inhibitory factor |
| α-MEM | Modified eagle's medium - alpha |

# Chapter 1: Introduction

## 1.1 Overview

Bone loss arising from trauma, disease or injury is a major cause of chronic morbidity, which results in reduced quality of life for many and represents a significant socio-economic burden. Currently, 1 in 3 women and 1 in 5 men are at risk of an osteoporotic fracture, which had an associated healthcare cost of £1.73 billion per year in 2012 and is expected to rise to over £2.1 billion by 2020 (Peto & Allaby n.d.). Osteoporotic fractures cause permanent disability in roughly 50% of patients, with a mortality rate of 15-20% within a year of injury (Johnell & Kanis 2006). Some have heralded tissue engineering as a new strategy for regenerating bone tissue. In essence, this discipline aims to combine cells capable of secreting bone matrix with biocompatible material and osteogenic growth factors in order to initiate bone regeneration and replace lost bone tissue (Rose & Oreffo 2002). This thesis aims to identify a suitable cell source for tissue engineering applications and investigate the use of bioactive signals such as miRNAs to promote osteogenic differentiation to further inform tissue-engineering strategies.

## 1.2 Bone Tissue Engineering

At present, autologous bone grafts are the gold standard in the repair of bone defects because they are histocompatible and non-immunogenic. Autografts possess the key components necessary to achieve osteoinduction, such as osteogenic growth factors, osteoprogenitor cells and a three dimensional matrix (Damien & Parsons 1991). Autografts are harvested from a patient's iliac crest and require two operations at the harvest site (Damien & Parsons 1991). Such bone grafts can result in significant harvest site injury, morbidity, deformity and scarring and are associated with an increased risk of inflammation, bleeding, chronic pain and infection (Palmer et al. 2008). Further, autografts might not even be a plausible treatment method in cases where the defect site requires a significant amount of bone tissue (Amini et al. 2012).

On the other hand, allografts represent the second most common bone-grafting technique. This method involves transplanting donor bone tissue, which is often obtained from cadavers (Boyce et al. 1999). An allograft may take various forms, including morcellised and cancellous chips, de-mineralized bone matrix, and whole-bone segments, depending on a case's specific requirements. Compared to autografts, allografts have a heightened risk of infection transmission and immunoreactions (Boyce et al. 1999). Since allografts are typically devitalised via irradiation or freeze-drying processing, allografts also have reduced osteoinductive properties due to their lack

of a cellular component, (Amini et al. 2012). Other bone repair techniques involve bone cement fillers and distraction osteogenesis. Although these current clinical interventions can improve the repair of bone, none possess the ideal characteristics of 1) high osteoinductive and angiogenic potentials, 2) high biological safety, 3) low patient morbidity, 4) no size restrictions, 5) adequate source availability and 6) reasonable cost (Amini et al. 2012). The field of bone tissue engineering focuses on alternative treatment options that will possess these ideal characteristics (Bhatt & Rozental 2012). The classic bone tissue engineering paradigm involves the following key elements: a biocompatible scaffold that closely mimics the natural extracellular bone matrix, osteogenic cells to synthesise a new bone matrix, a bioactive signal directing cells to differentiate into osteogenic cell types and a vascularization for nutrient supply (Rose & Oreffo 2002; Amini et al. 2012).

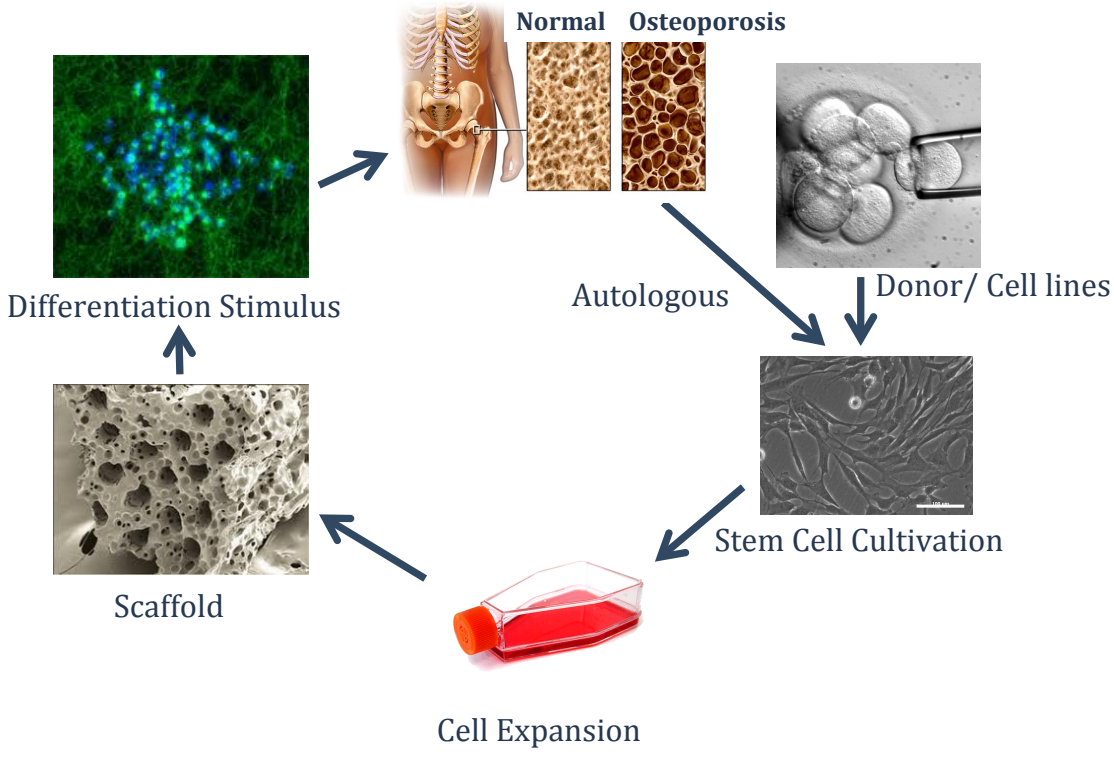


**Figure 1.1 Principles of bone tissue engineering.** Osteoprogenitor cells are harvested either from a patient or obtained from cell lines. These cells are then cultivated and expanded *in vitro* before being loaded into a biocompatible scaffold and treated with factors promoting osteogenesis. The resulting engineered bone tissue is then used as a bone graft.

## 1.3 Bone

### 1.3.1 Structure of Bone

Bone is characterised by its hardness, rigidity, and power of regeneration and repair. Bone protects vital organs, provides an environment for marrow (responsible for fat storage and haematopoiesis). Bone also acts as a reservoir of growth factors, cytokines and minerals (for calcium homeostasis). Bone is constantly undergoing change to adapt to biomechanical forces and to repair micro-damage in order to preserve bone strength (Fogelman et al. 2013).

Bone has two structural components: the cortical bone, which is dense and solid and surrounds the marrow space; and the trabecular bone, which is a honeycomb-like network of trabecular plates and rods. Cortical bone has an outer periosteal surface and inner endosteal surface (Fogelman et al. 2013). The periosteum is a fibrous connective tissue sheath surrounding the outer cortical surface. In addition, there are two types of bone based on the pattern of collagen formatting osteoid: woven bone, which is characterised by a haphazard organization of collagen; and lamellar bone, which is characterised by a regular parallel alignment of collagen into sheets (Fogelman et al. 2013). Because of the alternating orientation of collagen fibrils, lamellar bone has a significant mechanical strength and virtually all healthy bone in adults is lamellar bone. By contrast, woven bone has a disorganized structure, making woven bone weaker than lamellar bone (Bilezikian et al. 2008). Woven bone is only produced when osteoblasts are needed to produce osteoid rapidly, such as during foetal skeletogenesis and fracture healing. In normal individuals, woven bone is normally replaced by lamellar bone through the process of remodelling (Bilezikian et al. 2008).

### 1.3.2 Extracellular Matrix of Bone

The extracellular matrix (ECM) of bone comprises two main components: 1) an inorganic component, which consists mainly of hydroxyapatite crystals; and 2) an organic components known as osteoid, which consists of type I collagen embedded in a glycosaminoglycan gel containing specific glycoproteins such as chondroitin sulfate and osteocalcin. As a result of the deposition of hydroxyapatite (inorganic component) [$Ca_{10}(PO_4)_6OH_2$], osteoid gives bone its characteristic rigidity and functional strength (Bilezikian et al. 2008; Fogelman et al. 2013).

Type I collagen makes up roughly 95% of the osteoid. It is produced intracellularly as tropocollagen and then exported and associated into fibrils. The other 5% of osteoid is comprised of proteoglycans and non-collagenous proteins (Bilezikian et al. 2008). The non-collagenous proteins consist of osteocalcin, bone sialoprotein (BSP) and osteopontin, which act together in order to regulate mineralization of the matrix. Osteopontin is secreted by osteoblasts in the early stages of

osteogenesis and fosters bone remodelling and cellular signalling pathways via various receptors to encourage cell migration (Denhardt & Noda 1998). BSP is a multi-functional protein which is expressed at later stages of osteogenesis, promoting mineralization and bone growth and modulating the vascularisation of new bone (Nieden et al. 2003; Alford & Hankenson 2006; Malaval et al. 2008). Osteocalcin is the final component expressed during osteoblast differentiation and also fosters matrix mineralization and acts as a biochemical indicator of bone turnover (Nieden et al. 2003).

Crystalline hydroxyapatite is the main mineral component of bone, accounting for approximately half of adult bone mass (Fogelman et al. 2013). These crystals are deposited along bone collagen fibrils. Plate-like hydroxyapatite crystals are found in discrete spaces inside collagen fibrils (Figure 1.2), limiting growth of mineral crystals and forcing them to be discontinuous and discrete. This nano-crystalline organisation reduces the risk of fracture propagation and increases strength and toughness. The collagen fibrils and hydroxyapatite crystals are aligned along the direction of maximum stress in the bone. This provides an efficient structure capable of withstanding stress and the ability to detect and repair micro-damage (Rho et al. 1998).

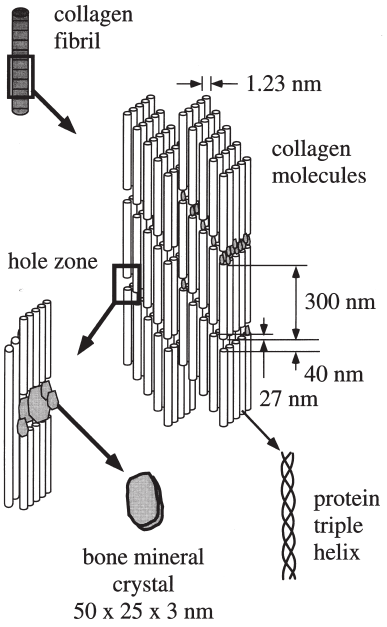


**Figure 1.2. The assembly of collagen fibrils and hydroxyapatite crystals.** Collagen fibrils are aligned with a 67nm periodic pattern resulting from the presence of a 40nm gap where hydroxyapatite crystals reside (Rho et al. 1998).

### 1.3.3 Skeletogenesis

Bone is derived from three distinct embryonic structures: 1) the somites, which generate the axial skeleton, 2) the lateral plates, which generates the limb skeleton and, 3) the neural crests, which generate the craniofacial bones. Depending on the site of development, bone is formed by one of two mechanisms: 1) intramembranous bone formation, which is mediated by the inner periosteal osteogenic layer where bone is synthesised without the mediation of a cartilage phase, giving rise to flat bone and 2) endochondral bone formation, where bone is formed by transformation of a cartilaginous template. Endochondral bone formation gives rise to long bones since its mechanism allows elongation and thickening of bone during foetal and post-natal skeletal development (Karsenty 1998). A developing long bone consists of the epiphyses and metaphyses at each end and the diaphysis in between. The epiphyses are responsible for the transverse and spherical growth of the ends of bones, the longitudinal growth of the metaphysis and the diaphysis and the shaping of the articular surfaces (Figure 1.3). The epiphyses are initially formed entirely of cartilaginous matrix and subsequently differentiate into three histologically distinct regions: 1) the articular cartilage, found at the outermost boundary, adjacent to the joint space, 2) the growth plate, found adjacent to the metaphysis and epiphyseal cartilage, containing hypertrophic chondroblasts and 3) the epiphyseal cartilage, found between the articular cartilage and growth plate, which forms the secondary ossification centre after vascular and osteoprogenitor cell invasion (Shapiro 2008). The growth plates undergo a temporal process of extracellular matrix synthesis, cell hypertrophy, mineralization of the matrix, cell proliferation, localised vascular invasion and, finally, apoptosis (Shapiro 2008).

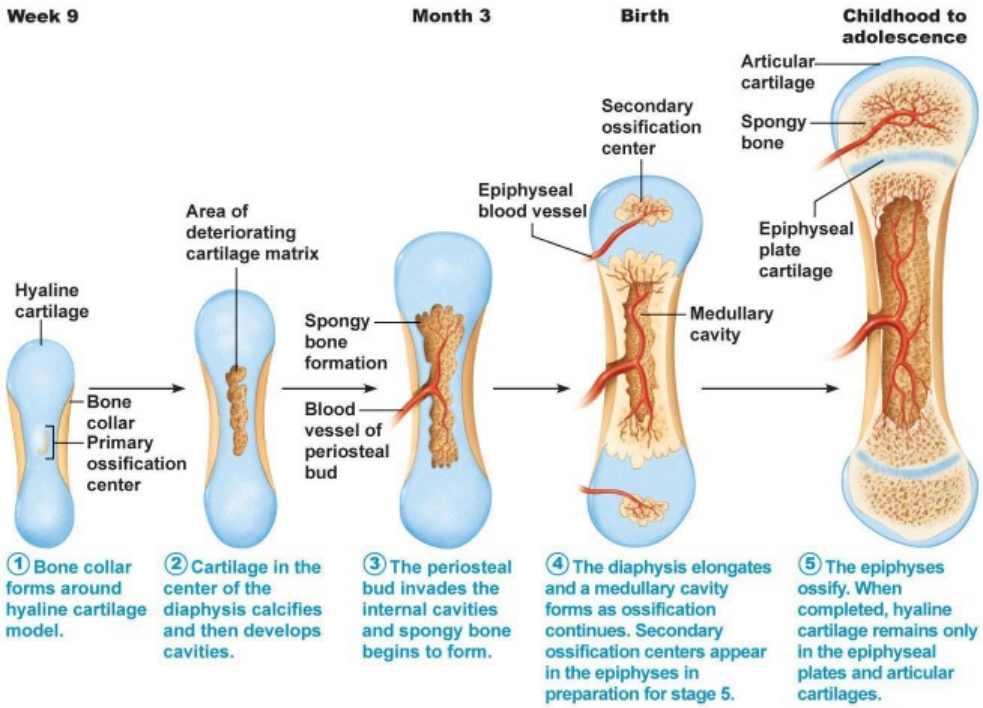


**Figure 1.3. The process of endochondral ossification**. Endochondral bone formation commences with the condensation of skeletal stem cells, which is followed by the formation of a cartilaginous template. Pre-hypertrophic cells differentiate in the centre of the cartilaginous template and induce differentiation of osteoblast precursors. During later stages, differentiated hypertrophic chondrocytes and osteoblasts produce the mineralised matrix. Blood vessels invade and allow migration of osteoprogenitor cells forming ossification centres. (Pearson education, Inc. http://www.kean.edu)

### 1.3.4 Bone Remodeling

Bone is a dynamic tissue undergoing constant change. This characteristic allows it to adapt to changing environmental stresses and to release stored phosphate ions and calcium to provide for calcium homeostasis (Summarised in figure 1.4). There are five stages of bone remodelling: 1) quiescence, 2) activation, 3) resorption, 4) reversal and 5) formation. Quiescent surfaces are resting bone areas in which a layer of inactive osteoblasts (bone lining cells) cover the surface, contributing to the regulation of extracellular bone fluid circulation and ion homeostasis (Teti 2011). The osteoclast is responsible for bone resorption and is composed of terminally differentiated myeloid cells which are rich in mitochondria and lysosome (Raggatt & Partridge 2010).

During the activation phase, Osteoclasts are recruited and activated to sites of micro-fracture by various paracrine factors like colony stimulating factor (*CSF-1*) and receptor activator of *NG-κB* ligand (*RANKL*) (Raggatt & Partridge 2010). The resorption phase is typically completed days after it commences. It is characterised by the presence of mature multinucleated osteoclasts where they

are adhered to substrate and initiate matrix degradation (Bilezikian et al. 2008). Activated osteoclasts form a ruffled cell border, sealing and degrading the underlying bone in a resorption pit by the release of hydrogen ions, hydrolytic enzymes and matrix metalloproteases. Resorption ends with the activation of apoptotic pathways in osteoclasts, liberating the remodelling area from the resorbing cells (Bilezikian et al. 2008). The reversal phase is not yet well understood, but is known to be characterised by the appearance of macrophage-like mononuclear cells (Teti 2011). Many believe these cells are involved in further collagen degradation and the removal of debris generated by osteoclasts (Busse et al. 2010).

Bone formation is comparatively slow and can take up to 120 days to complete. Bone formation is mediated by osteoblasts that replace removed bone with new bone. At the end of this phase, bone has been replaced, but the total amount remains unchanged as a result of the balanced osteoclast and osteoblast activity (Teti 2011).

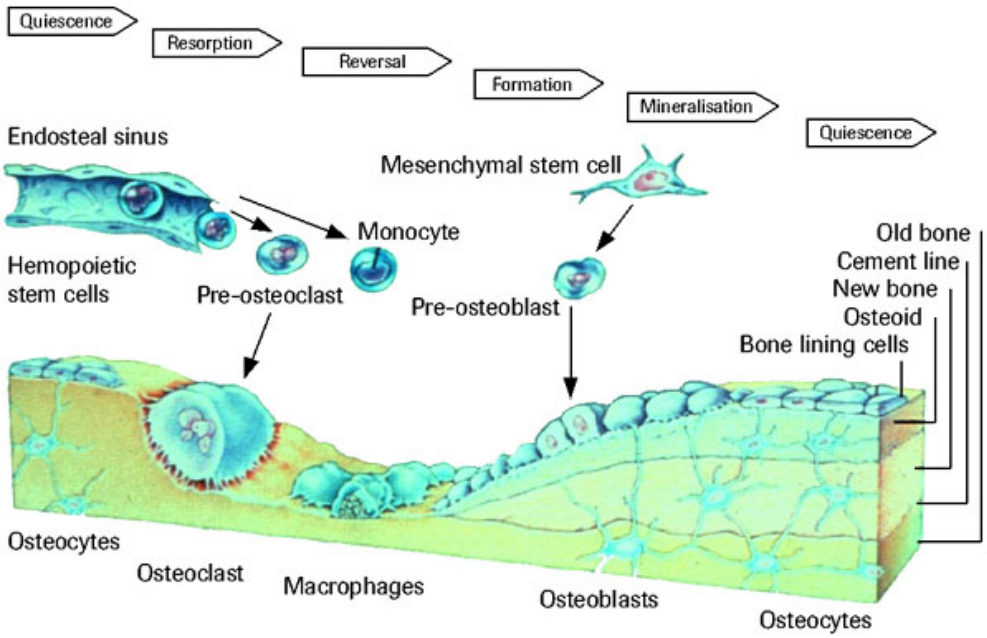


**Figure 1.4. Bone remodelling cycle.** Osteoclasts migrate via blood vessels to sites of micro-fractures and then adhere to substrate and initiate matrix degradation by releasing hydrogen ions, hydrolytic enzymes and matrix metalloproteases. Following resorption, macrophage-like mononuclear cells appear at the site of bone resorption, denoting the reversal phase. New bone formation is mediated by osteoblasts, completing the remodeling cycle. (www.Roche.com)

## 1.4 Skeletal Stem Cell

In 1966, Freidensten and colleagues described a plastic adherent cell population found in human bone marrow with osteogenic potential. This sub-population of marrow cells was shown to form colonies under monolayer culture and thus was described as colony-forming unit fibroblasts (CFU-F) (Friedenstein et al. 1966). Subsequently, similar cells have been isolated from other adult tissues such as deciduous teeth, cord blood, placenta, adipose tissue, synovial fluid, dermal tissue, and amniotic fluid (Lakshmipathy & Hart 2008). Although widely known as "Mesenchymal Stem Cells", it has not been formally proven that these cells differentiate beyond the skeletal lineages, but it has been shown that they differentiate into functional osteocytes, chondrocytes, bone marrow adipocytes, fibroblasts and bone marrow stromal cells (summarised in figure 1.5) (Tare et al. 2008; Mirmalek-Sani et al. 2006; Bianco et al. 2008). Accordingly, throughout this thesis the term skeletal stem cells (SSCs) will be used to describe this cell type, as it is a more accurate term to denote their differential potential. The ability of these cells to regenerate these phenotypes has led to their evaluation as potential therapeutic candidates for several diseases and degenerative applications requiring tissue regeneration.

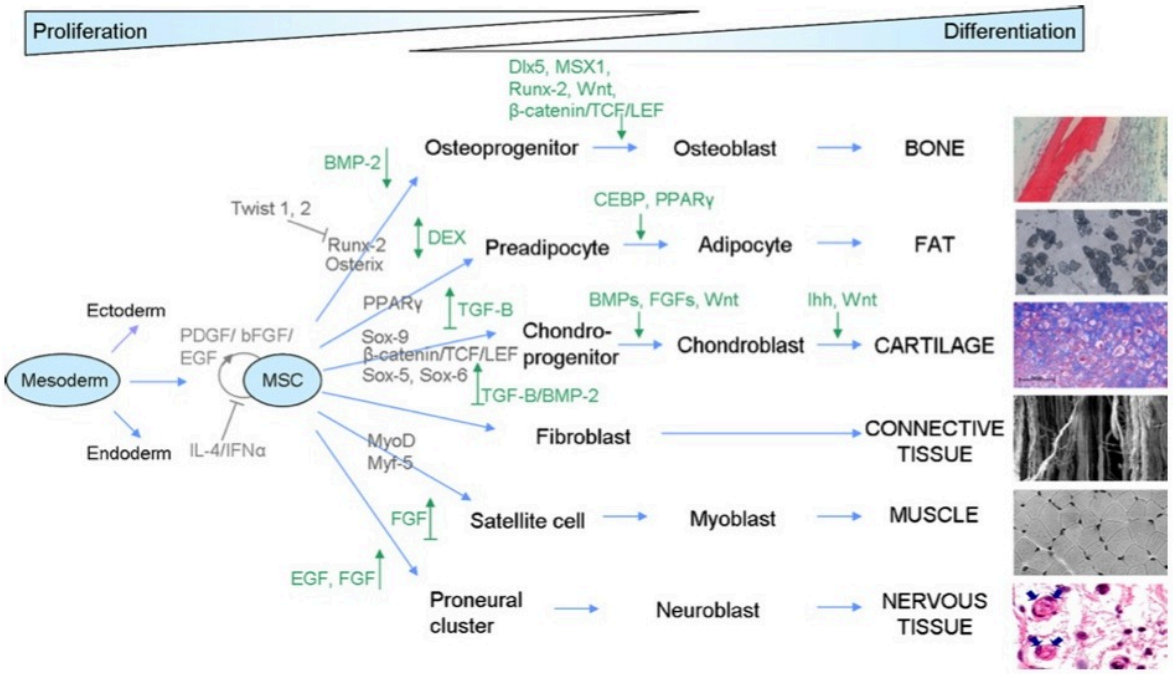


**Figure 1.5. Summary of the differentiation potential of skeletal stem cells**. SSCs can differentiate into their stromal lineages including osteoblasts, adipocytes, chondrocytes, fibroblasts, myoblasts and neuroblasts and are regulated by selected groups of growth and transcription factors (Tare et al. 2008).

### 1.4.1 Identification of the Skeletal Stem Cell

In monolayer culture, adherent SSCs display a spindle-like morphology with a dense cytoplasm, large nuclei and clear-cut nucleoli which are surrounded by chromatin particles (Friedenstein et al. 1966). SSCs isolated from human bone marrow or foetal femurs consist of a heterogeneous population with a varied potential to differentiate down specific stromal lineages including adipocyte, osteoblast and chondrocyte lineages (Mirmalek-Sani et al. 2006). As a result, a number of studies have attempted to classify SSCs into different sub populations and characteristics by their cell surface markers (Tare et al. 2008; Mirmalek-Sani et al. 2006). It is generally accepted that human SSCs do not express haematopoietic markers *CD45, CD34, CD14* and *CD11*, adhesion molecules such as *CD31*, *CD56* and *CD18* or co-stimulatory molecules such as *CD80*, *CD86* and *CD40*. However, SSC are thought to express *CD105*, *CD73*, *CD44*, *CD9*, *CD71* and *STRO-1* antigens and adhesion molecules *CD106*, *CD166*, *ICAM-1* and *CD29*. In addition, SSC expresses a number of cytokines, extracellular matrixes and growth receptors, which aid in the identification of SSCs (Kode et al. 2009) (summarised in table 1.1).

| **Maker Type** | |
|---|---|
| Surface markers | *CD13, CD29, CD44, CD73, CD90, CD105, CD106*, *STRO-1*, *SCA-1* |
| Cytokine receptors | *IL-1R, IL-3R, IL-4R, IL-6R, IL-7R* |
| Extracellular matrix receptors | *ICAM-1, ICAM-2, VCAM-1*, *ALCAM*, endoglin, hyaluronate receptor integrins a1, a2, a3, aA, aV, b1, b2, b3, b4 |
| Growth factor receptors | *BFGF-R, PDGF-R* |
| Other receptors | *THY-1, IFNGR1 (CD119), TGFBR, TNF-R* |

**Table 1.1. Commonly used cell surface proteins/receptors for isolation and characterisation of SSCs.** Adapted from Kode *et al* (Kode et al. 2009).

### 1.4.2 Immunomodulation Effect of Skeletal Stem Cells

In addition to their self-renewal and differentiation ability, SSCs have also been shown to possess immunomodulatory properties and to regulate transplantation tolerance, autoimmunity and tumour evasion (Petrie Aronin & Tuan 2010). The immunomodulatory effect of SSCs is thought to be mediated by a number of mechanisms: 1) suppression of T-cell functions, 2) inhibition of B-cell proliferation and differentiation into plasma cells (thus suppressing antibody formation), 3) suppression of natural killer cell proliferation and *INF-ϒ* production and 4) inhibition of monocyte maturation (Summarised in figure 1.6) (Kode et al. 2009). SSCs also lack MHC Class II molecules, indicating a potential immune evasion in allogeneic transplantation. These immuneregulatory properties enhance the potential applications of SSCs in tissue engineering strategies.

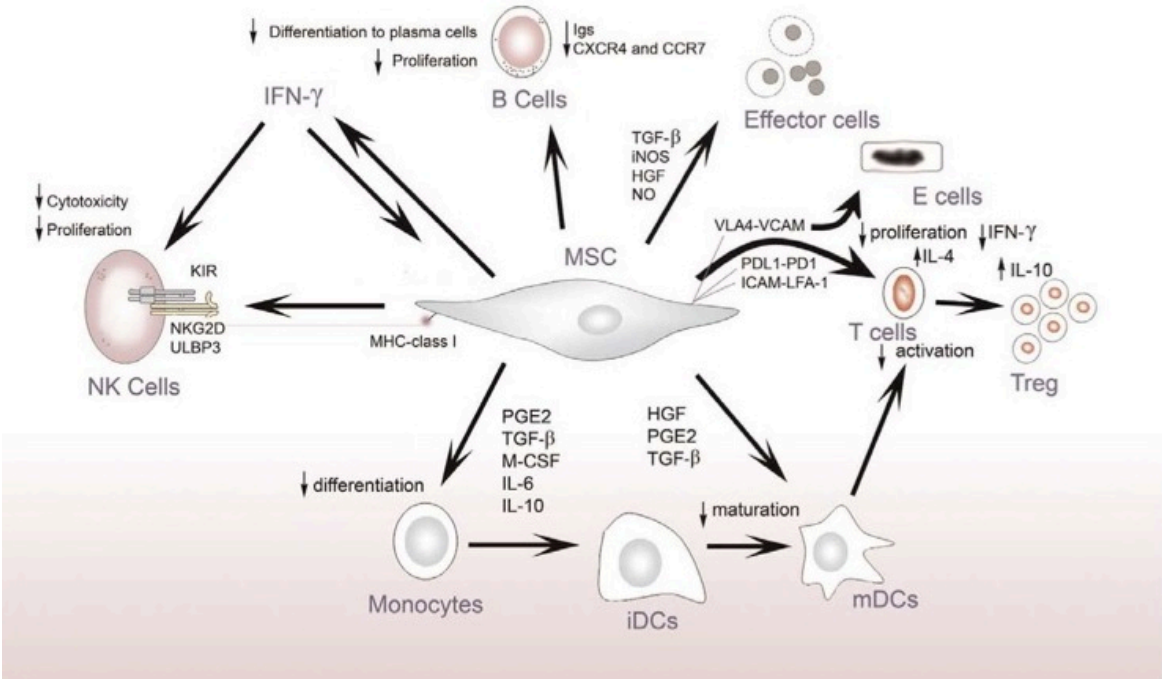


**Figure 1.6. The mechanisms of immunomodulation by skeletal stem cells.** SSCs inhibit differentiation and proliferation of B cells into plasma cells resulting in reduced antibody formation. SSCs suppress natural killer cell (NK) proliferation and IFN-ϒ release, thus suppressing NK cell function. SSCs inhibit differentiation of monocytes into immature dendritic cells and development into mature dendritic cells, suppressing innate immunity response (Kode et al. 2009).

## 1.5 Regulation of Osteogenic and Chondrogenic Differentiation

### 1.5.1 Transcription Control of Skeletal Stem Cell Differentiation

The differentiation of skeletal stem cells into specific stromal cells involves a complicated multistep pathway with various cell intermediates. In osteogenesis, SSCs progress through osteoprogenitor cells and osteoblasts into osteocytes. Each intermediate cell type secretes a number of matrix proteins and local factors required by developing bone matrix (Firth J 2008). Osteoprogenitor cells secrete Type I, III and V collagen, osteopontin, and fibronectin, which are the initial bone matrix. As osteoprogenitor cells differentiate into osteoblasts, alkaline phosphatase, type I collagen, osteocalcin, *SPARC* and *BSP* are produced in preparation for matrix mineralisation. Finally, osteocytes synthesise osteocalcin, *DMP1*, sclerostin and collagenase involved in mineralisation and remodelling of the previously secreted matrix (Hartmann 2009). Thus, the expression of osteogenic genes requires precise control of gene expression and is achieved through several key cell signalling pathways, transcription factors and miRNAs.

Progression from one stage of cell differentiation to the next cell intermediate requires specific nutrients, bioactive factors, and other environmental cues, which orchestrate differentiation (Firth J 2008). The exact mechanism of differentiation and renewal are not well understood, limiting the use of SSCs in clinical practice (Bruder et al. 1994). However, transgenic mouse models have helped to shed light on the function of various pathways and genes involved in osteogenesis (summarised in Table 1.2).

| Gene | Phenotype in knock-out mice | Role in skeletal genesis | Reference |
|---|---|---|---|
| *Ihh* | Reduces chondrocyte proliferation, maturation of chondrocytes at inappropriate position, and failure of osteoblast development in endochondral bones | Required for endochondral but not for intramembranous bone formation | (St-Jacques et al. 1999) |
| *sox9* | Perinatal lethality, hypoplasia and distortion of cartilage-derived skeletal structures and premature mineralization of bone | Required for chondrocyte development in endochondral bone formation | (Wright et al. 1993) |
| *runx2* | Absence of osteoblasts and impaired chondrocyte differentiation | Required for osteoblast differentiation of mesenchymal cells into preosteoblasts and hypertrophic chondrocytes | (Komori et al. 1997) |
| *osx* | Completely lack of bone formation but cartilage formation is normal | Required for differentiation of preosteoblasts into mature osteoblasts | (X. Zhou et al. 2010) |
| *β-catenin* | Blocks osteoblast differentiation and development into chondrocytes | Important for osteoblast differentiation, and prevents transdifferentiation of osteoblasts into chondrocytes | (DAY et al. 2005) |
| *Twist 1* | Leads to premature osteoblast differentiation | Antiosteogenic function by inhibiting *RUNX2* fuction during skeletogenesis | (Bialek et al. 2004) |
| *Atf4* | Delays bone formation during embryonic development and lowers bone mass throughout postnatal life | Critical regulator of osteoblast differentiation and function | (X. Yang et al. 2004) |
| *SatB2* | Involved in both craniofacial abnormalities and defects in osteoblast differentiation and function | A molecular node in the transcriptional network regulating skeletal development and osteoblast differentiation | (Dobreva et al. 2006) |
| *Shn3* | Involved in adult-onset osteosclerosis with increased bone mass due to augmented osteoblast activity | A central regulator of postnatal bone mass | (Jones 2006) |
| *Dlx5* | Delays ossification of the roof of the skull and abnormal osteogenesis | Positive regulator in osteoblast differentiation | (Acampora et al. 1999) |

**Table 1.2. The interaction of the transcription factors and their pathways.** Table summerises the effects of various transcription factors on skeletogenesis through gene knock-out mice studies (C. Zhang 2010).

Cbfa-1 (Core binding factor α1), also known as *RUNX2*, *Pebp2αA, AML3* is a runt-domain transcription factor expressed in early osteoblast progenitors at the site of bone formation (Banerjee et al. 2001). Its binding sites have been identified in the promoters of Type I Collagen, bone sialoprotein, osteopontin and osteocalcin (Banerjee et al. 2001). *RUNX2* has been identified as a downstream target of BMP and Transforming Growth Factor β (TGF-β) signalling, both of which are known to be potent inducers of osteogenesis *in vitro*. However, osteoblastic precursors that

produce active *RUNX2* are not fully committed to the osteoblastic lineage, as the downstream target Osterix *(OSX)* is also required (Figure 1.7) (C. Zhang 2010).

Osterix is a bone morphogenic protein-2 (*BMP2*) induced gene and is a downstream target of *RUNX2* (C. Zhang 2010). Although expressed at low levels in pre-hypertrophic chondrocytes, many think it to be a transcription factor that is specific for osteoblast development (C. Zhang 2010). In *Osx*-null mice, no cortical bone and no bone trabeculae were formed through either endochondral or intramembranous ossification and only a cartilaginous skeleton was observed (Nakashima et al. 2002). Although the phenotype of *Osx*-null and *runx2*-null mutants are both characterised by a lack of bone formation and an absence of differentiated osteoblasts, *runx2*-null mutants also display maturational disturbance of chondrocytes in addition to the failure of bone formation, which highlights the specificity of *OSX* expression to osteoblast development (Inada et al. 1999).

*SOX9* is a sex-determining region Y (SRY)-related high motility group box transcription factor and is expressed in skeletal precursors, a population of cells that give rise to chondrocytes as well as osteoblasts. *SOX9* ensures chondrogenic lineage commitment through direct inhibition of *RUNX2* and indirect transcriptional repression of *RUNX2* by up-regulating *Nkx3-2/Bapx1* (Yamashita et al. 2009). *SOX9* functions during both early and late chondrogenesis where knockout of *SOX9* expression before mesenchymal condensation results in absent cartilage development and loss of *SOX9* after condensation-caused general chondrogenic dysplasia (Firth J 2008).

Msh Homeobox *(MSX)* and Distal-less homeobox *(DLX)* homeodomain transcription factors are homologues of the Drosophila Distal-less and muscle-specific homoeobox genes with diverse roles in regulating development and patterning (Hassan et al. 2004). The involvement of *DLX* proteins in osteogenesis was suggested by some as a result of their expression at sites of bone formation during embrogenesis and in osteoblasts. *DLX3*, *DLX5* and *DLX6* have been implicated in osteogenic differentiation, with expression levels of the various *DLX* proteins changing during the course of osteogenic differentiation. *DLX3* is expressed early in osteogenesis with *DLX5* and *DLX6* expressed at later stages. *DLX5* and *DLX6* levels remain elevated through to matrix mineralization (Hassan et al. 2004).

*MSX2* is one of the three members of the *MSX* gene family thought to promote osteoblast proliferation and to inhibit osteoblast maturation (Firth J 2008). It has been observed that over expression of *MSX2* inhibits osteogenesis and that a reduction in endogenous *MSX2* promotes matrix mineralisation. In addition, *MSX2* is associated with the osteocalcin promoter only when the gene is inactive. Some evidence exists to support a positive role for *MSX2* in osteogenesis *in vivo* (Lallemand 2005; Satokata & Maas 1994), but it is thought that these observations were not based on the effect of *MSX2* alone but the overall effect when multiple signalling interactions are

interrupted. It is a more widely held view that *MSX2* and *DLX5* act antagonistically, with *MSX2* inhibiting and *DLX5* promoting osteogenesis (Firth J 2008). Ryoo et al, proposed that *MSX2* binds to elements in osteoblastic-specific genes, with *RUNX2* competing with and blocking *DLX5* binding (Ryoo et al. 2006). Bound *MSX2* represses gene transcription and promotes proliferation. In later stages of osteogenesis, increased levels of *DLX5* subsequently displace *MSX2* and activate transcription through *RUNX2* promoter interactions (Firth J 2008).

*Twist-1* and *Twist-2* are basic helix-loop-helix (bHLH) transcription factors which have negative effects on osteogenesis and which are thought to play a role in the timing of osteogenic differentiation required to create correctly patterned skeletal structures (Firth J 2008). Twist-mediated repression of osteogenesis is thought to act through pathways involving *RUNX2* and histone deacetylases. Repression through *RUNX2* is thought to be mediated via direct binding of *Twist* to *RUNX2*, inhibiting the binding and activation of osteogenic promoter by *RUNX2* (Firth J 2008; Pratap et al. 2003).

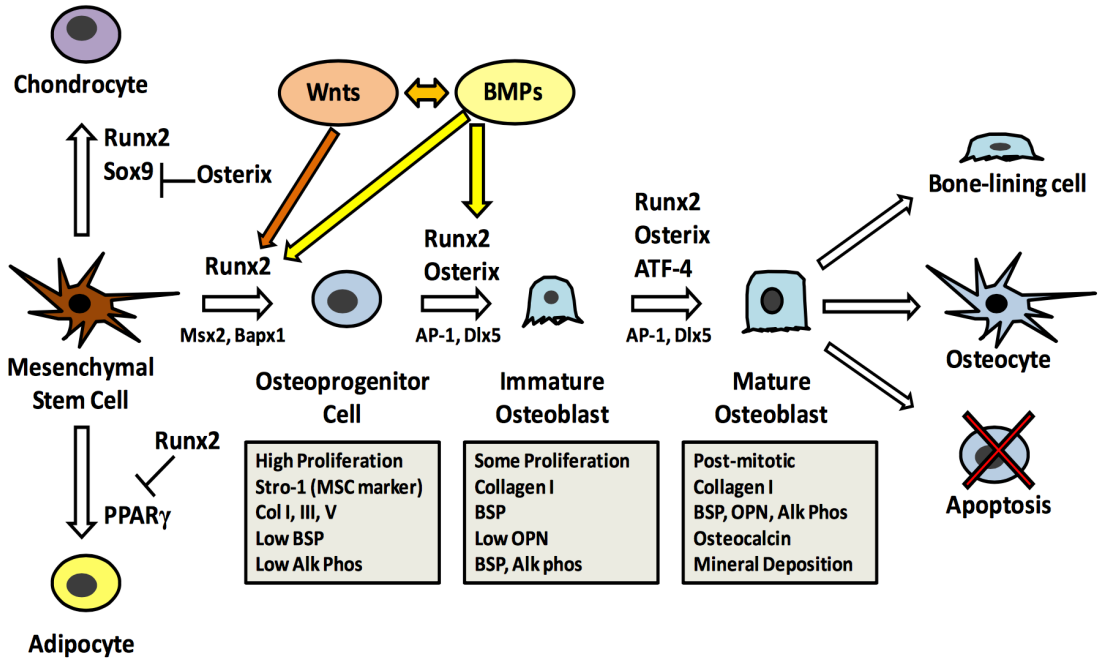


**Figure 1.7 Osteoblast differentiation pathway and factors regulating differentiation.** Differentiation of SSCs down osteogenic pathyway is orchestrated by a number of transcription factors. *RUNX2*, *MSX2* and *BAPX2* are involved in early lineage commitment of SSCs into osteoprogenitor cells while *RUNX2*, *OSX*, *AP-1* and *DLX5* are required for the progression of osteoprogenitor cells into immature osteoblasts. Abbreviations: Msh Homeobox 2 (Msx2), Bagpipe Homeobox Protein Homolog 1 (Bapx1), Activator protein 1 (AP-1), Distal-less homeobox 5 (Dlx5) and Activating Transcription Factor 4 (ATF-4) (Bryan Bell)

### 1.5.2 Transforming Growth Factor-β Pathway

Members of the transforming growth factor-β (TGF-β) family play a role in a variety of cellular processes including differentiation, growth and apoptosis. The human genome encodes 28 genes that encode members of this family, including the *TGF-β* and *BMPs* isoforms and activins (Moustakas et al. 2001). These proteins signal by stimulating formation of specific heteromeric complexes of type I and type II serine/threonine kinase receptors (Moustakas et al. 2001). When bound to ligands, type II receptors activate type I receptors by phosphorylation and type I receptors are responsible for downstream signalling. *SMADs* are substrate for type I receptor kinases with signalling function and act as intracellular signal transducers for the TGF-β pathway (Hellingman et al. 2011). There are eight *SMAD* isoforms and they fall into three functional sub-families: 1) receptor-activated *SMADs* (*R-SMADs*: Smad1/2/3/5/8) which are activated when phosphorylated by type I receptors; 2) common mediator *SMADs* (*Co-SMADs*: *SMAD4*), which oligomerise with activated *R-SMADs*; and 3) inhibitory *SMADs* (*I-SMADs*, *SMAD6* and *SMAD7*), which exert a negative feedback effect by competing with *R-SMADs* for receptor interaction and marking the receptors for degradation (Moustakas et al. 2001).

BMP/TGF-β signaling pathways have been shown to play an essential role in skeletogenesis (G. Chen et al. 2012). In the osteoblast, BMP signaling is required for the commitment of SSCs into an osteoblast lineage, while TGF-β/activin signaling is important in chondrogenesis and osteogenesis, working synergistically or antagonistically with BMP signaling, depending on the stage of differentiation (B. Song et al. 2009). BMP signaling regulates *SMAD1/5/8* and has been reported to progress osteogenesis through direct induction of *RUNX2*, *MSX2* and possibly *DLX5* in a *SMAD*-dependent manner (B. Song et al. 2009; Furumatsu et al. 2005). These molecules induce other important osteogenic gene expressions such as Osterix. *RUNX2* works with *R-SMADs* in an activator complex to activate BMP-responsive genes, and Osterix also activates osteogenic gene transcription, promoting osteogenic differentiation (B. Song et al. 2009). In chondrogenic differentiation, TGF-β stimuli are transducted by *SMAD2* and *SMAD3* signals (Furumatsu et al. 2005). Following ligand activiation, *SMAD2* and *SMAD3* work together to develop and maintain the phenotype of chondrocytes by forming a transcriptional complex with *SOX9* and have been shown to accelerate proteoglycan synthesis and type II collagen expression (Furumatsu et al. 2005).

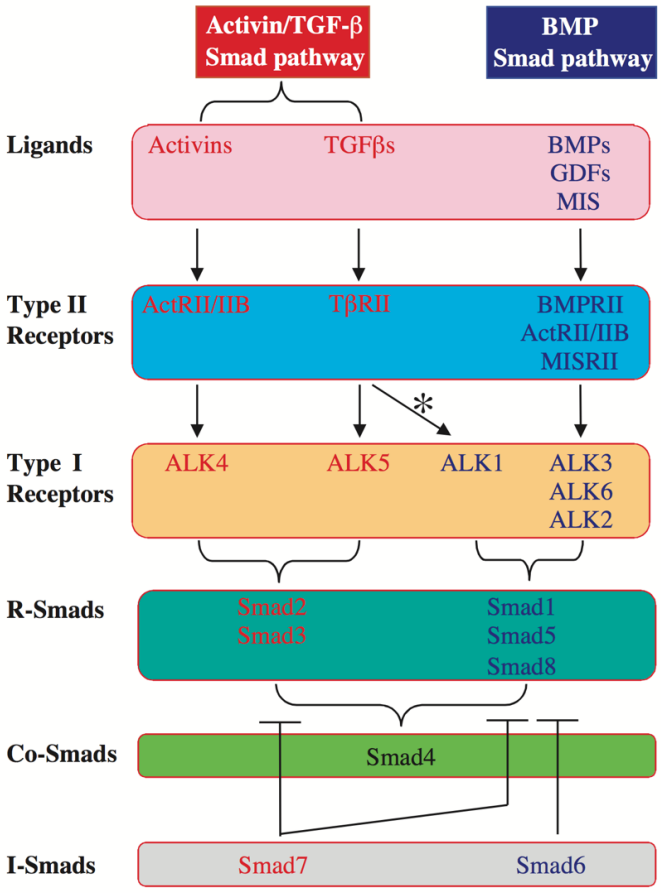


**Figure 1.8. Classification of mammalian Smad signalling cascade into activin-TGF- β and BMP pathways**. Classification of mammalian SMAD signalling cascade into activin-TGF- β and BMP pathways. Representative examples of ligands (pink), Type II receptors (blue), type I receptors (orange), R-SMADs (dark-green), Co-SMADs (light-green) and I-SMADs (grey). Divergence of the TGF- β pathway at the level of type I receptors towards both TGF-β and BMP SMADs is marked by an asterisk. Abbreviations: Growth and differentiation factors (GDFs), Mullerian inhibiting substance (MIS), activin type II and IIB receptors (ActRII/IIB), TGF-β type II receptor (TβRII), BMP type II receptor (BMPRII), Mullerian inhibiting substance type II receptor (MISRII), activin receptor-like kinases 1 to 6 (ALK1-ALK6). (Moustakas et al. 2001)

### 1.5.3 Wnt Signaling Pathways

Wnt proteins are cysteine-rich secreted glycol-lipoproteins that regulate development, cell proliferation, cell fate and generation of cell polarity (LEE et al. 2006). No less than 19 isoforms of Wnts have been identified. They function by binding to serpentine receptors of the Frizzled (FZD) family, initiating distinct cascades depending on if β-catenin is involved. Accordingly, this signalling is classified as either canonical (β-catenin dependent pathway) or non-canonical (β-catenin independent pathway) (Summarised in Figure 1.9) (Ling et al. 2009).

Wnt signalling plays a vital role in regulating the proliferation and differentiation of SSCs, which are known to express a number of Wnt ligands, including Wnt2, Wnt4, Wnt5a, Wnt11 and Wnt16, as well as several Wnt receptors, such as FZD2/3/4/5 and 6, and various co-receptors and Wnt inhibitors (LEE et al. 2006; Ling et al. 2009). The effect of Wnt signalling in SSCs depends on the context, and the function diversity of Wnt proteins is related to the specific surface receptors with which they interact and the particular intracellular signalling cascade that is subsequently stimulated.

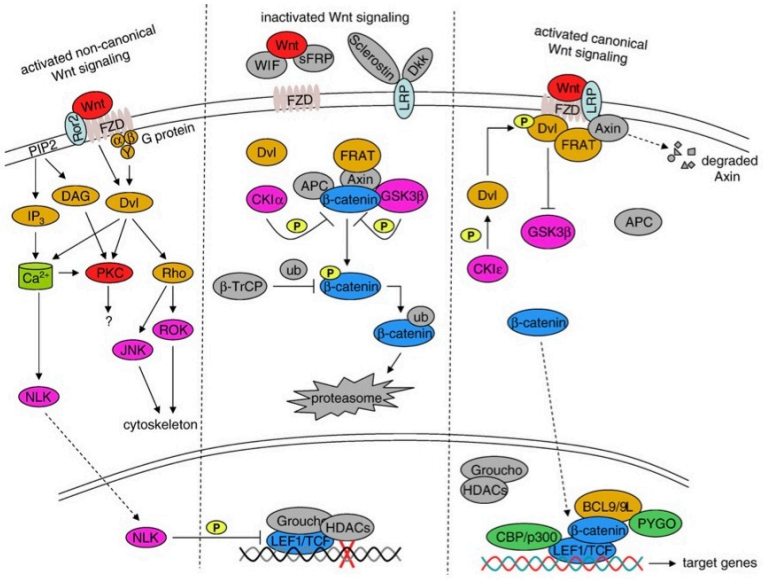


**Figure 1.9 Summary of Wnt signalling cascade**. Canonical Wnt signals are transduced through FZD receptors and low-density lipoprotein 5/6 co-receptors (LRP5/6 co-receptors) to the β-catenin signalling pathway. Non-canonical Wnt signals are transduced through FZD receptors and Rho2 co-receptors to the Dvl-dependent or $Ca^{2+}$-dependent pathways, activating downstream Rho/ROK, c-Jun N-terminal kinases (JNK), Protein kinase C (PKC) or Nemo-like Kinase (NLK), Wnt inhibitory factor (WIF), Secreted frizzled-related protein sFRP and Dickkopf-related protein (Dkk). Sclerostin acts as an inhibitor, inactivating Wnt signalling. Adenomatous polyposis coli (APC), Axin, Casein Kinase 1α (CKIα), Glycogene synthase kinase-3 β (GSK3β) and NLK negatively regulate Wnt signalling within the cytoplasm. (Ling et al. 2009)

### 1.5.4 Growth Factors Promoting Skeletal Stem Cell Differentiation

Transcription factors play an important role as proteins involved in the regulation of gene expression and a fundamental role in osteoblast and chondrocyte differentiation. Therefore, appropriate growth factors can be used to stimulate differentiation towards a particular pathway *in vitro* (Augello & De Bari 2010; Langenbach & Handschel 2013; S. J. Song et al. 2007; Scott et al. 2011). For chondrogenic differentiation, SSCs are typically cultured in a three-dimensional system by pelleting, in the absence of serum, and simulated with TGF-$\beta_3$ (Tare et al. 2005). TGF-$\beta_3$ has been widely used to promote SSC chondrogenesis in a variety of *in vitro* culture systems, where it is typically supplied intermittently to the cell culture medium during media changes (Augello & De Bari 2010). Although the optimal dose for *in vivo* chondrogenesis has not been systematically evaluated, 10ng/mL is most frequently used from chondrogenic differentiation of SSC *in vitro* (Augello & De Bari 2010). As the cells differentiate down the chondrogenic linage, an extracellular matrix typically consisting of type II collagen secreted by the chondrocytes can be detected.

To promote osteogenic differentiation *in vitro*, SSCs are usually cultured in ascorbate 2-phosphate, β-glycerol phosphate and dexamethasone. Dexamethasone induces *RUNX2* expression by *FHL2/β-catenin* mediated transcription activation promoting osteogenic differentiation (Langenbach & Handschel 2013). Ascorbate-2-phosphate is an enzyme co-factor for collagen synthesis (Takamizawa et al. 2004) and has been shown to increase secretion of *COL1A1*, which leads to increased COL1A1/α2β1 integrin-mediated intracellular signalling (Langenbach & Handschel 2013). The phosphate from β-glycerol phosphate serves as a source for the hydroxyapatite and promotes matrix mineralization (Langenbach & Handschel 2013) but has been shown to cause widespread non-specific mineralisation, a phenomenon that differs greatly from true bone formation and is associated with reduced cell viability (Orriss et al. 2014).

1,25-dihydroxyvitamin $D_3$, (vitamin $D_3$) is often used in combination with ascorbic acid and dexamethasone and has been established to induce a dose-dependent osteogenic response in human bone marrow stromal cells, with increased *ALP*, *COL1A1* and osteocalcin expression (Beresford et al. 1986; Skjødt et al. 1985). Another group of osteo-inductive factors are BMPs. A fundamental function of the BMPs is to induce the differentiation of mesenchymal osteoprogenitor cells towards cells of the osteoblastic linage and then to promote osteoblastic maturation and function (Ono et al. 2011). Bone morphogenetic proteins (BMPs) are well known to induce bone formation in animal models (Diefenderfer et al. 2003). In addition, *BMP2* has been shown to increase the expression of early markers of osteogenic differentiation *ALP* and osteoprotegerin *in vitro* (S. J. Song et al. 2007).

To promote adipogenic differentiation, SSCs are cultured in a medium together with 3-isobutyl-1-methylxanthine (IBMX), dexamethasone, insulin and indomethacin (Scott et al. 2011). Adipogenesis can be confirmed by morphology, with accumulation of lipid-rich vacuoles (Scott et al. 2011). Adipocytes will express peroxisome proliferation-activated receptor γ (*PPAR-γ*), lipoprotein lipase (LPL) and fatty acid binding protein aP2 (Scott et al. 2011).

## 1.6 MicroRNAs

### 1.6.1 Overview

In 1993, Lee et al described a 22-nucleotide (nt) gene lin-4, functionally known to downregulate target the protein lin-14, which is involved in the developmental timing of *Caenorhabditis elegans* (R. C. Lee et al. 1993). Lin-4, did not encode any protein, but instead contained sequences complementary to the 3' untranslated region (3'UTR) of lin-14 *mRNA* (R. C. Lee et al. 1993). This observation demonstrated that the gene regulatory properties of small non-protein coding RNAs or "MicroRNAs" (miRNAs) occur via antisense RNA-RNA interaction (R. C. Lee et al. 1993). Over the last two decades, the gene regulatory effects of miRNAs have been extensively studied and shown to participate in the regulation of almost every cellular process examined (Großhans & Filipowicz 2008). To date, 940 human miRNA sequences have been identified (miRBase Release 15), which are thought to control over 60% of all human protein coding genes (Liang et al. 2009). MicroRNAs have been shown to influence developmental timing (Pepper 2004), cell death (P. Xu et al. 2003), cell proliferation (L. Huang et al. 2010), haematopoiesis and the patterning of the nervous system (Fiore & Schratt 2007). These discoveries offer new strategies for the use and control of genomic information, with the potential to improve the prevention, diagnosis, prognosis and treatment of disease.

### 1.6.2 MicroRNA Biosynthesis and Mechanism of Gene Regulation

MicroRNAs are transcribed by RNA polymerase II as long primary transcripts of several kilobases in length with a hairpin structure (pri-miRNA). These are then processed by RNase III enzyme Drosha into shorter hairpin structures of ~80 bases long (pre-miRNA). Finally, pre-miRNAs are exported into the cytoplasm by exportin 5 mediated mechanisms where they are trimmed by RNase III enzyme Dicer into mature double-stranded miRNAs with ~20 bases. The biosynthesis of mircoRNA is summarised in figure 1.10. These two strands then separate to give a guide strand and a passenger strand. The guide strand is the functional strand and becomes incorporated in the complex known as miRNA-containing ribonucleoprotein complex (miRNP), miRgonaute or miRNA-containing RNA-induced silencing complex (miRISC). The passenger strand, usually marked with an asterisk, is

thought to be subjected to degradation (Iorio et al. 2010). miRISC can negatively regulate gene expression by direct *mRNA* cleavage, *mRNA* decay by deadenylation or translational repression, depending on the pairing complementarity. MicroRNAs usually base pair to target 3' UTR with imperfect complementarity, resulting in translational repression. With perfect pairing to the target *mRNAs*, miRNA can also induce *mRNA* degradation (Lewis et al. 2005). The principle of perfect/imperfect complementary binding results in numerous pair partnerships between individual miRNA*s* and *mRNA* targets. The *mRNA* targets of vertebral miRNA*s* were estimated by comparing conserved complementarily to the seed sequence of the miRNA*s*, suggesting an average of 200 *mRNA* per miRNA molecule. This plastic miRNA/*mRNA* binding relationship forms a complex network of inter*acting* post-transcriptional regulation of gene expression. This allows for the complex, system-wide signalling network needed for the global programmatic function of each cell type and still maintains flexibility for fine-tuning of segmental signalling operations.

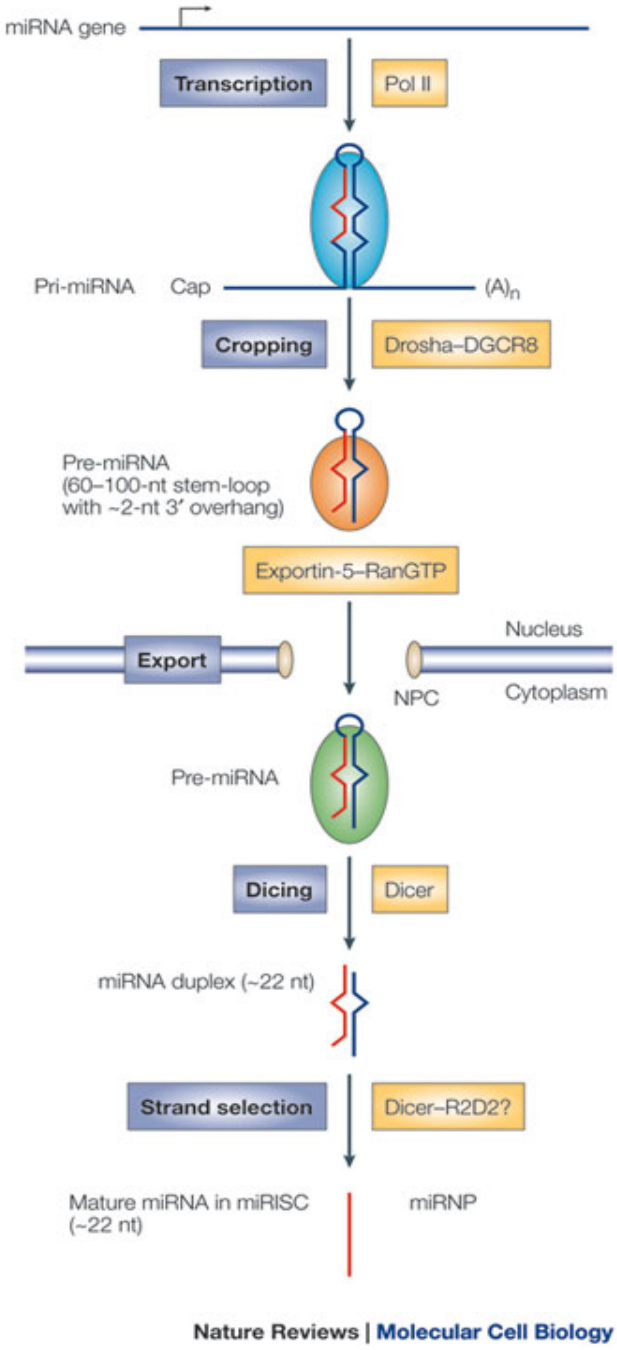


**Figure 1.10. MicroRNA processing.** MicroRNA are transcribed as long primary transcripts by RNA polymerase II (pri-miRNA) and subsequently processed by Drosha cleaving transcripts into short hairpin structures (pre-miRNA). Pre-miRNAs are exported into the cytoplasm by exportin 5, where Dicer further processes them into mature, double-stranded miRNAs. (V. N. Kim 2005).

### 1.6.3 MicroRNA Genomics and Gene Structures

The sequence coding for miRNAs are spread throughout the genome, including exons, introns, 3'-UTRs and genomic repeat-areas, and are situated either in the sense or antisense orientation with respect to the overlapping protein-coding gene (Suomi et al. 2008). Roughly 50% of the loci for mammalian miRNA are located in close proximity to each other, often in cluster sequence domains, with a "master" promoter for the production of a single polycistronic transcription unit (V. N. Kim et al. 2009). The remaining miRNA loci may then be structured as individual units, each controlled by its own separate promoter element. Approximately 40% of miRNA loci are located in the intronic region, and 10% in the extronic region of non protein-coding transcripts and 40% of miRNA loci are found within introns of protein-coding genes, and are known as microtrons (Bartel 2004). The mature miRNAs coded by clustered polycistronic transcripts may be either functionally related or distinct (Bartel 2004). Most intergenic human pri-miRNA genes measure 3-4 kbp, with a distinct 5' transcription start site and a CpG island located within the upstream proximal 2 kb region, and also flanked by a poly(A) site within the downstream 2 kb region of the embedded pre-miRNA code (Lewis et al. 2005). The transcription factor binding site for primary miRNAs are often found in clusters within the upstream 2 kb region of the pre-miRNAs. The transcription factors controlling signalling for growth and development are predicted by bioinformatic models to target these clusters (Min & Yoon 2010). Initiation of transcription is activated by RNA polymerase II binding to their specific target binding sequence elements within the core promoter. There are two distinct types of core promoters: 1) focus promoters, which contain either a single transcription start site (TSS) or a unique cluster of TSS's and 2) dispersed promoters containing several TSS's over 50-100nt and which are typically embedded in CpG islands in vertebrates (Min & Yoon 2010). In evolutionary terms, focused promoters are more conserved and are found in both invertebrates and vertebrates. Within vertebrates, dispersed promoters are more commonly identified than the focus type (Bartel 2004).

### 1.6.4 Regulation of MicroRNA Expression

The expression of miRNAs can be regulated at both a transcriptional and at a post-transcriptional level. At the transcription level, miRNA expression can be affected by mechanisms such as genomic changes, transcription factors, DNA methylation and histone modification (Iorio et al. 2010). In addition, altered expression of Drosha and DICER enzymes are important in the biosynthesis of mature miRNAs and may affect the level of miRNAs post-transcriptionally (Iorio et al. 2010). A number of factors are key for cell renewal and pluripotency, in particular, transcriptional factors, Octamer-binding transcription factor 4 (*OCT4*), Sex determining region Y-box 2 (*SOX2*), *NANOG* and Transcription Factor 3 (*TCF3*) determine the pluripotent and self-renewing properties of embryonic

stem (ES) cells. These four factors were predicted to occupy 55 unique miRNA polycistronic transcription units in murine ES cells, giving rise to 81 mature miRNAs, suggesting that up to 11% of mammalian miRNA is controlled by these four transcription factors (Liang et al. 2009). However, stimulation of estrogen receptors E2 and the ERα have been shown to decrease miRNA expression, suggesting transcription factors may also inhibit the expression of miRNA (Adams et al. 2007).

Approximately half of miRNAs are associated with CpG islands, suggesting their regulation by DNA methylation (Weber et al. 2007). An *in vitro* study demonstrated that treating T24 bladder cancer cells with 5-AZA-2' deoxycytidine, a DNA methyltransferase (DNMT) inhibitor, led to a strong up regulation of miR-127 (Saito et al. 2006). A similar study has also been conducted in colorectal cancer cells (Lujambio et al. 2008). On the other hand, miRNA with a hypermethylated promotor are generally down-regulated (Lujambio et al. 2008).

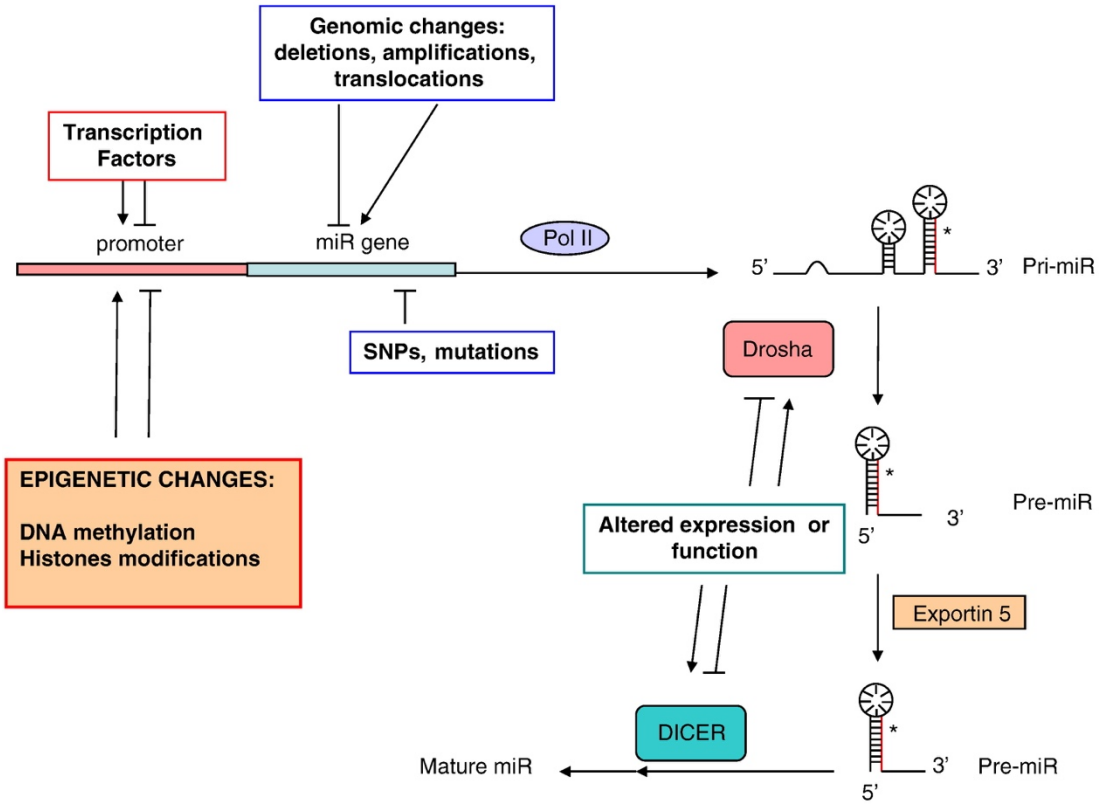


**Figure 1.11. Mechanisms regulating microRNA expression.** MicroRNA expression can be affected by epigenetic changes, transcription factors, chromosomal abnormalities, mutations, polymorphisms (SNPs). (Iorio et al. 2010)

### 1.6.5 Interaction of microRNAs in Epigenetics

A group of miRNAs, also known as "epi-miRNAs", (summarised in Figure 1.12) have been shown to regulate the expression of both DNA methyltransferase (Iorio et al. 2010) and enzymes regulating histone acetylation (J.-F. Chen et al. 2005). Their ability to affect the expression of these components of the epigenetic machinery suggests this group of miRNAs may constitute a highly-controlled feedback mechanism in the regulation of gene expression (Iorio et al. 2010). Khraiwesh *et al*, found the loss of dicer-like-B1 gene in mutant *Physcomitrella patens* moss did not impair normal miRNA maturation but impaired the cleavage of the target *mRNA* by the affected miRNAs (Khraiwesh et al. 2010). It was found that the accumulation of miRNA:target-RNA duplexes subsequently leads to hypermethylation of the genes encoding the target RNA, causing gene silencing. Khraiwesh et al proposed that the initiation of epigenetic silencing by DNA methyltransferase might be dependent on the ratio of the miRNA to its target *mRNA* (Khraiwesh et al. 2010).

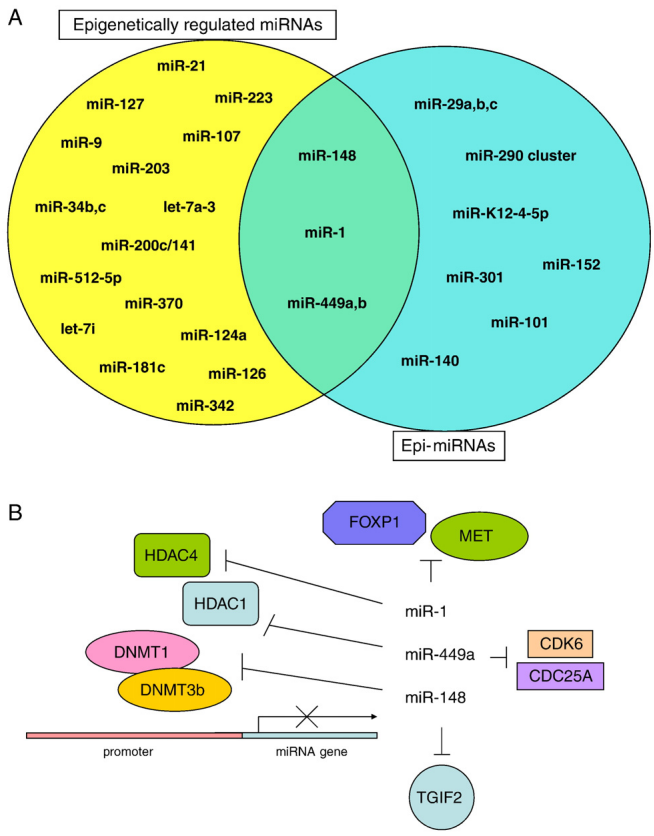


**Figure 1.12. Interactions between microRNAs and epigenetic machinery**. Diagram A details the most important miRNAs that are epigenetically regulated and the so-called epi-miRNAs, with the ability to directly and indirectly target members of the epigenetic machinery. Interestingly, the expression of some epi-miRNAs is in turn affected by epigenetic events, giving rise to possible feedback regulation loops (Diagram B). From Lorio *et al* 2010 (Iorio et al. 2010).

### 1.6.6 MicroRNA in Stem Cell Renewal and Differentiation

The role of miRNAs in stem cell self-renewal is suggested by the observation that loss of Dicer I, an enzyme essential to miRNA synthesis, resulted in embryonic lethality and loss of stem cell populations (Bernstein et al. 2003; Wienholds et al. 2003). During stem cell differentiation, there is a need to downregulate stem cell maintenance genes and activate lineage-specific genes. These transitions require a rapid switch in gene expression profiles. Although the transcription factor pool is replaced, remaining transcripts that were highly expressed in the previous stage need to be silenced to allow further progression of differentiation. miRNA can rapidly affect such changes through simultaneous repression of many remaining transcripts (J.-F. Chen et al. 2005). In a murine model, it has been shown that miR-291-3p, miR-294 and miR-295 are specific to embryonic stem cells and increase the efficiency of reprogramming by *Oct4*, *Sox2* and *Klf4* (Judson et al. 2009). By introducing miR-291-3p, miR-294 and miR-295 using retrovirus into murine embryonic fibroblasts, Judson *et al* have shown the ability to induce a homogenous population of pluripotent stem cell colonies (Judson et al. 2009). This observation suggests miRNAs play a key role in regulating stem cell renewal and differentiation.

### 1.6.7 MircoRNA Regulation of Cell Cycle and Apoptosis

microRNA-16, miR-24a and miR-106b families all regulate the G1 to S transition within the cell cycle. miR-16 and miR-34a are negative regulators of G1 progression, whereas miR-106b accelerates this transition (Ivanovska & Cleary 2008). The miR-16 family has been shown to modulate G1/S transition by regulating Cyclin-dependent kinase 4 *(Cdk4)* /6-cyclin D complexes and Cdk2-cyclin E complexes. These complexes cooperate in phosphorylation and prevention of Retinoblastoma protein (pRb) binding to E2F, thus activating E2F-mediated transcription and driving cells from G1 into S phase (Cimmino 2005). Moreover, miR-16 can induce apoptosis by downregulation of anti-apoptosis protein *BCL2*. These findings suggests that the miR-16 family can trigger an accumulation of cells in G0/G1 by silencing multiple cell cycle genes simultaneously (Cimmino 2005).

A number of genome profile studies indicate a general downregulation of miRNA in various tumors, suggesting a possible negative regulation of cancer growth by miRNAs (Y. S. Lee & Dutta 2006). Several studies positively support this hypothesis: miR-143 and miR-145 are two co-expressed miRNAs shown to be downregulated in colorectal adenocarcinoma. miR-15 and miR-16 are located within a 30 kb region at chromosome 13q14, a region deleted in more than half of patients with B-cell Chronic Lymphocytic Leukaemia (Ng et al. 2009). Overexpression of miR-15 and miR-16 results in downregulation of *BCL2*, an anti-apoptotic protein shown to induce apoptosis in a leukemic cell line (Cimmino 2005).

### 1.6.8 MicroRNAs involved in Osteogenic Differentiation

Various miRNAs have already been identified to play a role during SSC differentiation through regulating various transcriptions and the interplay with signalling pathways involved in SSC differentiation (Z. Liu et al. 2011; J. Huang et al. 2009; Dong et al. 2012). Of these, miR-93 has been shown to target the *OSX* gene (L. Yang et al. 2012). As previously described, *OSX* is a critical regulator of osteoblast differentiation and subsequent mineralisation. Overexpression in primary mouse osteoblasts has been shown to inhibit mineralisation through downregulation of *OSX* expression (L. Yang et al. 2012). In addition, miR-31 was reported to degrade *OSX mRNA* expression, and overexpression of miR-31 in HBMSC leads to osteogenic inhibition (Baglìo et al. 2013). MicroRNA has also been shown to interact with *RUNX2*, a transcription factor essential for osteoblast differentiation and bone formation (Kundu et al. 2002). miR-133 has been found to target *RUNX2 mRNA* resulting in inhibition of BMP2-induced osteoblast differentiation in murine C1C12 cells (Z. Li et al. 2008). In addition to miR-133; miR-23a, miR-30c, miR-34c, miR-133a, miR-135a, miR-137, miR-204, miR-217 and miR-388 have also been reported to regulate *RUNX2* gene expression, and overexpression of these miRNAs in SSCs have been shown to inhibit osteoblast differentiation (Y. Zhang et al. 2011; Y. Zhang et al. 2012). In addition to *RUNX2* and *OSX*, there are many important regulators of SSC differentiation which have also been shown to be regulated by miRNAs (Summarised in table 1.3).

Skeletal development and bone formation is regulated by various signalling pathways such as BMP/TGF-β and Wnt signalling (G. Chen et al. 2012; DAY et al. 2005; Ling et al. 2009). Therefore, miRNAs' regulating components of these signalling pathways will, by extension, affect osteogenic differentiation. For example, miR-135a has been reported to downregulate *SMAD5* protein translation, leading to the inhibition of osteogenesis and bone development (Z. Li et al. 2008). miR-210 has been found to target activin A receptor type Ib, thereby reducing the signal transduction of TGF-β and promoting osteoblastic differentiation (Mizuno et al. 2009). Activation of Wnt signalling has been reported to be mediated by miR-27 (Tao Wang & Z. Xu 2010) where miR-27 has been shown to inhibit the expression of *APC* and promote osteoblastic differentiation (Tao Wang & Z. Xu 2010). Furthermore, miR-346 was shown to stimulate osteogenesis in HBMSC by downregulating GSK-3β protein transition and subsequently activating Wnt/β-catenin signalling through increasing the level of β-catenin(Qing Wang et al. 2013). Collectively, these studies suggest a vast network of miRNAs is working in concert to regulate osteogenic differentiation.

| microiRNA | **Target Gene** | **Osteogenesis** | **Cell Line** |
|---|---|---|---|
| let-7f | Axin2 | + | hBMSC |
| miR-10a | KLF4 | + | hBMSC |
| miR-15b | SMURF1 | + | hBMSC |
| miR-196a | HOXC8 | + | hADSC |
| miR-20a | PPARγ Bambi Crim1 | + | hBMSC |
| miR-29a | osteonectin | + | MC3T3 |
| miR-29b | AcvR2a CTNNBIP1 DUSP2 TGF-$\beta_3$ HDAC4 | + | MC3T3 |
| miR-29c | osteonectin | + | MC3T3 |
| miR-346 | GSK-3β | + | hBMSC |
| miR-548d-5p | PPARγ | + | hBMSC |
| miR-133 | Runx2 | – | C2C12 |
| miR-135a | Smad5 | – | C2C12 |
| miR-138 | *FAK* | – | hBMSC |
| miR-140-5p | BMP-2 | – | hBMSC hADCS hUCSC |
| miR-141 | Dlx5 | – | MC3T3 |
| miR-143 | Osx | – | MC3T3 |
| miR-145 | Osx | – | C2C12 MC3T3 |
| miR-204 | RUNX2 | – | ST2 hMSC |
| miR-211 | RUNX2 | – | ST2 hMSC |
| miR-214 | Osx | – | C2C12 |
| miR-217 | Runx2 | – | MC3T3 |
| miR-23a | Runx2 | – | MC3T3 |
| miR-23a~27a~24-2 | SATB2 | – | MC3T3 |
| miR-26a | SMAD1 | – | hADSC |
| miR-30c | *Runx2* | – | MC3T3 |
| miR-31 | OSX | – | hBMSC |
| miR-338 | *Runx2* | – | MC3T3 |
| miR-338-3p | *Runx2/* Fgfr2 | – | mouse BMSC |
| miR-34a | JAG1 | – | hBMSC |
| miR-34b | SATB2 | – | primary mouse osteoblasts |
| miR-34c | SATB2 | – | primary mouse osteoblasts |
| miR-542-3p | BMP-7 | – | primary mouse osteoblasts |
| miR-637 | OSX | – | hBMSC |
| miR-654-5p | BMP2 | – | hBMSC |
| miR-93 | Osx | – | primary mouse osteoblasts |

**Table 1.3 Summary of microRNAs known to regulate osteoblast differentiation with confirmed target gene.** (Fang et al. 2015).

### 1.6.9 Identification of *Novo* MicroRNAs Involved in Skeletal Stem Cell Differentiation

A variety of techniques and strategies have been developed to examine specific miRNAs or prolife miRNA expression. MicroRNA cloning in combination with bioinformatics was first used to detect miRNA (R. C. Lee et al. 1993; Vanderpuye et al. 1992; Wightman et al. 1993). MicroRNA cloning is unique in its ability to reveal new miRNAs, however it is very labour intensive and relatively costly. Alternative techniques include 1) northern blotting, 2) profiling using microarrays and 3) miRNA specific PCR (C.-G. Liu et al. 2008; Fu et al. 2006; Várallyay et al. 2008). Northern blotting is the traditional technique for measuring RNA molecules with known sequences (Várallyay et al. 2008). The drawback of northern blotting is it has relatively lower sensitivity and might not be able to identify miRNA with lower expression (Várallyay et al. 2008). Microarray utilizes synthetic probes to profile miRNA expression in extracted RNAs (C.-G. Liu et al. 2008). The advantage of miRNA microarray is its ability to simultaneously detect hundreds of miRNAs with a change in expression during SSC differentiation (C.-G. Liu et al. 2008). Many investigators have already performed miRNA expression in attempts to identify the miRNAs involved in SSC differentiation. For example, *Li et al* have shown 58 miRNAs are upregulated and 10 are downregulated during the mineralization stage of murine calvaria-derived preosteoblast (Z. Li et al. 2009). In addition, the levels of 33 miRNAs have been shown to be modulated between differentiated and undifferentiated HBMSC, among which miR-26a, miR-26b, miR-30c, miR-101 and miR-143 were found to be upregulated and a downregulation of miR-138 and miR-222 was shown during osteoblast differentiation (Eskildsen et al. 2011). Although a plethora of miRNAs have been identified to have a change in level of expression during SSC differentiation, it is important to note that many of the miRNA targets could be involved in other cellular functions such as regulation of housekeeping genes instead of being directly involved in osteogenic and chondrogenic differentiation. Therefore, careful putative target analysis and functional analysis is required to confirm the role of miRNAs identified through miRNA arrays.

## 1.7 Conclusion

As a result of an aging population, there is a growing socio-economic need for an effective strategy to repair damaged or lost bone tissue. Bone tissue engineering offers treatment strategies for diseases which require regeneration of bone tissue, by using a combination of osteoprogenitor cells, bioactive factors to promote osteogenic differentiation and a biocompatible scaffold that closely mimics the natural bone structure. At present, the lack of a clear understanding of the complex processes involved in skeletal stem cell differentiation has hampered the use of bone tissue engineering in clinical practice. Therefore, a detailed characterisation of SSCs to provide an appropriate cell source and identification of new factors involved in SSC differentiation may help

inform bone tissue engineering strategies to restore function of the skeletal system. MicroRNA has emerged as an important regulator of a host of cellular processes including skeletal stem cell differentiation. By profiling and investigating miRNA functions during skeletal stem cell differentiation, new miRNA targets with osteogenic properties may be identified and can be used to enhance bone formation in clinical practice, offering new treatment avenues for conditions such as osteoporosis, as well as to play a role in tissue engineering applications by promoting bone formation.

## 1.8 Hypothesis

Foetal femur-derived SSCs possess enhanced differentiation and renewal capacity and can potentially be use as a cell source for tissue engineering applications. Cells with distinct differential potential can be isolated from the developing foetal femur. Novel miRNA targets can be identified through characterisation of subpopulations of SSCs derived from foetal femur. Functional analysis of newly identified miRNA targets may further our understanding of the processes involved in orchestrating SSC differentiation.

## 1.9 Aims and Objectives

- To derive an appropriate cell source for bone and cartilage tissue engineering applications through characterisation of a subpopulation of skeletal stem cells found within the developing foetal femur.
- To identify new miRNA targets involved in skeletogenesis and osteogenesis.
- To derive a robust culture model to identify miRNAs involved in SSC differentiation and allow functional analysis of miRNAs.
- To develop an effective transfection protocol for miRNA functional interrogation.
- To develop a miRNA gene delivery system to enhance osteogenic and chondrogenic differentiation.
- To examine the function of new miRNAs identified through characterisation of foetal femur-derived SSCs.

# Chapter 2: Materials and Methods

## 2.1 Materials and Reagents

Cell culture: all tissue culture reagents, growth factors, chemicals and other materials were supplied by Sigma-Aldrich unless otherwise stated. Penicillin/Streptomycin was purchased from PAA Laboratories. Foetal calf serum was purchased from Invitrogen, Paisley, UK. Collagenase B was purchased from Roche Diagnostics Ltd., East Sussex, UK. Histological analysis: all reagents used in histological analysis were supplied by Sigma-Aldrich unless specified. Histo-Clear was purchased from National Diagnostics, Atlanta, USA. DAPI (4',6-diamidino-2-phenylindole) nuclear counter stain (D3571) was purchased from Invitrogen. STRO-1 monoclonal antibody (STRO-1 hybridoma gifted from Dr J. Beresford, University of Bath). Molecular analysis: mirVana RNA isolation kits were obtained from ThermoFisher Scientific. All reagents for RT-qPCR including TaqMan miRNA assays and TaqMan Array were purchased from Applied Biosystems and Life Technologies unless otherwise stated. Primer sets were obtained from Sigma-Aldrich; primer sequences are given in section 2.10. In-situ hybridization: all reagents used for in-situ hybridization were obtained from Sigma-Aldrich unless specified. Blocking reagent was purchase from Roche. Salmon Sperm DNA was purchased from Fisher Scientific. MicroRNA-146a miRCURY LNA™ detection probes used for ISH were purchased from Exiqon. MicroRNA overexpression: Dharmafect and miRNA miRIDIAN mimics were purchased from Dharmacon. Western blot: all reagents used to make buffer solutions and protease inhibitor cocktail were purchased from Sigma-Aldrich. A BCA protein assay kit was obtained from Pierce. *SMAD2* and *SMAD3* antibody and DDT were supplied by Cell Signaling. SDA sample buffer and Any kD precast gel was purchased from BioLabs. PVDF immobilon-FL transfer membrane was obtained from Milipore. IRDye 800CW goat anti-rabbit and IRDye 800CW rabbit anti-HRP were obtained from LI-COR biosciences. Spermine-pullulan complex synthesis: 1,1 carbonyldimidazole was purchased from naclci tesque Inc., Japan. Pullulan P-50 Mw 47,300 was obtained from Sanko Pharmaceutical Co. Ltd, Tokyo. Spermine was acquired from Sigma-Aldrich Ltd, USA and Cellulose tube - Molecular Weight Cut Off 12,000-16,000g was purchased from Sanko Pharmaceutical Co. Ltd, Tokyo.

## 2.2 Tissue Culture

### 2.2.1 Human Bone Marrow Preparation and Stromal Cell Culture

Bone marrow tissues from femoral reaming waste were obtained from haematologically normal patients undergoing total hip replacement surgery. Ethical approval was obtained from the Southampton & South West Hampshire Local Research Ethics Committee (LREC-194-99). Marrow tissue was shaken in 10 ml of α-MEM four times and the resulting suspension was centrifuged at x270 g for four minutes at room temperature. The supernatant was discarded and the pellet was resuspended with α-MEM supplemented with 10% (v/v) foetal calf serum (FCS) and 1% (v/v) penicillin/streptomycin (P/S) and passed through a 70 μm filter to remove larger debris. The filtered cell suspension is then plated in a tissue culture flask at appropriate densities. Cells are then cultured under standard condition (humidified, 37 $^{o}$C with 5% $CO_2$) for four to five days before first PBS wash and media change. PBS wash and Media change is then carried out every three to four days until 95% confluence.

### 2.2.2 Isolation and Culture of Foetal Femur-Derived Cells

Human foetal tissue was obtained with informed and written consent from women undergoing termination of pregnancy procedures according to guidelines issued by the Polkinghorne Report. Ethical approval was obtained from the Southampton & South West Hampshire Local Research Ethics Committee (LREC 296100). Foetal femur samples at 7-12 weeks post conception were isolated from foetuses provided by Professor Neil Hanley and Professor David Wilson of Human Genetics Division, University of Southampton. Surrounding skeletal muscle and connective tissues were removed from the collected foetal femur samples by rolling the sample on filter paper and careful dissection. Depending on the experimental requirement, foetal femur samples might be processed as whole or separated into epiphysis and diaphysis sections by division at the metaphysis regions. Femurs were plated into a well of a 6-well plate overnight in 2 ml α-MEM containing collagenase B. The cell suspension was then passed through a 70 μm filter, centrifuged at x270 g for four min and suspended in α-MEM supplemented with 10% (v/v) FCS and 1% (v/v) P/S. Cells were maintained in monolayer culture under standard condition until 95% confluence prior to cell passage. Foetal age was determined by measuring foetal foot length and described as weeks post conception (WPC) (Table 1).

| Foetal foot length (mm) | Days post conception (DPC) | Weeks post conception (WPC) |
|---|---|---|
| 3.75 | 52 | 7.5 |
| 4.0 | 53 | 7.5 |
| 4.5 | 54 | 7.5 |
| 5.0 | 55 | 7.5 |
| 5.5 | 56 | 8.0 |
| 6.0 | 59 | 8.5 |
| 6.5 | 61 | 8.5 |
| 7.0 | 63 | 9.0 |
| 7.5 | 65 | 9.0 |
| 8.0 | 68 | 9.5 |
| 8.5 | 70 | 10.0 |
| 9.0 | 72 | 10.0 |
| 9.5 | 73 | 10.5 |
| 10.0 | 77 | 11.0 |

**Table 2.2. Foetal age in days and weeks post conception determined by foetal foot length measurement.**

For STRO-1 positive SSC isolation, whole foetal femurs were cut into small segments and collagenase B digested overnight in preparation for STRO-1 immunoselection. Individual isolated cells were passed through a 40 µm sieve (BD Biosciences) to remove large clumps and mineralised bone collar, and resuspended in basal medium (α-MEM, 10% foetal calf serum (FCS, Invitrogen), penicillin (100 U/mL) and streptomycin (0.1 mg/mL,)). Cells were initially incubated with blocking buffer (α-MEM, 10% human serum, 5% FCS and 1% bovine serum albumin (BSA, PAA Laboratories)) before incubation with primary STRO-1 antibody (undiluted hybridoma culture supernatant). Cell suspensions were subsequently washed three times in isolation buffer (2 mM ethylenediaminetetraacetic acid (EDTA) and 1% BSA in phosphate buffered saline (PBS)) before incubation with magnetic bead-conjugated secondary antibody (200 µL in 1 mL isolation buffer, Miltenyi Biotec). Samples were then washed and target cells isolated by magnetic-activated cell sorting (MACS) prior to suspension and culture in basal medium.

### 2.2.3 Cell Passage

After the culture medium was removed, monolayer cells were washed with PBS twice to remove debris and remaining media. Cultured cells were then incubated in 1X trypsin-EDTA solution under standard culture condition for 5 mins to break down adhesion proteins, releasing cells from tissue culture plastic. αMEM containing 10% (v/v) FCS was added to the resultant cell suspension to deactivate trypsin. The cell suspension was transferred to a sterile tube and centrifuged at x270 g for four min. The supernatant was discarded and cells were suspended in αMEM containing 10% (v/v) FCS for use in experiments, or in FCS containing 10% (v/v) DMSO for cryogenic storage at -80 $^{o}$C.

### 2.2.4 3D Pellet Formation and Organotypic Culture

Cells were isolated from foetal femur as previously described in section 2.2.2. Cells were expanded in monolayer culture until 90% confluence and passage as described in section 2.2.4. A cell count was performed and a cell suspension containing $1.25x10^5$ cells/ml of αMEM supplemented with 10% (v/v) FCS was prepared. 2 ml of the cell suspension was added to each 10-ml Falcon tube ($2.5x10^5$ cells) and a pellet was formed by centrifugation at x270 g for 4 min. The resulting pellet was incubated in standard culture conditions (humidified, 37 $^{o}$C with 5% $CO_2$) for 48 hours to allow formation before transfer to organotypic culture on polytetrafluoroethylene (PTFE) confetti membranes (BioCell Interface) on tissue culture flask-well inserts. Organotypic pellets were cultured for 21 days in either basal, osteogenic or chondrogenic medium as described in section 2.2.4. After 21 days, pellets were prepared for histological analysis or for RNA extraction and subsequent RT-qPCR analysis as described in section 2.3 and 2.5 respectively.

### 2.2.5 Micromass Culture

2.5 x $10^5$ cells per micromass were suspended in 10-20 µL basal medium, pipetted carefully into a 6-well plate and incubated for 1 hour, allowing attachment to the plate and cell/cell adhesion. Basal medium was removed and chondrogenic medium (α-MEM, 10 nM Dex, 100 µM Asc, 10 ng/mL TGFβ-3 (Peprotech) and 10 µg/mL insulin (in the form of 100x insulin/tranferrin/sodium selenite (ITS)) solution) was carefully added so as not to disturb the micromass. After 21 days, cultures were fixed in 4% (w/v) PFA and stained with Alcian blue (0.5% (w/v) in acidic $H_20$ (0.01% acetic acid)).

### 2.2.6 Differentiation Media

To encourage SSCs to differentiate down chondrogenic, adipogenic and osteogenic linages, culture media was supplemented with different combinations of soluble factors. For chondrogenic

conditions, cells were cultured in α-MEM containing 10% (v/v) FCS, supplemented with 100 µM ascorbic-2-phosphate, 10 nM dexamethasone, 10 µl/ml 100x Insulin-transferrin-sodium selenite solution (ITS solution) and 10 ng/ml TGF-β3. To promote adipogenic differentiation, confluent cell cultures were treated with appropriate media containing 10% (v/v) FCS, 1 µM dexamethasone, 10 µl/ml 100x ITS solution, 0.5 mM 3-isobutyl-1-methylxanthine (IBMX) and 100 µM indomethacin. Finally, supplementing culture media with 100 µM ascorbic-2-phosphate and 10 nM dexamethasone enhances osteogenic differentiation.

## 2.3 Histological Analysis

### 2.3.1 Samples Fixation and Sectioning

Foetal femur and cell pellets were washed in PBS and incubated in 4% (w/v) paraformaldehyde in PBS overnight for fixation. For monolayer culture, samples were washed with PCS and fixed by adding 90% (v/v) ethanol for 15 min. Whole foetal femurs and cell pellet samples were processed through graded ethanol (90% and 100%) for 30 min each after fixation. Then immersed in 50% (v/v) chloroform/ethanol and 100% (w/v) chloroform twice for 30 min. Samples were then soaked in paraffin wax at 60 $^{o}$C for 30 min to allow full penetration of paraffin wax. Finally, the samples were embedded in paraffin wax blocks. Sectioning was performed on a Microm 330 at 7 µm and the cut sections were transferred to a pre-heated glass slide. Prior to staining, the samples were processed through histoclear solution twice to remove paraffin wax and rehydrated by a 2 mins immersions in four reverse-graded methanol solutions (100%, 100%, 90% and 50%).

### 2.3.2 Live/Dead Staining

To examine cell viability, the following stains were added to samples prior to fixation: Cell Tracker Green™ (5 chloromethylfluorescein diacetate), which labels metabolically active cells green, and ethidium homodimer-1, which labels necrotic or damaged cells red. 20 µl of absolute ethanol was used to dissolve 50 µg of cell tracker green and subsequently added to 5 ml of plain medium along with 25 µg of ethidium homodimer-1. The mixture was added to cell cultures and incubated under standard conditions for one hour. After incubation, the staining mixture was removed and cell cultures were rinsed in PBS twice to remove any residual staining solution. Finally, samples were fixed in 90% (v/v) ethanol for 15 min before being re-immersed in PBS for microscopy.

### 2.3.3 Alcian Blue/ Sirius Red Staining

To allow visualization of cell nuclei, Weigert's haematoxylin solution was prepared and added to rehydrated samples for 10 min. Excess staining solution was then removed with water and acid alcohol. To stain for proteoglycans, samples were immersed in 0.5% (w/v) Alcian blue 8GX solution for 10 min, followed by a water rinse. Samples were then placed in 1% (w/v) molybdophosphoric acid for 20 min, followed by one hour incubation in 0.1% (w/v) Sirius red F3B solution to stain for collagen. Slides were rinsed thoroughly with water and dehydrated in revers-graded methanol back into histoclear before mounting in dibutyl phthalate xylene (DPX).

### 2.3.4 Alkaline Phosphatase Staining

To assess alkaline phosphatase activity, samples were fixed in 90% (v/v) ethanol as described in section 2.3.1. A staining solution was prepared by adding 4% (v/v) Napthol AS-MX phosphate and 0.024% (w/v) Fast Violet B salt to water. After staining solution was added, samples were incubated under standard culture conditions for up to 60 min. The reaction was terminated by rinsing cells with distilled water and air-drying them for microscopy.

### 2.3.5 Von Kossa Staining

Slides were de-waxed and rehydrated as described in section 2.3.1 before treatment with 1% (w/v) silver nitrate solution and placed under ultra-violet light (U.V.) irradiation for 20 min followed by rinsing in distilled water. Slides were then treated with 2.5% (w/v) sodium thiosulfate for 8 min. then rinsed once more. A counterstain was then performed with Alcian blue for 1 min and van Gieson for 5 min. Finally, the slides were dehydrated through graded alcohols, starting at 90% (v/v) methanol, placed through histoclear and mounted in DPX. Deposits of calcium or calcium salt could then be visualized with pink sections of the slide stain osteoid and brown/black colour highlighting mineralized matrix.

### 2.3.6 Goldner's Trichrome Staining

Slides were processed through histoclear solution twice to remove paraffin wax and rehydrated by 2 min immersions in four reverse-graded methanol solutions (100%, 100%, 90% and 50%), then treated with haematoxylin for 10 min and washed in distilled water. Samples were then placed in 0.5% (w/v) acid alcohol for 10 seconds followed by washing in running water for 20 min. Slides were then treated with 10% (v/v) ponceau-fuchsin (0.75% (w/v) and 0.25% (w/v), respectively in 1% acetic acid) and 2% (v/v) azophloxin solution (0.5% (v/v) in 0.6% acetic acid) in acetic acid (0.2% in $dH_2O$) treated for 5 min then rinsed in 1% acetic acid for 10 seconds. Slides were subsequently

placed in 0.6% (w/v) phosphomolybdic acid and 0.4% (w/v) orange G solution in distilled water with thymol for 20 min before counterstaining with 0.2% (w/v) light green solution in 0.2% (w/v) acetic acid. Stained sections were blotted dry and directly mounted with DPX. Nuclei are shown in blue/black, mineralized bone stains green and Osteoid/collagen stains red.

### 2.3.7 Immunocytochemistry

After removal of excess wax and rehydration as described in section 2.3.1, samples were treated with 3% (v/v) hydrogen peroxide ($H_2O_2$) solution for 5 min to exhaust endogenous peroxidase activity and blocked with 1% (w/v) bovine serum albumin (BSA) in PBS for 30 min. The sections were then incubated with relevant primary antibody overnight at 4 $^{o}$C. Negative controls were performed by replacing the primary antibody with 1% (w/v) BSA in PBS. For SOX9 immunocytochemistry staining, the protein cross-links that could mask the antigen/epitope in paraffin-embedded sections must be broken prior to incubation with primary antibody. This is achieved by boiling the sections in 0.01 M citrate buffer solutions for 5 min using a microwave oven. Following incubation, residual primary antibodies were removed by rinsing samples in water and wash buffer (0.1% (v/v) tween in PBS) for 5 min. The sections were then incubated in the appropriate biotin-linked secondary antibody for one hour. Samples were rinsed and incubated for 30 min in ExtrAvidin peroxidase solution. Antibody binding was developed using 3-amino-9-ethyl-cardazole (ACE) in acetate buffer containing $H_2O_2$ to yield a reddish-brown reaction product. Slides were washed in water bath and counterstained in Alcian blue for one minute before final wash and being mounted with crystal mount.

### 2.3.8 MicroRNA *In Situ* Hybridization

Solutions and buffers used for *in situ* hybridization were made with the following recipes. For 1 liter of 20x saline sodium citrate (SSC solution): 175.3 g sodium chloride (NaCl) is combined with 88.2 g of sodium citrate and dissolved in ultra-pure water (up$H_2O$). The pH of the solution is then adjusted with hydrochloric acid (HCl) and the volume is adjusted to 1 L with up$H_2O$. To make 100 ml of 50x Denhardt's Solution: 1 g of Ficoll 400, 1 g of Polyvinilpyrolidone and 1 g of bovine serum albumin is added to 100 ml up$H_2O$, mixed using a magnetic stirrer for 30 min and then filter sterilized. Phosphate-buffered saline with Tween (PBST) is made by combining 49.5 ml of sterile PBS with 500 µl of Tween-20. To make 10 ml of blocking solution, 200 µl of normal goat serum is mixed with 20 mg of bovine serum albumin (BSA) and 9.4 ml of PBST. Denaturing solution is made by combining 10 ml of formamide with 5 ml of 20x SSC solution, 2 ml of 50x Denhardt's solution, 250 u(l of yeast RNA, 500 µg of salmon sperm DNA, 500 µl of 10% (v/v) CHAPS, 100 µl of 20% (v/v) Tween-20 and 400 µg of blocking reagent (Roche). Solution B1 is made by combining 100 ml 1-M

TRIS (pH 7.5) with 30 ml of 5-M NaCl and made up to 1 L with up$H_2O$. For pre-hybridization solution: 10 ml of formamide is combined with 5 ml of 20x saline sodium citrate (SSC), 2 ml of 50x Denhardt's solution, 250 µl of yeast RNA (Stock 20mg/ml), 1000 µl of salmon sperm DNA (Stock 500 µg/ml), 500µl l % (v/v) CHAPS, 100 µl 20% (v/v) Tween-20 and 400 mg of blocking reagent in 1150 µl RNase free water. Finally, development solution is made by combining 24.08 mg tetramisole hydrochlrode, 5 ml of 1 M Tris-HCl (pH 9.5), 2.5 ml 1-M magnesium chloride, 1 ml of 5-M NaCl and 500 µl 10% (v/v) Tween made up to 50 ml with up$H_2O$. All solutions are either filter sterilized or autoclaved to ensure sterility and absence of RNase.

Freshly-prepared foetal femur samples were placed in sterile 2 ml glass vials and fixed with sterile 4% (w/v) PFA in PBS for 4 hours followed by a three-time washing with PBS. Foetal femur samples were immersed in acetylation solution followed by washing in PBS for 5 min then incubated in 10 ml PBS containing 2 µg of protease K (Roche) for 30 min. Samples were then washed with PBS three times before incubating in pre-hybridization solution for 5 hours. The pre-hybridization solution was then poured off and replaced with hybridization probe mix containing 20 mM of ISH Probe then incubated in the hybridization oven at 60 $^{o}$C overnight. After incubation in hybridization probe mix, samples were washed with 5x SSC solution, followed by incubation in 0.2x SSC for 1 hour. 0.2x SSC solution was removed and replaced with B1 solution (TRIS-Saline solution) and incubated in RT for 1 hour. B1 solution was replaced with blocking solution and samples were incubated in RT for 1 hour. Antibody solution containing Anti-DIG antibody was then added to samples and incubated overnight at 4 $^{o}$C. Finally, for colour development, NBT/BCIP solution was added to the development solution before adding it to the samples. Samples were incubated in the dark until colour reaction intensified. Washing in PBS-T three times stopped the colour reaction. Samples were photographed as soon as possible using a Canon G10 camera.

### 2.3.9 Image Capture and Analysis

Images of samples were captured using a Zeiss Axiovert 200 inverted microscope running Zeiss Axiovision software version 4.7. Light microscopy images were taken using an Axiocam HR camera, and fluorescent images were captured using an Axiocam MR camera.

## 2.4 Transfection Protocols

### 2.4.1 Synthesis of Spermine-Introduced Pullulan Complex

To produce spermine-introduced pullulan complex (spermine-pullulan) suitable for oligonucleotide transfection, pullulan with a molecular weight of 47,300 g was used. Spermine was introduced to the hydroxyl groups of pullulan molecule using N,N'-carbonyldiimidazole (CDI) activation method (Figure 2.2). 2.95 ml of spermine and 216.6 mg of CDI were added to 50 ml of dehydrated DMSO containing 50 mg of pullulan. The reaction mixture was then agitated at 35 $^{o}$C for 20 hours using a magnetic stirrer. The resultant mixture was dialyzed against up$H_2O$ for 48 hours through a dialysis membrane with a molecular weight cut-off of 12,000-14,000 g. After dialysis, the solution was freeze-dried to obtain a dried sample of spermine-pullulan. The degree of spermine introduction was then determined from conventional elemental analysis expressed by molar percentage of spermine introduced to the hydroxyl group of pullulan.

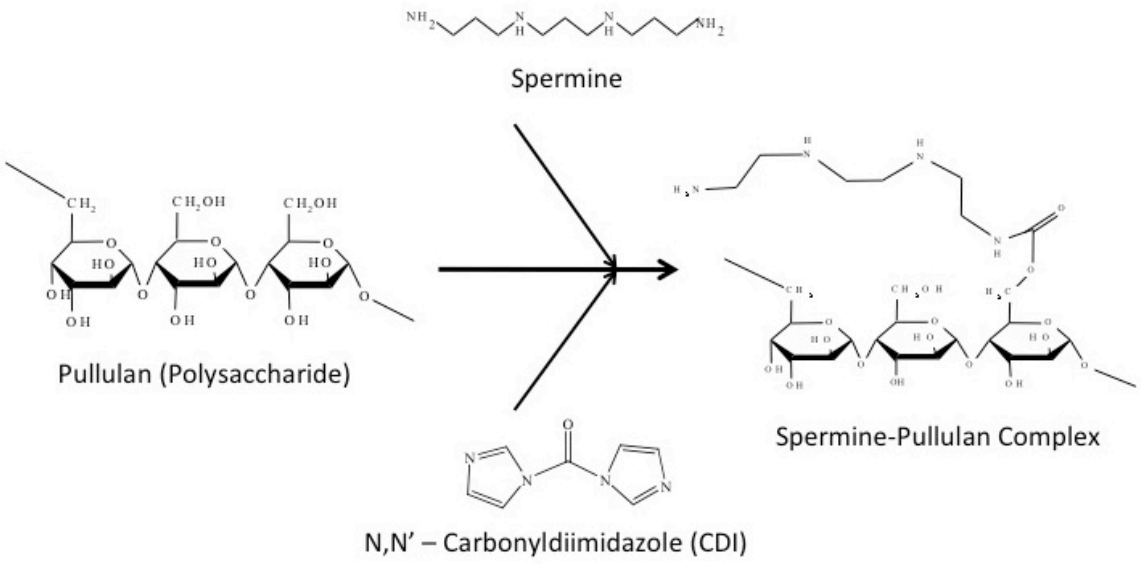


**Figure 2.1. Summary of chemical reaction involved in the production of spermine-pullulan complex**

### 2.4.2 Spermine-Pullulan Transfection

A stock aqueous solution of spermine-pullulan was prepared by adding 4 mg of dried spermine-pullulan to 1 ml of up$H_2O$. An appropriate amount of spermine-pullulan stock solution was then diluted in 100 µl of up$H_2O$ to give a working solution and mixed with 100 µl of PBS containing 40 pmol of oligonucleotide. The mixture was vortexed for 15 seconds and allowed to stand for 15 min to obtain polyion complexes for transfection. Cell samples were passaged as described in section

2.2.3. A cell count was performed and a cell suspension containing 50,000 cells/ml of media supplemented with 10% (v/v) FCS was prepared. 2 ml of the cell suspension was added to each well in a six-well plate and incubated under standard culture conditions until the monolayer culture reached 80% confluence (typically for 24-48 hours). Once ready for transfection, the culture medium was removed and the cells were washed with PBS twice to remove any residual medium containing FCS. 2 ml of plain medium was then added to the cells and incubated under standard conditions for 30 min. The prepared polyion complexes were then added to the culture and incubated under standard conditions for 3 hours. 1 ml of FCS was added to the culture and the samples were incubated for a further 1 hour. The medium containing polyion complexes was then removed and replaced with appropriate medium supplemented with 10% (v/v) FCS and 1% (v/v) P/S.

### 2.4.3 MicroRNA Transient Overexpression Using Lipofection

Cells were extracted from foetal femur samples and passaged as previously described in section 2.2.2 and 2.2.3. Following cell passage, a cell count was performed and a $5x10^4$ cell/ml stock was made. 500 µl of cell suspension containing $2.5x10^4$ cells was added to each well of a 24-well plate and culture under basal conditions for 48 hours to allow cell adhesion and proliferation. For transfection, a miRNA mimic working solution was prepared by adding 10 µl of 50 µM miRNA mimic stock solution to 240 µl up$H_2O$ to give a solution containing 2 µM miRNA mimic. For each well, 25 µl of 2 µM mimic solution was added to 25 µl of plain medium and allowed to stand in RT for 5 min (mimic mix). A second solution was prepared by adding 5 µl of Dharmafect 1 to 45 µl of plain medium and being left to stand in RT for 5 min (liposome mix). The mimic mix was then combined with the liposome mix, mixed by gentle pipetting, and allowed to complex for 20 min in RT. 400 µl of medium containing 10% (v/v) FCS was added to the liposome-miRNA complex mixture to produce the transfection solution. Cells were rinsed with PBS twice and the transfection solution was added to the cells. 48 hours following transfection, cells were fixed using 4% (w/v) PFA for microscopy or prepared for RNA extraction and subsequent RT-qPCR analysis as described in section 2.5. For western blot analysis, cells were lysed for protein extraction 72 hours following transfection.

## 2.5 Molecular Analysis

### 2.5.1 RNA Extraction

RNA extraction was performed using a mirVana™ RNA Isolation System Kit according to the manufacture's protocol. Briefly, cultured samples were placed on ice and washed twice in PBS. For monolayer culture, 500 µl of the supplied lysis buffer was added to the sample, followed by incubation on ice for 15 min to allow cell lysis before the lysate was transferred to a molecular-grade eppendorf. For pellet culture, the pellet along with the attached confetti were transferred to an eppendorf containing 500 µl of lysis buffer and incubated on ice for 30 min. 50 µl of miRNA homogenizing agent was added to each sample, mixed by vortex and incubated on ice for a further 10 min. 500 µl of acid phenol-chloroform solution was then added to the lysate, mixed by vortex and spun at x15682 g for 10 min to separate the organic phenol layer from the inorganic aqueous layer containing total RNA. The aqueous phase was transferred to a new eppendorf and absolute ethanol was added at 1.25x the aqueous phase volume. The mixture was then passed through the supplied column by centrifugation at x9278 g. The column embedded with RNA was then washed with 700 µl of miRNA wash solution followed by two washes with 500 µl of RNA wash solution. Total RNA was then eluted in up$H_2O$ at 90 $^oC$. The extracted RNA samples were stored at -80 $^oC$ until needed, or used immediately for cDNA synthesis.

### 2.5.2 cDNA Synthesis (*mRNA*)

cDNA was produced using a SuperScript®VILO cDNA Synthesis Kit. Between 150-500 ng of RNA was dissolved in 7 µl of up$H_2O$. 2 µl of the supplied 5X VILO™ reaction mix and 1 µl of 10X SuperScript® enzyme mix was added to the RNA sample. The mixture was then incubated at 25 $^oC$ for 10 min followed by 42 $^oC$ for 2 hours. The reaction was terminated by 5 min incubation at 85 $^oC$. 40 µl of up$H_2O$ was then added to the cDNA sample to give a 1:4 dilution and stored at -20 $^oC$ or used immediately for quantitative RT-PCR analysis.

### 2.5.3 Quantitative RT-qPCR (*mRNA*)

Quantitative RT-PCR was performed using SYBR-Green PCR master mix: 10 µl of SYBR-Green master mix; 5 µl of up$H_2O$; 2 µl of forward and reverse primers for the gene of interest (details summarized in table 2.2) and 1 µl of cDNA sample. The final mixture (20 µl) was added to each well of a 96-well-plate, then loaded into the Applied Biosystem (Life Technology, USA), 7500 Real Time PCR system for reaction run. The initial holding stages were 50 $^oC$ for 2 min then 95 $^oC$ for 10 min. The cycling stage (n=40) consisted of a 15-second denaturing step at 95 $^oC$ followed by a 1-minute

annealing/extension step at 60$^{o}$ C. A dissociation stage (95 $^{o}$C for 15 seconds, 60 $^{o}$C for 1 minute and 95 $^{o}$C for 15 seconds) then followed to assess the quality of the PCR product. All reactions were performed in triplicate and included a negative control lacking cDNA. The data was analyzed using the Applied Biosystem 7500 System SDS Software, version 2.0.5 program. Ct value for each sample was normalized to *β-ACTIN*, an endogenous housekeeping gene known to be expressed at a stable level in SSCs, and fold expression levels for each target gene were calculated using the delta-delta Ct (crossover threshold) method. For quality control, a minium Ct value of 22 is required for the housekeeping gene to calculate the delta-delta Ct of genes examined.

| Gene | Primer sequences | Amplicon size |
|---|---|---|
| Human $\beta$- *ACTIN* | F: 5’ ggc atc ctc acc ctg aag ta 3’<br>R: 5’ agg tgt ggt gcc aga ttt tc 3’ | 82 bp |
| Human *RUNX-2* | F: 5’ gta gat gga cct cgg gaa cc 3’<br>R: 5’ gag gcg gtc aga gaa caa ac 3’ | 78 bp |
| Human Osterix | F: 5’ atg ggc tcc ttt cac ctg 3’<br>R: 5’ ggg aaa agg gag ggt aat c 3’ | 75 bp |
| Human *ALP* | F: 5’ gga act cct gac cct tga cc 3’<br>R: 5’ tcc tgt tca gct cgt act gc 3’ | 86 bp |
| Human *COL1A1* | F: 5’ gag tgc tgt ccc gtc tgc 3’<br>R: 5’ ttt ctt ggt cgg tgg gtg 3’ | 52 bp |
| Human *COL2A1* | F: 5’ cct ggt ccc cct ggt ctt gg 3’<br>R: 5’ cat caa atc ctc cag cca tc 3’ | 58 bp |
| Human *COL10A1* | F: 5’ ccc act acc caa cac caa ga 3’<br>R: 5’ gtg gac cag gag tac ctt gc 3’ | 95 bp |
| Human Osteonectin | F: 5’ gag gaa acc gaa gag gag g 3’<br>R: 5’ ggg gtg ttg ttc tca tcc ag 3’ | 95 bp |
| Human Osteocalcin | F: 5’ ctc aca ctc ctc gcc cta tt 3’<br>R: 5’ gct cac aca cct ccc tcc tg 3’ | 211 bp |
| Human *SMAD3* | F: 5’ tga atc cct acc act acc aga g 3’<br>R: 5’ gga tgg aat ggc tgt agt cg 3’ | 117 bp |
| Human *SMAD2* | F: 5’ gat cct aac aga act tcc gcc 3’<br>R: 5’ cac ttg ttt ctc cat ctt cac tg 3’ | 146 bp |
| Human *SOX9* | F: 5’ ccc ttc aac ctc cca cac ta 3’<br>R: 5’ tgg tgg tcg gtg tag tcg ta 3’ | 74 bp |
| Human Nucleostemin | F: 5’ ggg aag ata acc aag cgt gtg 3’<br>R: 5’ cct cca aga agt ttc caa agg 3’ | 98 bp |
| Human *CD63* | F: 5’ gcc ctt gga att gct ttt gtc g 3’<br>R: 5’ cat cac ctc gta gcc act tct g 3’ | 87 bp |
| Human *ALCAM* | F: 5’ acg atg agg cag acg aga taa gt 3’<br>R: 5’ cag caa gga gga gac caa caa c 3’ | 96 bp |

**Table 2.2. Forward and reverse primers used for RT-PCR**

### 2.5.4 MicroRNA Expression Analysis

MicroRNA expression was interrogated using TaqMan® miRNA Assays (Applied Biosystem, Life Technology). Each assay is comprised of two primers, one for cDNA synthesis and the other for TaqMan RT-PCR. cDNA specific to each assay-specific miRNA was generated using a TaqMan® MiRNA Reverse Transcription Kit from total RNA using a modified manufacturer's protocol. In brief, a reaction mixture containing 50 mM dNTPs, 25 units of Mutiscribe™ RT enzyme, 0.75 µl 10x buffer, 1.88 units of RNase inhibitor, 3.58 µl up$H_2O$, 1.5 µl of primer and 10 ng of total RNA was made. The reaction mixture was then mixed by pipetting and incubated at 16 $^{o}$C for 30 min followed by 42 $^{o}$C for 30 min. The reaction was then terminated by an incubation of 5 min at 85 $^{o}$C. The cDNA sample was stored at -20 $^{o}$C if not used immediately for RT-PCR analysis.

For RT-PCR reaction, TaqMan® Universal PCR Master Mix with No AmpErase® UNG was used. A reaction mixture containing 5 µl TaqMan master mix, 3.335 µl of up$H_2O$, 0.5 µl of RT-PCR primer and 0.7 µl of cDNA was made. The mixture was then transferred into a well of a 96-well plate and loaded into the Applied Biosystem (Life Technology, USA), 7500 Real Time PCR system for reaction run. All reactions were performed in duplicate and included a negative control lacking cDNA. The data was analyzed using the Applied Biosystem 7500 System SDS Software, version 2.0.5 program. Ct value for each sample was normalized to MammU6, an endogenous control for miRNA, and fold expression levels for each target gene were calculated using the delta-delta Ct (crossover threshold) method.

### 2.5.5 MicroRNA Arrays

RT-PCR miRNA arrays were performed using the TaqMan® Low Density Array system. cDNA was generated using Megaplex™ RT Primers Human Pool A v2.1 kit. Briefly, 400 ng of total cellular RNA was combined with 10X RT Buffer, 25x dNTP, Megaplex™ RT primers, Mutiscribe™ RT enzyme, RNase inhibitor and magnesium chloride. The reaction mixture was placed in a thermocycler and underwent 40 cycles of 16 $^{o}$C for 2 min, 42 $^{o}$C for 1 minute and 50 $^{o}$C for 1 second. The reaction was then terminated at 85 $^{o}$C for 5 min. The cDNA sample was combined with TaqMan® Universal PCR Master Mix and up$H_2O$ and loaded into the array card. The card was placed into an Applied Biosystem 7900 System for the reaction run. The generated data was then analyzed using Sequence Detection System Enterprise Edition v2.4 (Applied Biosystem). Relative expression of all the miRNAs detected was calculated using the delta-delta Ct method. MammU6, RNU44 and RNU48 were proposed reference miRNA according to manufactor protocol. Of these, MammU6, was found to be the most stably expressed miRNA in SCCs and was chosen as the endogenous control.

### 2.5.6 Western Blot Analysis

Cells were lysed with RIPA buffer (750 mM NaCl, 5% (w/v) IgePal CA-630, 2.5% (w/v) DOC, 0.5% (w/v) (SDS, 250 mM Tris (pH 8.0)) supplemented with a protease inhibitor cocktail (1:100; Sigma). Cell lysates were centrifugation at x270 g for 20 min at 4 $^{o}$C, and the supernatant collected. Protein concentration was determined using Pierce BCA protein Assay Kit (Pierce). 20 µg of each sample, combined with DTT (Cell Signaling) and SDA sample buffer (BioLabs), was analysed by SDS gel electrophoresis using Any kD precast gels (Mini-PROTEAN TGX; Bio-rad) and transferred onto a polyvinylidene fluoride (PVDF) immobilon-FL transfer membrane (Millipore). Immunoblots were probed with *SMAD3* and *SMAD2* antibody (1:1000; Cellsignalling), then with anti-*β-ACTIN*-Peroxidase (1:10000; Sigma). IRDye 800CW goat anti-rabbit (LI-COR Biosciences) and IRDye 800CW rabbit anti-HRP (LI-COR Biosciences) were used as secondary fluorescent antibodies respectively. The anti-*β-ACTIN*-Peroxidase was used as loading control to which protein expression across the membrane was normalized. The blots were scanned individually on an Odyssey Infrared Imaging System (LI-COR Biosciences), and densitometry analyses were run calculating the signal intensity ratio between samples and loading control. Image Studio software (LI-COR, Biosciences) was employed to obtain the signal intensity values, which were transformed into percentages of intensity for the statistical analysis.

## 2.6 Statistical Analysis

Statistical analysis was carried out using Student's t-test or One-way Analysis of Variance (ANOVA) with Tukey-Kramer multiple comparison post-test using the statistics software integrated into GraphPad software version 3.05. Values were expressed as mean ± standard deviation. All experiments were performed using at least three separate samples unless other stated. $p \leq 0.05$ were considered statistically significance.

# Chapter 3: Characterisation of Foetal Femur Cell Populations

## 3.1 Introduction

Adult bone marrow stromal cells (HBMSCs) contain a diminutive bone stem cell population (1 in 10,000 to 50,000) often referred to as mesenchymal stem cells (MSCs). A number of studies have shown that HBMSCs are capable of generating tissues within the skeletal system, namely bone, cartilage, fat, ligament, muscle and tendon. Since these "mesenchymal stem cells" have only been shown to reliably differentiate into cells from the musculoskeletal system, the term skeletal stem cells (SSCs) will be applied to restrict the description to stem cells from bone able to generate all skeletal tissue (Bianco et al. 2008).

Conventional SSC populations are found in the bone marrow as first described by Friedenstein *et al* in 1966 (Friedenstein et al. 1966). However, conventional SSC populations are highly heterogeneous and as a result, there remains significant controversy over their exact identity and differentiation potential. The observed heterogeneity is likely a consequence of their derivation from a multitude of adult tissues, including adipose tissue, muscle, placenta, and umbilical cord blood (Tare et al. 2008). This highlights the need for a robust *in vitro* clonal analysis of exact differentiation capacity given heterogeneity and the lack of clear markers for SSC populations impacts on the aplication of SSCs in clinical applications.

An alternative cell source to adult tissue is foetal tissue. Foetal tissue has been shown to contain cell populations with comparable if not enhanced reparative function (Mirmalek-Sani et al. 2006; Mirmalek-Sani et al. 2009). Furthermore, foetal-derived cells are thought to be less immunogenic and tumorigenic, particularly in foetal cell populations extracted during the first trimester (Tuch 1988; Kirste et al. 1989). Foetal femurs are composed of proliferative osteochondral progenitor cells capable of self-renewal, differentiation, and most importantly bone and cartilage formation. A previous report by Mirmalek-Sani *et al* (Mirmalek-Sani et al. 2009; Mirmalek-Sani et al. 2006) has shown that whole foetal femur-derived cell populations may offer an alternative to adult HBMSC populations for tissue engineering applications, specifically for *in vitro* investigation of human skeletal development. The report from MIrmalek-Sani and colleagues indicated foetal cells displayed significantly enhanced proliferation and multi-lineage differentiation capacity. However, the heterogeneity of foetal femur-derived cell populations has not been explored. One surface marker which has been shown to reduce heterogeneity of SSC populations is the trypsin-resistant cell surface antigen 1 (STRO-1). Adult STRO-1 positive populations exhibit enhanced colony-forming

unit fibroblastic (CFU-F) capacity and elevated osteogenic differentiation both *in vitro* and *in vivo* in comparison to unsorted adult HSMSCs (Gronthos et al. 1994). Therefore, the STRO-1 surface marker could potentially be used to identify sub-populations of SSCs within the developing human foetal femur. Other markers have been used to characterise and identify SSC cell populations, namely CD105 (SH2/Endoglin), CD73 (SH3/4), CD44, CD90 (Thy-1), CD71, as well as the adhesion molecules CD106 (VCAM-1), CD166 (*ALCAM*), ICAM-1 and CD29; but a unique, specific single-cell surface marker that specifically identifies the SSC has, to date, remained elusive (Tare et al. 2008).

MicroRNAs (miRNAs) are a class of non protein-coding small RNA molecules of 21-25 nucleotides in length. Along with the RNA-induced-silencing complex (RICS), miRNAs act to regulate protein translation by inhibiting their target mRNAs' function (Pillai 2005). There is growing evidence to suggest miRNAs play an important role in a number of cellular processes including cell cycle and stem cell differentiation (N. Xu et al. 2009; Ivanovska & Cleary 2008). Various miRNAs have already been shown to play a role in SSC differentiation. A recent review by *Lian et al* summarised the effects of 42 miRNAs on osteoblast differentiation through targeting various cell-signalling pathways such as Wnt and TGF-β, transcription factors such as *RUNX2* and Osterix and epigenetic machineries such as histone deacetylase 5 (HDAC5) (Lian et al. 2012). Data gathered through proteomic approaches have demonstrated that a single miRNA can repress the translation of hundreds of proteins, however the effect of a single miRNA on protein translation is surprisingly small (D. Baek et al. 2008). Therefore, it can be difficult to determine how a single miRNA is able to provoke a detectable functional change.

In this chapter, the aim of the studies presented was to identify subpopulations of SSC within the foetal femur through histological analysis and STRO-1 immunostaining. The presence of distinct regional cell population with reduced heterogeneity displaying specific chondrogenic and osteogenic differentiation capacity will be examined. In addition, differentiation in the absence of supplements to promote specific lineage differentiation was examined.

Derivation of specific osteogenic and chondrogenic cell populations from foetal femur-derived SSCs, with retained capacity for self-renewal and differentiation into other lineages may be used as a cell source for tissue engineering applications. Furthermore, distinct regional cell populations could be used as a model to interrogate miRNA expression profiles during differentiation and identify novel miRNAs involved in SSC differentiation. Finally, miRNA expression profiles could act as a marker to identify or reduce the heterogeneity of skeletal stem cell populations.

### 3.1.1 Hypothesis

SSCs can be isolated from distinct regions of the developing foetal femur with defined and distinct differentiation capacity. Cells from the diaphyseal region, where mineralised bone first occurs in development, is predicted to posses enhanced osteogenic differentiation capacity while cells in the epiphyseal region is expected to have an increased affinity toward chondrogenic differentiation. MicroRNA expression profiling in the subpopulation of SSCs could potentially identify new miRNAs involving in skeletogenesis.

### 3.1.2 Aims and Objectives:

- To identify sub-populations of SSCs and their locality within the foetal femur and attempt to isolate sub-populations using micro-dissection techniques.
- To characterize the phenotype of cells from the epiphyseal and diaphyseal region of human foetal femur through histological and molecular analysis.
- To validate the stemness of epiphyseal and diaphyseal SSC populations by verification of stem cell marker expression and capacity to differentiate into osteogenic, chondrogenic and adipogenic lineages.
- To identify miRNAs involved in SSC osteogenic and chondrogenic differentiation using miRNA microarrays and to revalidate potential targets identified using TaqMan miRNA RT-qPCR assays.
- To analyse potential mechanisms of action of miRNA identified by predicting their miRNA targets.

## 3.2 Result

### 3.2.1 Isolation of Diaphyseal and Epiphyseal Foetal Femur Cell Population

To assess the difference in phenotype at different stages of development, human foetal femurs covering a range of development stages from 47 to 69 days post conception were fixed, sectioned and stained with Alcian blue and Sirius red. It was noted that with increasing age (expressed by days post conception), femurs increased considerably in size with the occurrence of key developmental events (Figure 3.1 A). High magnification images showed foetal femur samples were composed primarily of a cartilage anlage with a developing bone collar marked by type I collagen deposition, as evidenced by Alcian blue and Sirius red staining (Figure 3.1 B). Within the epiphyseal regions, cells were observed to be smaller and densely packed, while cells from the diaphyseal region displayed a hypertrophic phenotype (Figure 3.1B). Foetal femur samples available for the experimental work in this study ranged from 47 to 69 days post conception as calculated by measuring foetal foot length. At day 47, the femur was a predominantly cartilaginous anlagen with modest development of hypertrophic cells at the diaphyseal region (Figure 3.1B). By day 54, the development of a bone collar and periosteum became evident as evidenced by the Sirius red stain highlighting the type I collagen deposition within the diaphyseal region and the difference in phenotype between epiphyseal and diaphyseal cells became more distinct (Figure 1.1B). At day 69, the diaphyseal region of the femur displayed a relatively thick mineralized bone collar macroscopically and was more susceptible to fracture on sectioning. The cells found within the epiphyseal region of the femur remained small and densely packed throughout day 47 to day 69 (Figure 1.1B). These finding indicate the heterogeneity of cells within a developing foetal femur and suggest different cell phenotypes may be isolated from distinct locations within the foetal femur. Furthermore, cells isolated from the foetal femur at different developmental stages may have different differentiation potentials.

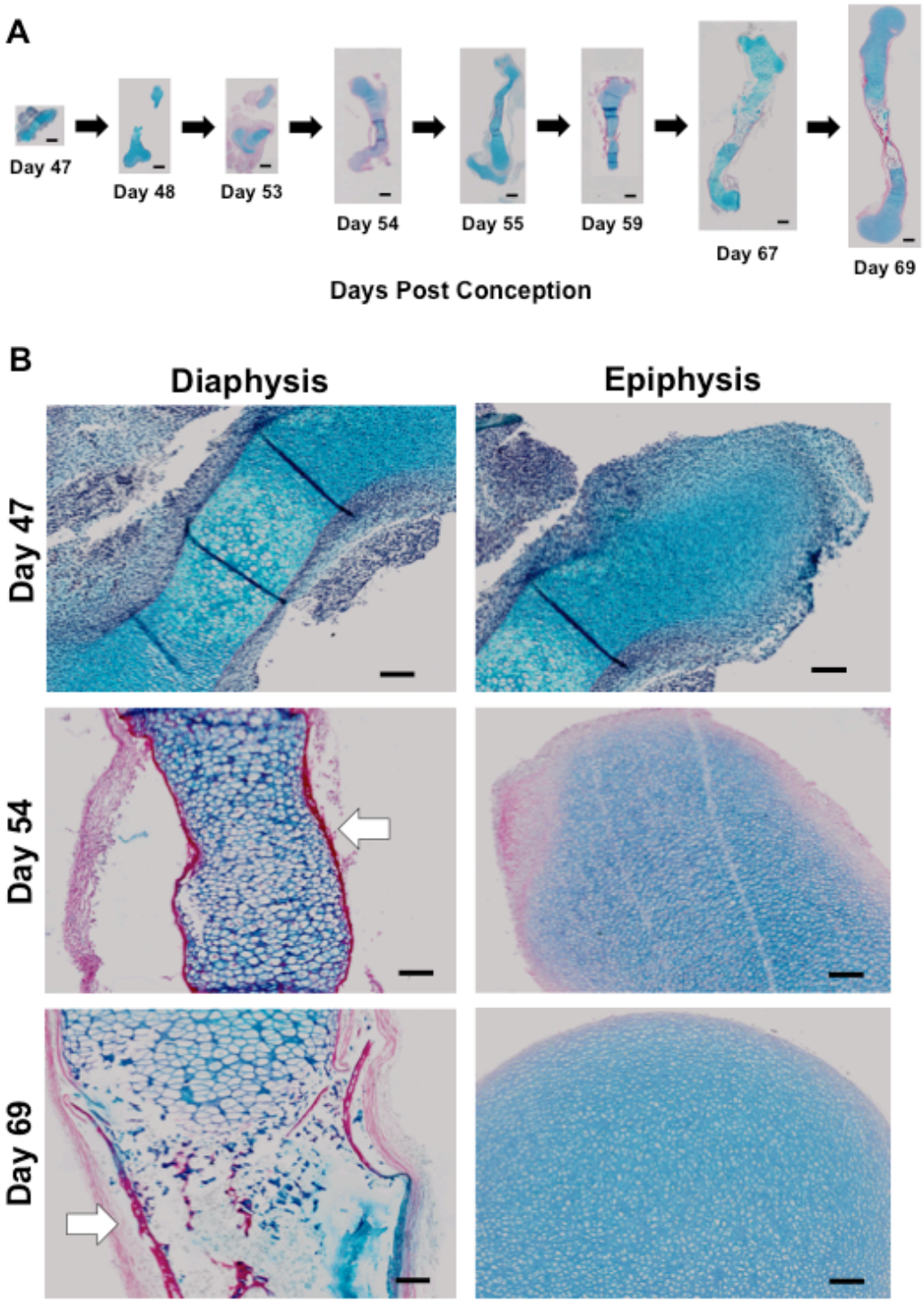


**Figure 3.1. Development of human foetal femurs and bone collar formation**. A) Human foetal femurs covering a range of developmental stages from 47 to 69 days post conception. Femurs increase significantly in size and exhibit both mineralisation and marrow cavity formation. B) High magnification images showing morphology of cells and formation of bone collar marked by arrows. Scale bars measure 100 µm (high magnification images) and 500 µm (low magnification images). (n=1)

### 3.2.2 Foetal Femur-derived Cells Contain STRO-1 Expressing Cells

Gronthos and co-workers found that the heterogeneity of the stromal cell population could be reduced by cell isolation using the monoclonal antibody STRO-1, which recognizes a trypsin-resistant cell surface antigen present on a subpopulation of adult bone marrow cells (Gronthos et al. 1994). However, STRO-1 expression in foetal femur-derived cells has not been examined in detail to date. To assess STRO-1 expression in developing human foetal femur samples, human foetal femurs covering a range of developmental stages; day 47 to 69 days post conception were fixed, sectioned and STRO-1 immuno-labelled (Figure 3.2). Early STRO-1 expression was observed around 47 days post conception, prior to bone collar formation (Figure 3.2). STRO-1 expression was noted to reduce by day 53. With the development of the bone collar, STRO-1 expressions was observed to recur and expression was observed in cells within the diaphyseal region until day 69 and within the epiphyseal region until day 61. Thus, temporal analysis across foetal developmental stages indicates STRO-1 expression follows a temporal and spatial pattern and may be associated with various developmental events.

To assess whether STRO-1-positive cells can be isolated from foetal femur tissue, foetal femurs were dissected and treated with collagenase and labelled with STRO-1 antibody and isolated using magnetic activated cell-sorting techniques as described in section 2.2.2 STRO-1+ cells could be enriched from whole human foetal femur cell populations and cultured *in vitro* in basal medium (Figure 3.3).

HBMSC is known to exhibit decreased STRO-1 expression following *in vitro* expansion. However, the expression of STRO-1 of HBMSC typically wanes within one passage. In comparison, foetal femur-derived cell populations maintained STRO-1 expression over multiple passages (Figure 3.3). STRO-1 positive cells were observed in culture over 5 passages. A significant reduction in STRO-1 expression was observed at passage 6 until loss of expression observed on passage 8 (Figure 3.3). This observation suggests STRO-1-enriched populations from foetal femur cells exhibit phenotype stability over several passages.

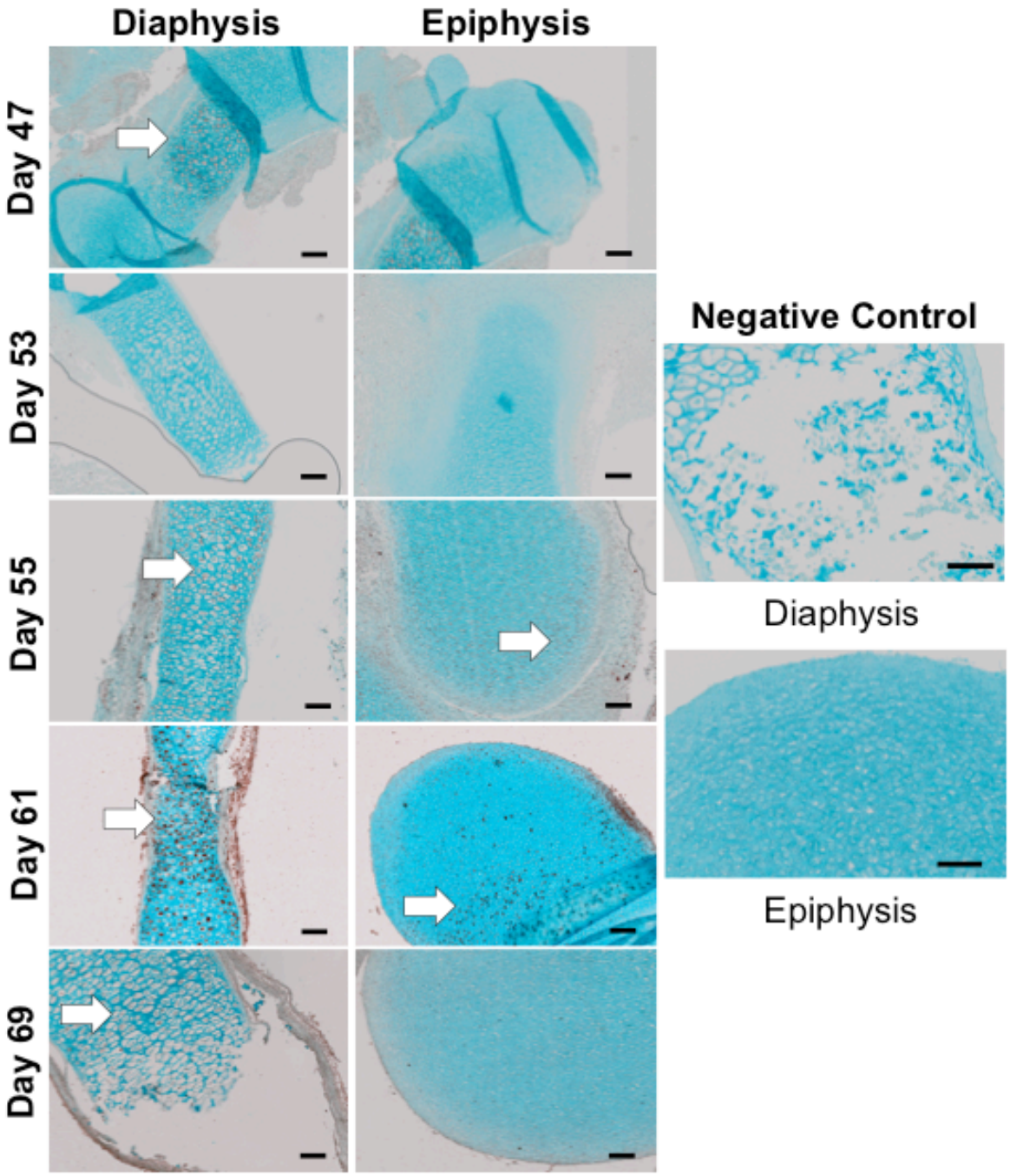


**Figure 3.2. Development of human foetal femurs and STRO-1 expression**. Human foetal femurs covering a range of developmental stages from 47 to 69 days post conception were fixed, sectioned and immunolabelled with STRO-1 antibody. STRO-1 expression (marked by arrows) appeared to be related to key developmental events and followed a distinct spatial pattern largely restricted to the diaphyseal region. Scale bars measure 100 µm (high magnification images). (n=1)

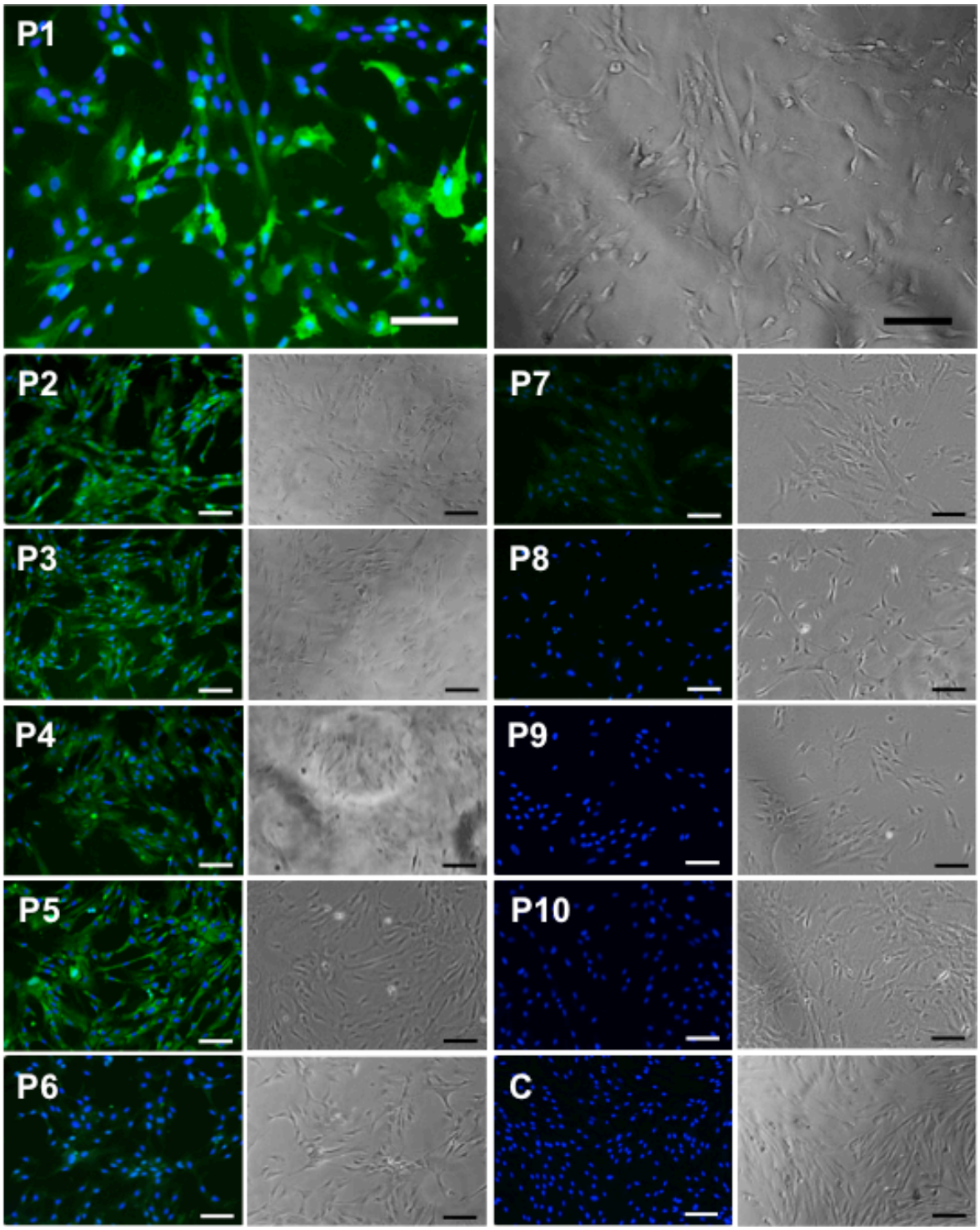


**Figure 3.3. Maintenance of STRO-1 expression following MACS isolation over serial passage *in vitro*.** Isolated cells were seeded (1 x $10^3$ cells/$cm^2$) at each passage (P). Cells were cultured for 3 to 5 days to allow cell adhesion and proliferation prior to further passaging. Cells were fixed in 4% PFA at the end of each passage and immuno-labelled with STRO-1 antibody (Green) and counterstained with DAPI (Blue). STRO-1 positive cells could be isolated from foetal femur-derived cells with expression maintained up to passage 7 and lost at passages 8. C = Negative Control. Scale bars indicate 50 µm. (n = 3)

### 3.2.3 Diaphyseal Cell Population Have Higher Affinity toward Osteogenic Differentiation

Previous results showed a difference in phenotype between cells found in the epiphyseal region and diaphyseal region along with STRO-1 expression largely restricted in the diaphyseal region (Figure 3.1 - 3.3), suggesting cells from the epiphyseal and diaphyseal contain two distinct subpopulations of SSC. To assess whether difference in differentiation capacity existed between epiphyseal cell populations and diaphyseal populations, the epiphyseal and diaphyseal region were separated from the foetal femur and placed under monolayer culture.

Epiphyseal and diaphyseal cells were isolated from three unrelated, similar age patient femur samples. Following 7 days in monolayer culture under basal conditions, cells were fixed in ethanol and examined for alkaline phosphatase (*ALP*) expression. A significant variation in *ALP* expression was seen between different patient samples in both epiphyseal (Figure 3.4 A – C) and diaphyseal cell populations (Figure 3.4 D-F). However, within each patient sample, the diaphyseal cell populations consistently displayed enhanced *ALP* activity when compared to the corresponding epiphyseal sample (Figure 3.4 A and D, B and E, C and F). These results indicate diaphyseal cells have a higher affinity towards osteogenic differentiation compared to epiphyseal cell populations.

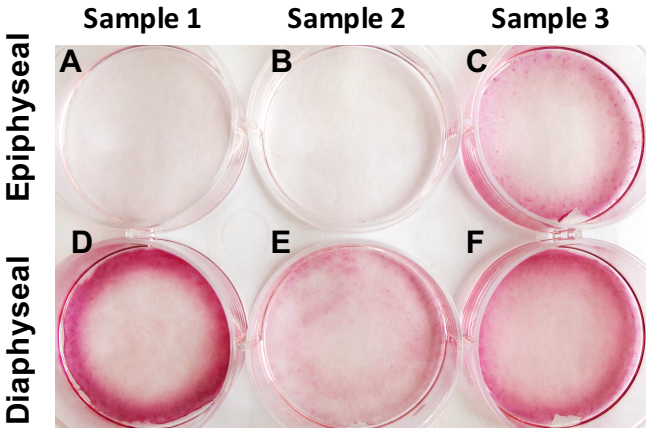


**Figure 3.4. Macroscopic appearances after *ALP* staining of monolayer culture in three unrelated foetal femur samples.** A-C are epiphyseal cell populations with corresponding diaphyseal cells below (D-F). A significant degree of variation in *ALP* activity across different patient samples in both epiphyseal (A-C) and diaphyseal cell populations (D-F). When comparing cells isolated within each sample (A and D, B and E, C and F), the diaphyseal cell populations consistently display higher *ALP* activity to the corresponding epiphyseal cell population. (n=3)

### 3.2.4 Epiphyseal and Diaphyseal Cells Express Distinct gene associated with Osteogenic and Chondrogenic Differentiation

To assess osteogenic and chondrogenic-associated gene expression between epiphyseal and diaphyseal cell populations, epiphyseal and diaphyseal cells were isolated from three unrelated patient samples. Following 7 days in monolayer culture under basal conditions, RNA was extracted from each individual sample for gene expression analysis. Using RT-qPCR, diaphyseal cells were shown to express higher levels of genes associated with osteogenic differentiation; Osterix, *RUNX2*, *ALP*, *COL1A1* and Osteonectin (Figure 3.5 A-E). Of note, Osteocalcin, a late osteogenic differentiation marker gene was expressed at a lower level in the diaphyseal cell populations (Figure 3.5 F).

Epiphyseal cell populations expressed increased level of genes associated with chondrogenic differentiation; *SOX9* and *COL2A1* (Figure 3.5 G-H). Importantly, the marker for hypertrophic chondrocyte differentiation, *COL10A1*, were found to have a 20-fold increase in expression in diaphyseal cells compared to epiphyseal cell populations (Figure 3.5 I). These results suggest epiphyseal cells have a tendency towards chondrogenic differentiation while diaphyseal cells express high level of genes associated with hypertrophic chondrocyte phenotype with an increased affinity for osteogenic differentiation.

To examine the effects of osteogenic and chondrogenic culture medium on gene expression in epiphyseal and diaphyseal cell populations, cells were cultured in differentiation medium for 7 days prior to RNA extraction and RT-qPCR analysis. When epiphyseal cell populations were cultured under osteogenic media, expression of genes associated with osteogenic differentiation, namely; *RUNX2*, *ALP* and *COL1A1* were shown to be increased while the expression of *SOX9*, a gene associated with chondrogenic gene expression was seen to be decreased compared to basal conditions (Figure 3.6 B-E). Interestingly, chondrogenic medium had a similar effect to osteogenic medium on gene expression in epiphyseal cell populations; with the expression of *RUNX2*, *ALP* and *COL1A1* all increased (Figure 3.6 B-D) and the expression of *SOX9* decreased following culture under chondrogenic medium (figure 3.6 E).

In diaphyseal cell populations, only *ALP* expression was significantly enhanced by culture in osteogenic medium (Figure 3.7 C), and like the epiphyseal cell populations, *SOX9* gene expression was reduced following culture in osteogenic medium. After 7 days of monolayer culture in chondrogenic medium, diaphyseal cell populations displayed a modest increase in *COL1A1* expression. Interestingly *SOX9* expression was not significantly affected by chondrogenic medium simulation (Figure 3.7 E).

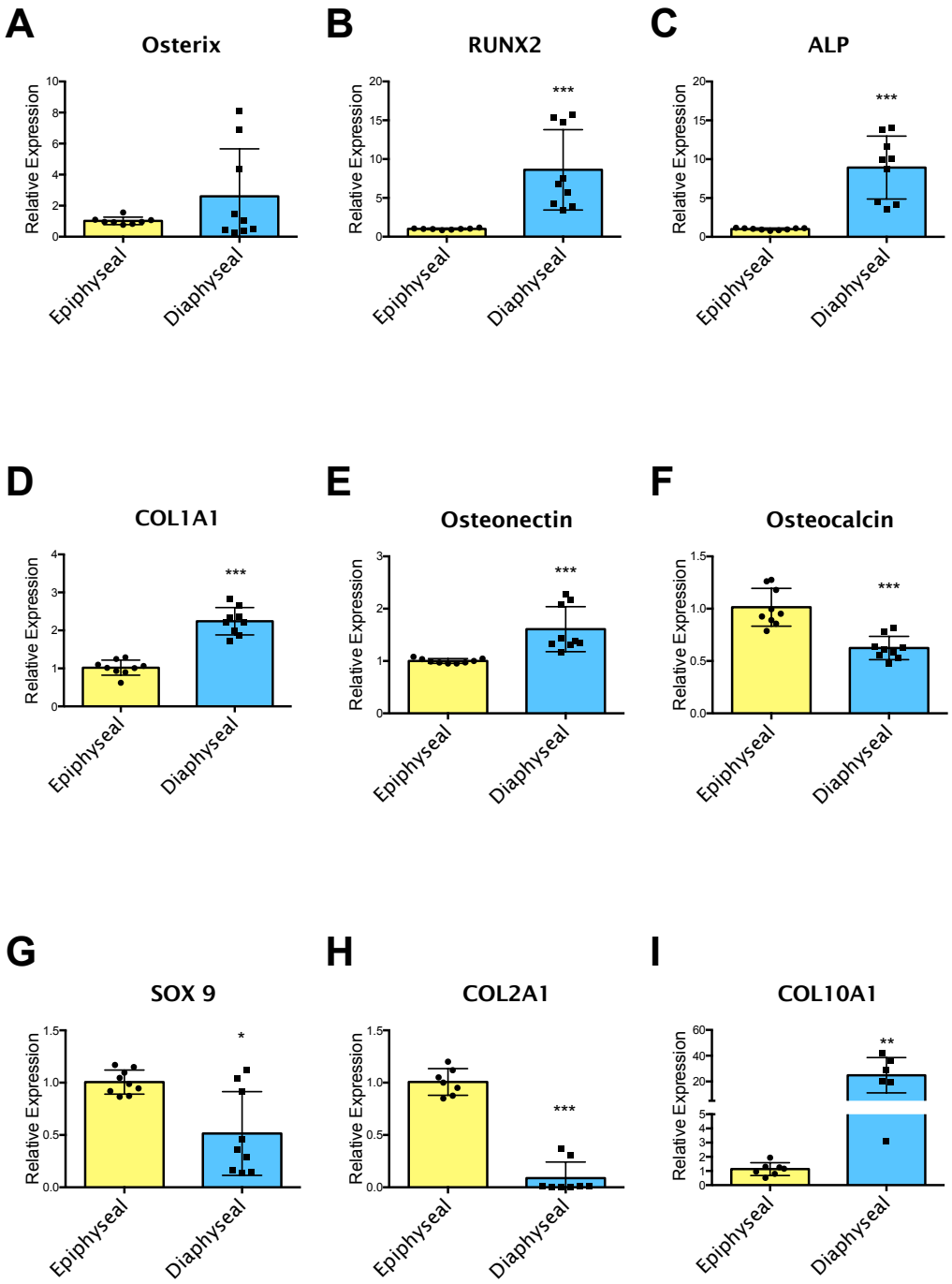


**Figure 3.5. RT-qPCR result showing the expression of osteogenic associated genes in epiphyseal and diaphyseal cell populations after 7 days in monolayer culture under basal conditions**. Osterix (A), *RUNX2* (B), *ALP* (C), *COL1A1* (D), Osteonectin (E) were expressed at a higher level in diaphyseal cell populations. Interestingly, epiphyseal cells displayed a higher expression of Osteocalcin (F). *SOX9* (G) and *COL2A1* (H), genes associated with chondrogenesis. Diaphyseal cell populations displayed a 20-fold increase in *COL10A1* (I) compared to epiphyseal cell populations. Data represents an average of three independent patient samples, and error bars represent mean and standard deviation. *P<0.05, **P<0.01, ***P<0.001 calculated using the Mann-Whitney Test.

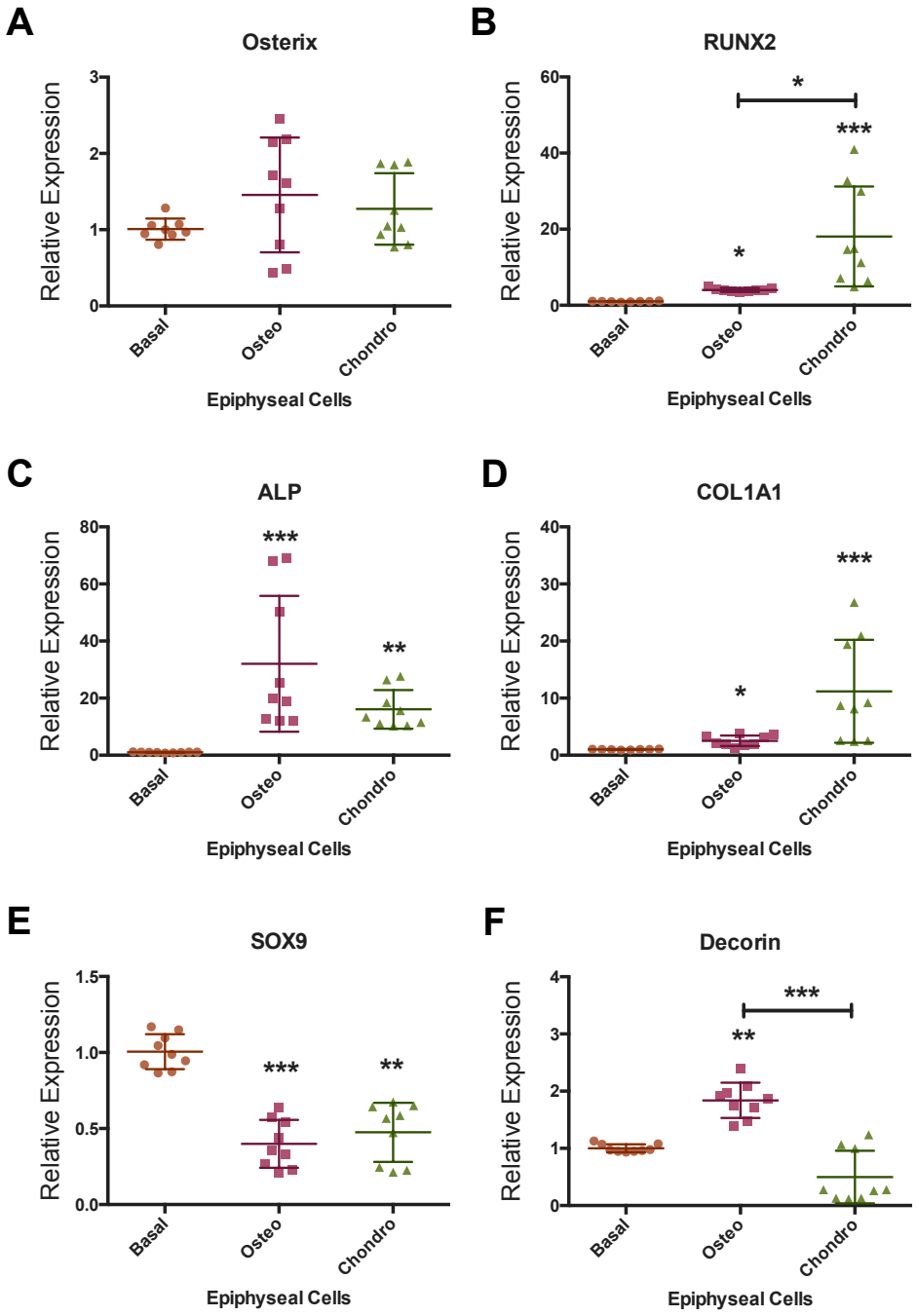


**Figure 3.6. RT-qPCR result showing the effects of osteogenic and chondrogenic culture media on Osterix (A), *RUNX2* (B), *ALP* (C), *COL1A1* (D), *SOX9* (E) and Decorin (F) in epiphyseal cell population**. Osteogenic medium increased the expression of *RUNX2*, *ALP* and *COL1A1* (B-D) while decreased the expression of *SOX9* (E). Chondrogenic medium had similar effects on gene expression with a higher augmentation on *RUNX2* and *COL1A1* expression (B and D). Interestingly, chondrogenic medium decreased the expression of the chondrogenic differentiation associated gene *SOX9* similarly to osteogenic culture condition (E). Data represents an average of three independent patient samples, and error bars represent mean and standard deviation. *P<0.05, **P<0.01, ***P<0.001 calculated using ANOVA test. (n=3)

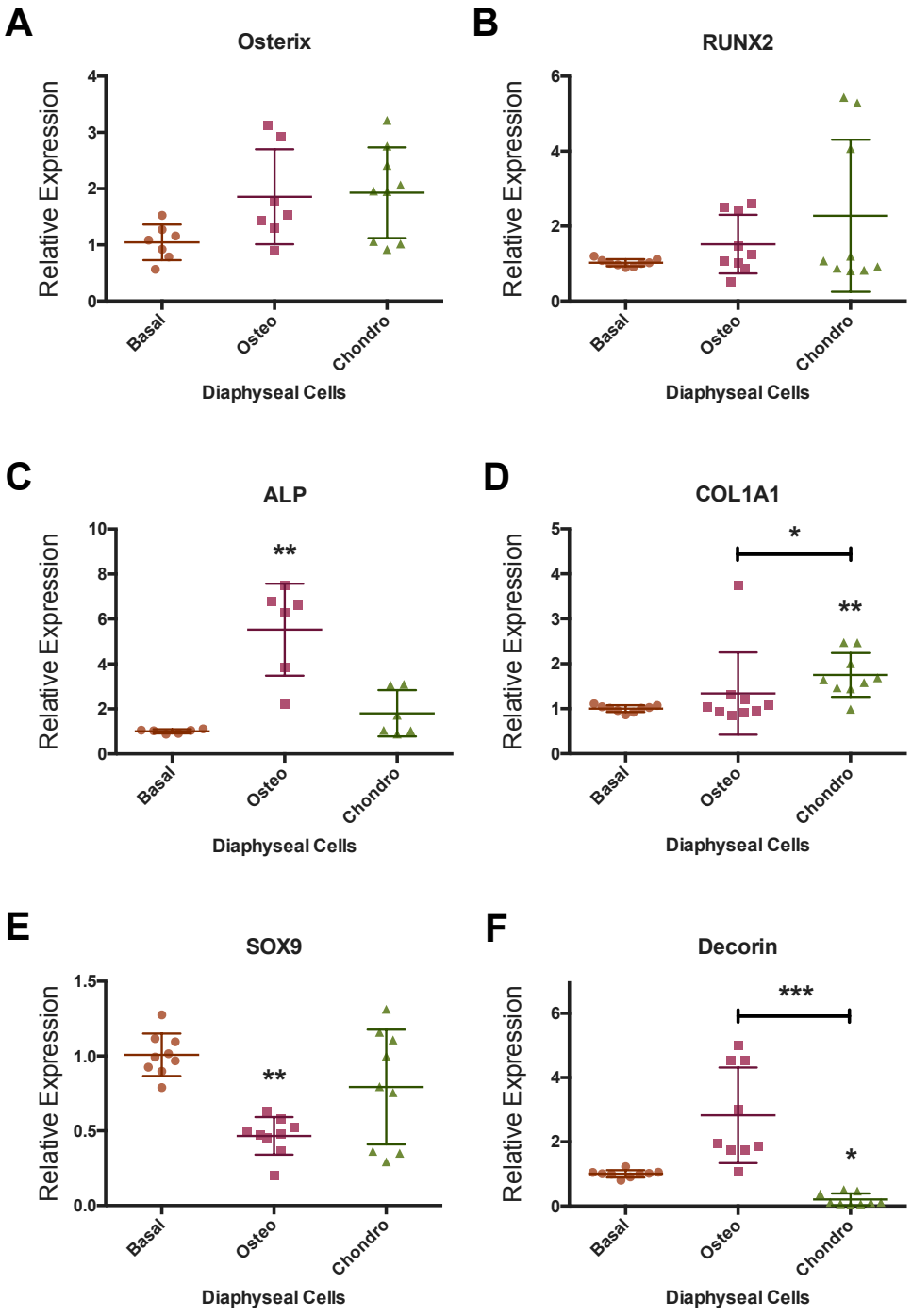


**Figure 3.7. RT-qPCR showing the effects of osteogenic and chondrogenic culture medium on Osterix (A), *RUNX2* (B), *ALP* (C), *COL1A1* (D), *SOX9* (E) and Decorin (F) in diaphyseal cell population**. Osteogenic medium increased the expression of *ALP* by 5-fold (C) with no effect of Osterix, *RUNX2* and *COL1A1* (A, B and D). Osteogenic culture conditions resulted in decreased expression of *SOX9* (E). Chondrogenic medium increased expression of *COL1A1* and had no effects on the chondrogenesis marker gene *SOX9* (E). Data represents an average of three independent patient samples, and error bars represent mean and standard deviation. *P<0.05, **P<0.01, ***P<0.001 calculated using ANOVA test.

### 3.2.5 Confirmation of Stromal Antigens and Nucelostemin expression by Foetal Femur Cell Populations

Following isolation and monolayer culture, both epiphyseal and diaphyseal-derived cell populations formed distinct cell colonies displaying a fibroblastic morphology similar to the human bone marrow stromal cell populations (Figure 3.8 A-C). RT-qPCR confirmed expression of the stromal antigens *CD63* and *ALCAM* in epiphyseal and diaphyseal cells although at a lower level in comparison to HBMSC (Figure 3.8 D and E). Epiphyseal cells expressed *ALCAM* at a similar level to HBMSC while diaphyseal cells appeared to express lower levels of *ALCAM* (Figure 3.8 E). Nucleostemin, a putative stem cell marker, was found to be expressed by both epiphyseal and diaphyseal cells (Figure 3.8 F). The expression of *CD63*, *ALCAM* and Nucelostemin by epiphyseal and diaphyseal cells confirms these cell populations retain mesenchymal progenitor cell-like characteristics.

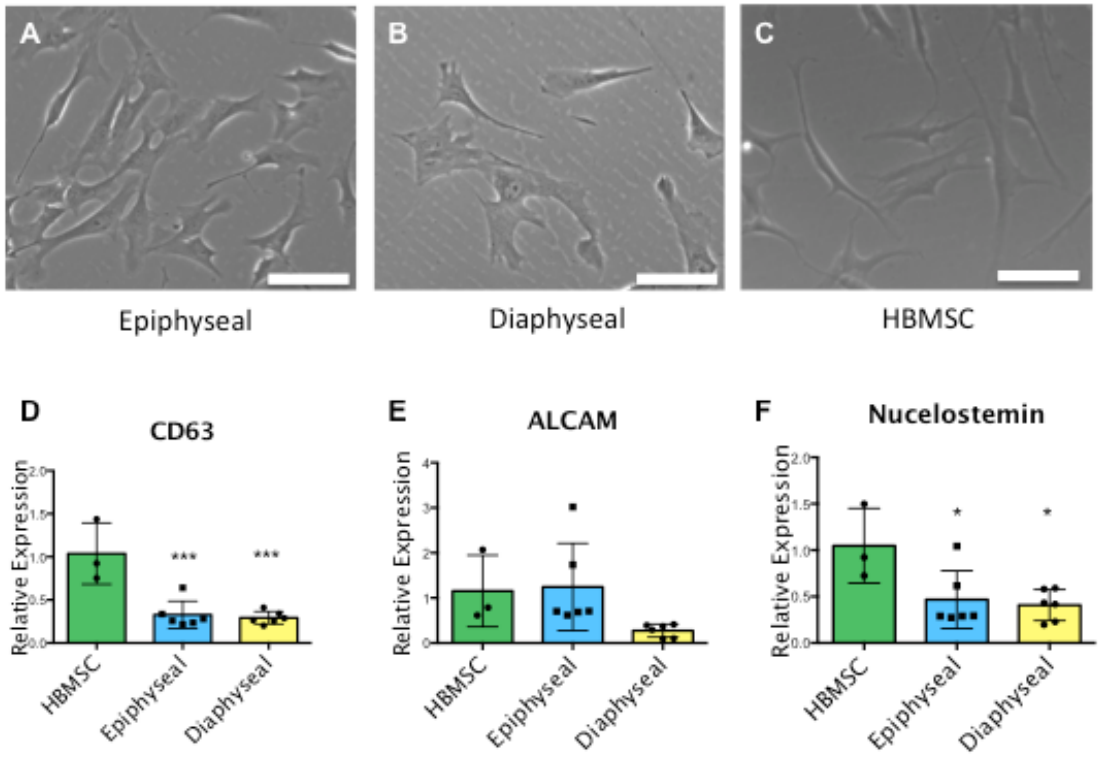


**Figure 3.8. Morphology and stem cell marker expression of different SSC populations.** Fibroblastic morphology of epiphyseal cells (A), diaphyseal cells (B) and Human Bone Marrow Stromal Cells (C) under monolayer culture. RT-qPCR showing Epiphyseal cells, diaphyseal cells and HBMSC express stromal antigen *CD63* (D), *ALCAM* (E) and putative stem cell marker nucelostemin (F). Scale bar = 100 µm. Data represents an average of three independent patient samples, and error bars represent standard deviation. * P<0.1, *** P<0.001 calculated using ANOVA *test.

### 3.2.6 Epiphyseal and Diaphyseal Cells Differentiation Capacity

To validate both epiphyseal and diaphyseal cell populations have the capacity to differentiate down osteogenic, chondrogenic and adipogenic linages, epiphyseal and diaphyseal cell populations were extracted and seeded at 1 x $10^3$ cells/$cm^2$ and treated with osteogenic and adipogenic (rosiglitazone) medium for 14 days. Cultures were subsequently stained with Alizarin red to show mineralised matrix and Oil red to display lipid deposition. Micromass cultures (2.5 x $10^5$ cells per pellet) were treated with chondrogenic medium for 14 days and stained with Alcian blue to show proteoglycan secreted by chondroblast.

After 14 days in monolayer culture with osteogenic medium, both epiphyseal and diaphyseal cell populations were shown to contain mineralised matrix as shown by alizarin red staining (figure 3.9). Diaphyseal cells displayed an enhanced quantity of mineralised matrix compared to epiphyseal cells, supporting molecular data showing a higher affinity for osteogenic differentiation (Figure 3.9). Under adipogenic culture conditions, both epiphyseal and diaphyseal cell populations were shown to differentiate down the adipogenic lineage with cells positive for lipid deposition evidenced by by Oil red O staining. Epiphyseal cells appeared to differentiate more readily towards adipocytes when compared to diaphyseal cell populations (Figure 3.9).

Under chondrogenic culture conditions, both epiphyseal and diaphyseal cell populations were able to differentiate down the chondrogenic lineage as evidenced by proteoglycan deposition (Alcian blue staining) (Figure 3.9). Micromass culture of epiphyseal cells displayed a more intense Alcian blue stain, denoting an increased level of proteoglycan compared to diaphyseal cells.

The above results correspond strongly with previously shown molecular data (Figure 3.5), suggesting epiphyseal and diaphyseal cell populations display distinct differentiation potentials while retaining the ability to differentiate into osteoblast, chondrocyte and adipocytes.

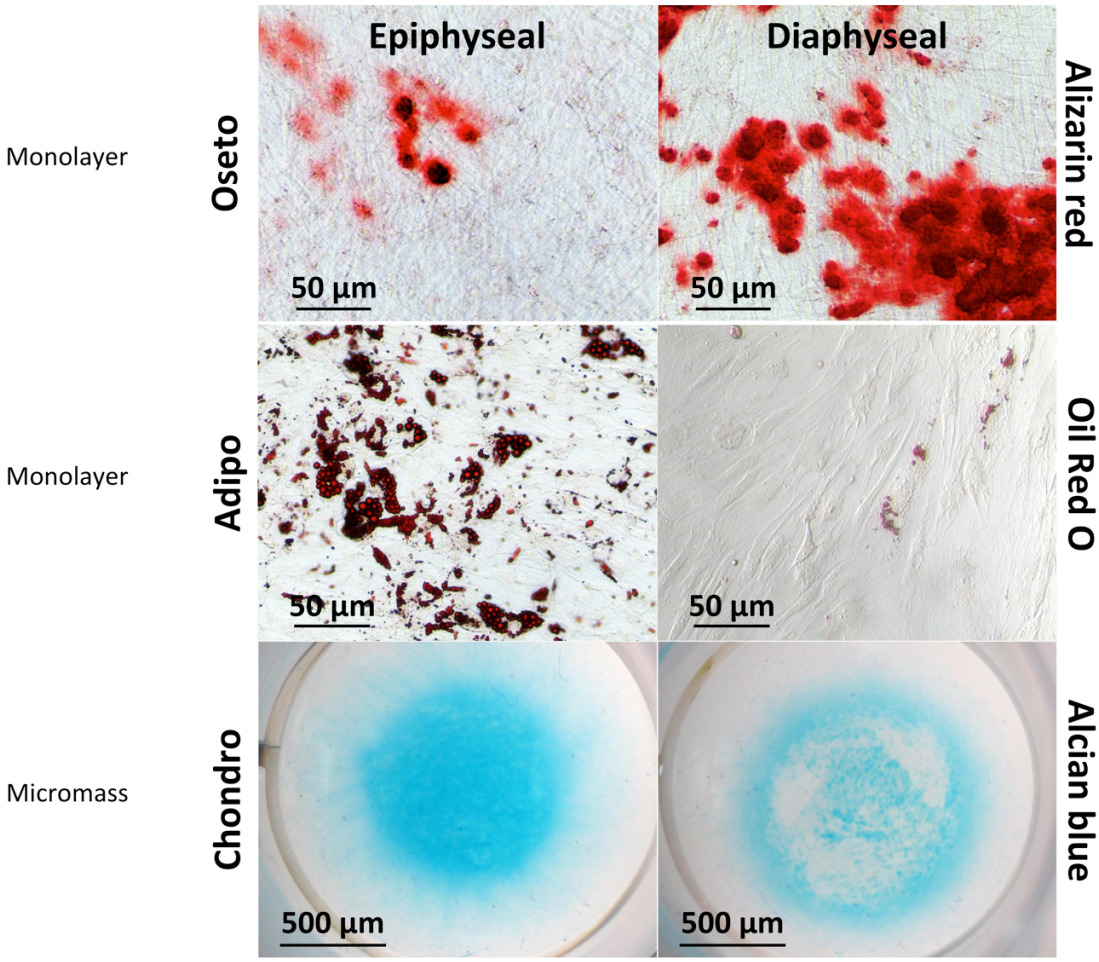


**Figure 3.9. Multi-lineage differentiation potential of epiphyseal and diaphyseal cell populations.** Following monolayer culture under osteogenic medium, both epiphyseal and diaphyseal cells displayed areas of mineralized matrix evidenced by Alizarin red stain. Diaphyseal cells displayed increased areas of mineralized matrix compared to epiphyseal cell populations. Adipogenic culture conditions generated cells with lipid deposition in both epiphyseal and diaphyseal cell populations. However, while most epiphyseal cells were positive for Oil red staining, only a few cells displayed lipid deposition in the diaphyseal cell population. Micromass culture with chondrogenic medium induces proteoglycan matrix secretion by both epiphyseal cell and diaphyseal cell population as shown by Alcian blue staining. There were increased levels of proteoglycan deposition found in epiphyseal cell populations compared to diaphyseal cell populations. (n=3). (Staining and microscopy by Dr. David Gothard in collaboration)

### 3.2.7 Characterisation of Epiphyseal and Diaphyseal Cell Population in 3D Organotypic Culture

To characterize epiphyseal and diaphyseal-derived cell populations in 3D pellet cultures, primary cultures were expanded in monolayer culture and tripsinized. Pellets were formed at a density of $2.5 \times 10^5$ cells by centrifugation. The pellets were cultured in basal media in centrifugation tubes for 48 hours before transfer to 3D organotypic culture. Cells were cultured for 21 days before RNA extraction and RT-qPCR analysis.

RT-qPCR results showed diaphyseal 3D pellets exhibited a higher level of genes associated with osteogenic differentiation, namely *ALP*, *COL1A1* and *RUNX2,* compared to epiphyseal 3D pellets (Figure 3.10 A-C). These results were comparable to data obtained in monolayer culture (figure 3.5). However, there were no significant differences in Osteonectin and Osteocalcin expression between epiphyseal and diaphyseal pellets (Figure 3.10 D and E). No significant difference in *SOX9* and *COL2A1* gene expression was observed between epiphyseal and diaphyseal cell populations in the 3D pellet culture model (Figure 3.10 F and G). The *COL10A1* expression pattern was reversed to that observed in monolayer culture with a lower level of *COL10A1* expression observed in diaphyseal cell 3D pellets (Figure 3.10H). These results suggest 3D organotypic culture model affects the pattern of gene expression and differentiation of epiphyseal and diaphyseal cell populations in comparison to cells cultured in monolayer culture.

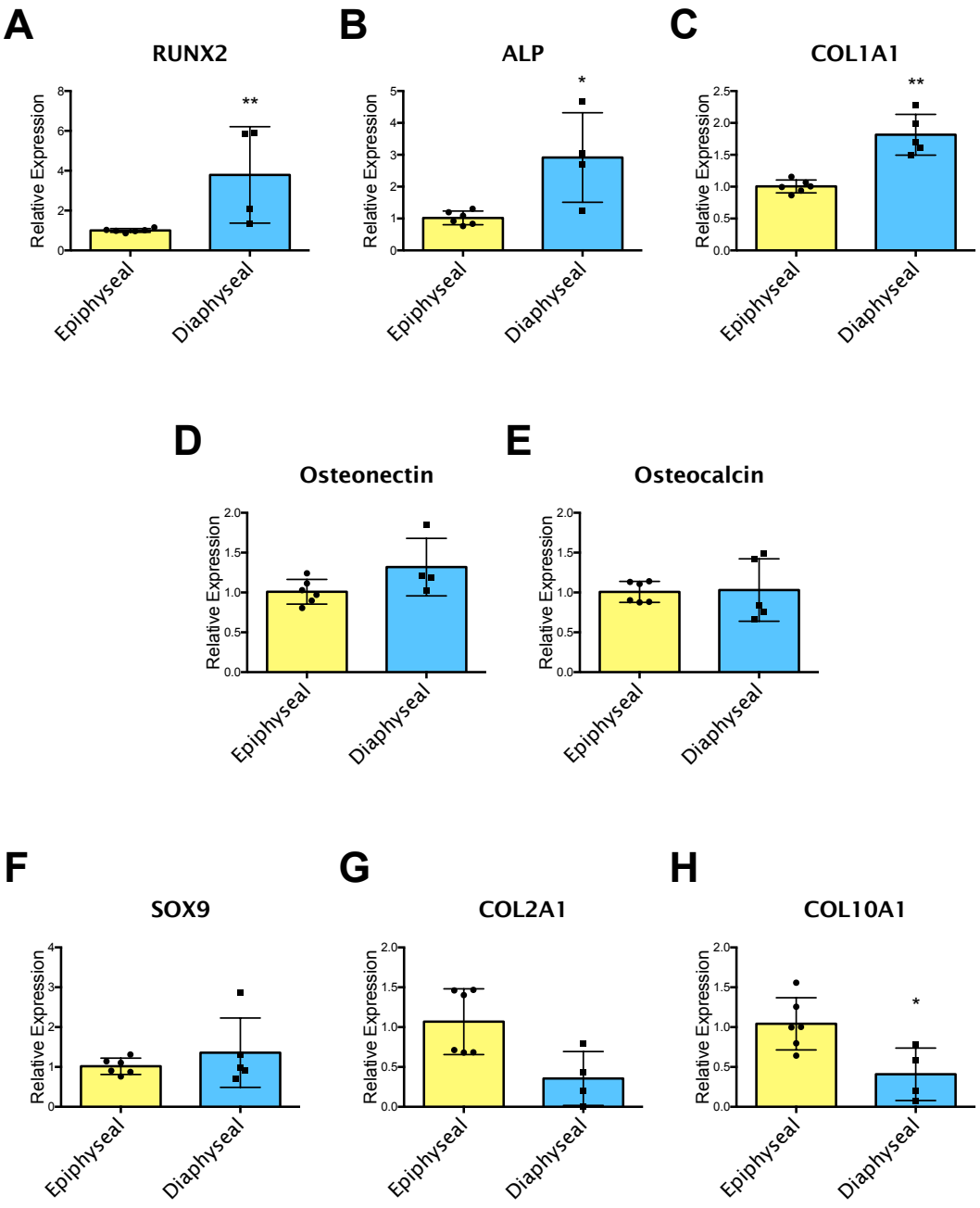


**Figure 3.10. Osteogenic and chondrogenic-related gene expression in 3D pellet culture.** RT-qPCR results showing differences in *RUNX2* (A), *ALP* (B), *COL1A1* (C), Osteonectin (D), Osteocalcin (E), *SOX9* (F), *COL2A1* (G) and *COL10A1* (H) between epiphyseal and diaphyseal cell populations in 3D organotypic culture. Diaphyseal cell populations showed increased expression of *RUNX2* (A), *ALP* (B) and *COL1A1* (C). No difference in Osteonectin, Osteocalcin, *SOX9* and *COL2A1* expression was seen between epiphyseal and diaphyseal cell populations in 3D organotypic culture. *COL10A1* was expressed at a higher level in epiphyseal cell populations (H). Data represents an average of three independent patient samples, and error bars represent mean and standard deviation. * P<0.1, *** P<0.001 calculated using Mann-Whitney test.

### 3.2.8 Histological Analysis of 3D Organotypic Culture

To characterize epiphyseal and diaphyseal-derived cell populations in 3D pellet culture, primary cells were expanded in monolayer culture and tripsinized. Pellets were formed using 2.5 x $10^5$ cells by centrifugation. Pellets were cultured in basal media for 48 hours before transfer to basal, osteogenic and chondrogenic media for 21 days in organotypic culture. As previous results have suggested diaphyseal cell populations have a propensity to differentiate towards the osteogenic lineage while epiphyseal cell populations favours chondrogenic differentiation; Diaphyseal pellets were cultured in basal and osteogenic media, whilst epiphyseal pellets were cultured in basal and chondrogenic media.

Alcian blue and Sirius red staining showed epiphyseal cell and diaphyseal cell pellets secrete proteoglycan and collagenous matrix (Figure 3.11). Both diaphyseal and epiphyseal cell pellets appeared to contain increased type I collagen deposition when cultured in differentiation medium (Figure 3.11). Von Kossa stain revealed the presence of mineralised matrix formation in diaphyseal pellets under basal and osteogenic conditions (Figure 3.11). Immunocytochemistry was used to confirm Type I collagen, Type II collagen and *SOX9* expression (Figure 3.11). Type I collagen was found to be expressed in both epiphyseal and diaphyseal pellets with increased level of expression following culture in differentiation media. Type II collagen expression was found with different spatial distribution in diaphyseal and epiphyseal pellets. In Diaphyseal pellets, expression of type II collagen was located in cells central to the pellet where oxygen tension and nutrient levels might be relatively lower, while type II collagen was observed in in cells on the peripheral region in the epiphyseal cell pellets (Figure 3.11). *SOX9* expression was not observed in either diaphyseal or epiphyseal cell pellets under basal conditions. Interestingly, only epiphyseal pellets cultured in chondrogenic media exhibited *SOX9* expression and osteoid formation as highlighted by Goldner's Trichrome stain.

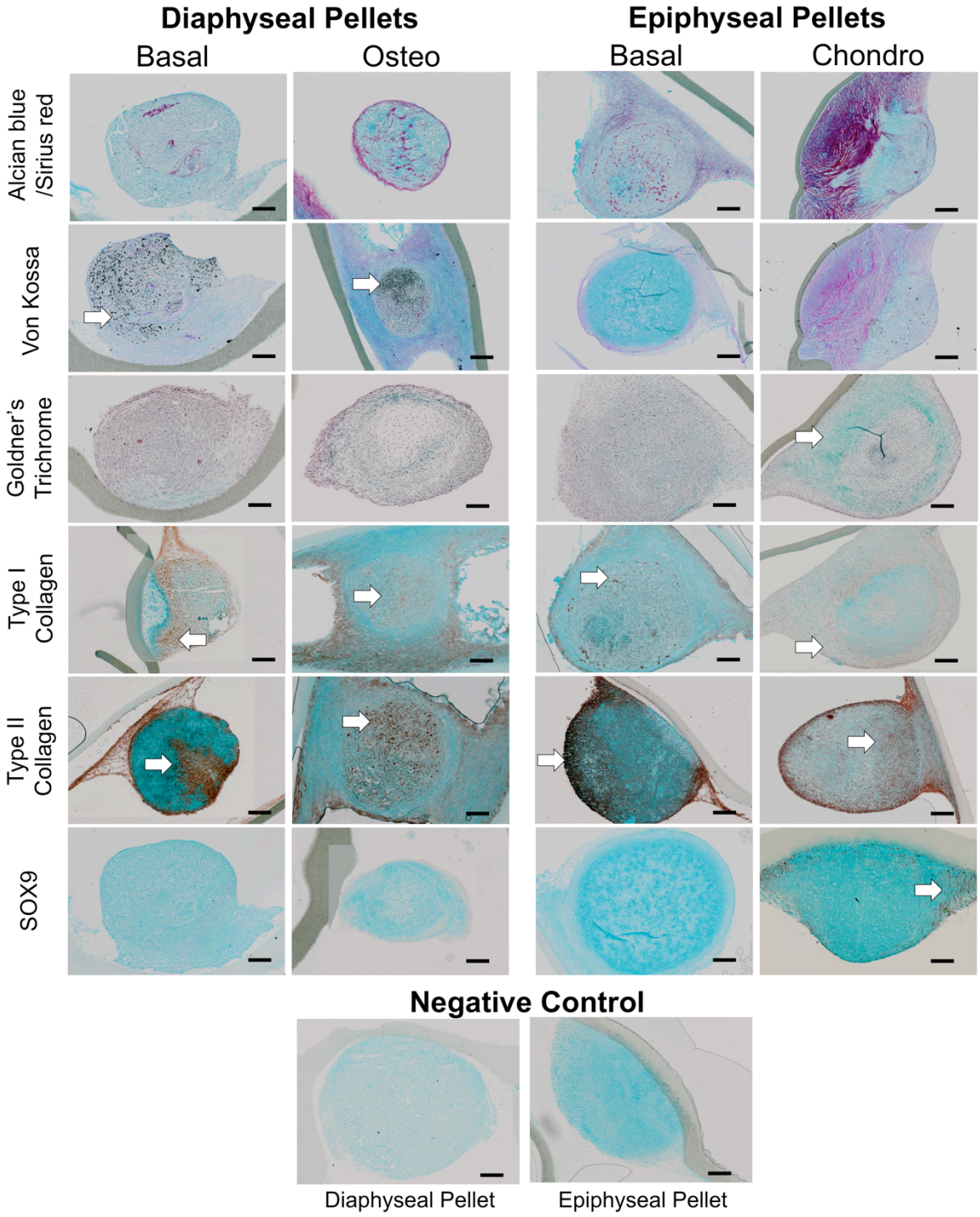


**Figure 3.11. Characterisation of epiphyseal and diaphyseal-derived cell populations in 3D pellet culture**. Alcian blue and Sirius red stain showing proteoglycan and collagenous matrix. Von Kossa stain shows mineralised matrix formation. Goldner's Trichrome shows osteoid formation. Immunocytochemistry identifying Type I collagen, Type II collagen and *SOX9* protein expression. Scale bars measure 200 µm. (n = 6)

### 3.2.9 Epiphyseal and Diaphyseal Cells Express Distinct MicroRNAs

The above results (Figure 3.1 – 3.11) demonstrated that cells found within the foetal femur are heterogeneous with different affinities for osteogenic and chondrogenic differentiation. Epiphyseal cells favoured chondrogenic differentiation while diaphyseal cells favoured osteogenic differentiation. To examine wither a difference in miRNA expression profiles exists between the two foetal femur derived cell populations, a RT-qPCR miRNA array was employed. Three unrelated foetal femur samples were used; the epiphyseal and diaphyseal regions were separated using micro-dissection. Cells were released using collagenase digestion and were cultured in monolayer under basal conditions for 7 days prior to RNA extraction and array analysis.

MicroRNA array expression analysis indicated 156 out of the 377 detecteable miRs were expressed in the samples. Of these, 67 miRs were found to have a difference in expression of greater then 1.5 fold between epiphyseal and diaphyseal cells with 12 miRs expressed at an elevated level in epiphyseal cells and 55 miRs in the diaphyseal cell population (Figure 3.12 A and B).

A heat map was employed to demonstrate the difference in selected miRs expression between epiphyseal and diaphyseal cells (Figure 3.12 C). With the use of a scatter chart (Figure 3.13) plotting each miR dCt normalised to MammU6, where lower dCt values denote higher expression and high dCt reports low levels of expression, 7 miRs were identified with a statistically significant difference in expression between epiphyseal and diaphyseal cells, namely miR-146b-5p, miR-301b and miR-138 (Higher expression in epiphyseal cells) and miR-143, miR-145, miR-146a and miR-34a (increased expression in diaphyseal cells) (Figure 3.13).

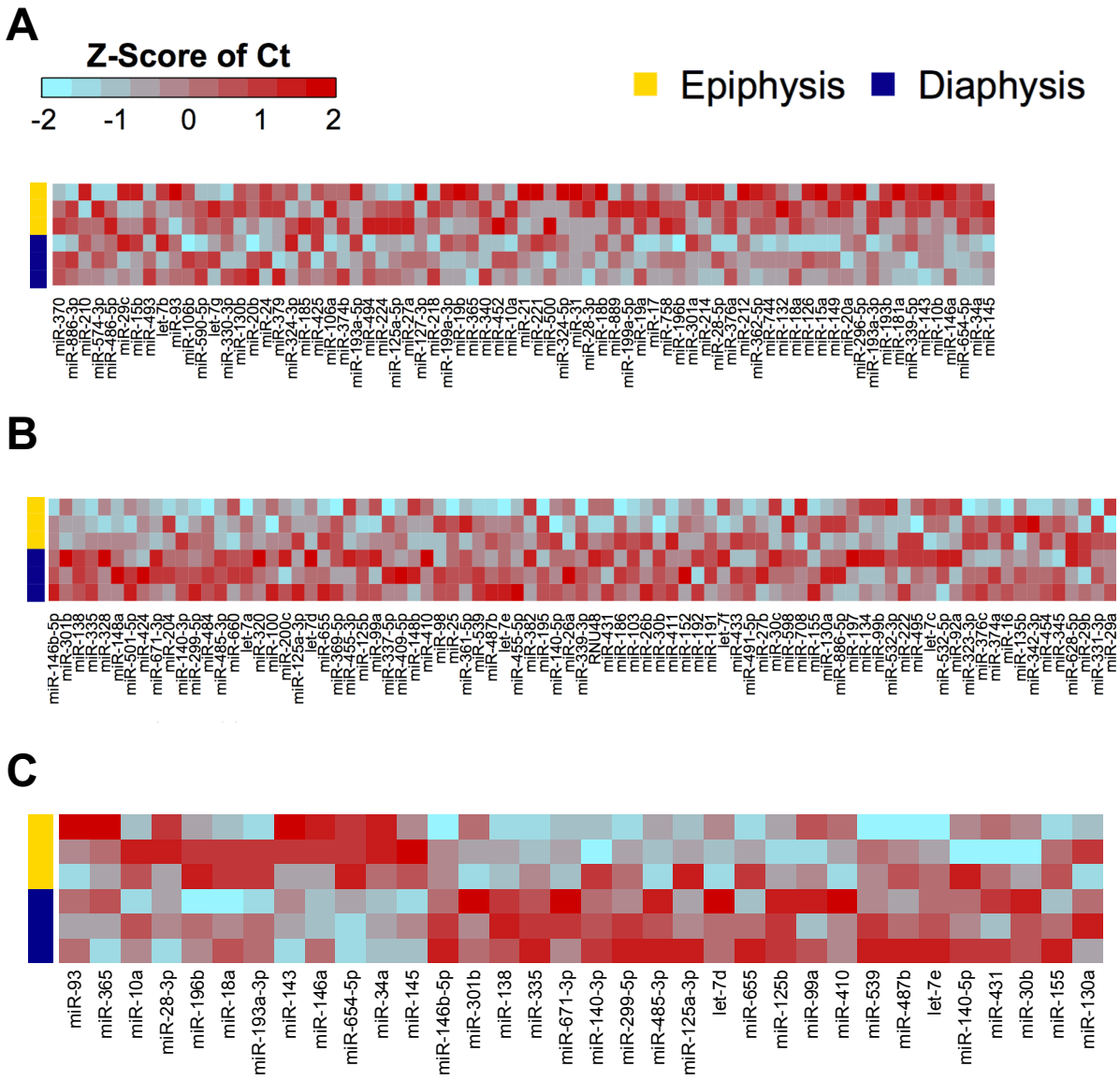


**Figure 3.12. Heat map of microRNA expression between epiphyseal and diaphyseal cell populations**. A) Showing miRNAs with a higher expression in epiphyseal population, B) Showing miRNA with higher expression in diaphyseal cells and C) Showing miRNAs with the greatest difference between epiphyseal and diaphyseal cell populations. Heat map represents z-transformed expression, blue represents higher level of expression and red represents lower level of expression. (n=3)

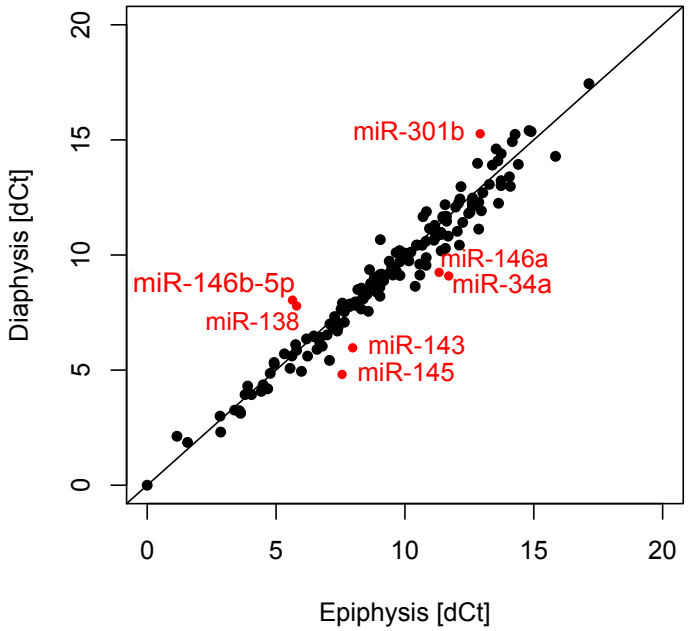


| | Epiphyseal Cells dCT Mean | Diaphyseal Cells dCT Mean | Difference | P Value |
|---|---|---|---|---|
| miR-146b-5p | 5.64 | 8.04 | -2.40 | 0.013 |
| miR-301b | 12.92 | 15.27 | -2.35 | 0.016 |
| miR-138 | 5.80 | 7.79 | -1.99 | 0.040 |
| miR-143 | 7.97 | 5.97 | 2.00 | 0.039 |
| miR-146a | 11.33 | 9.25 | 2.08 | 0.032 |
| miR-34a | 11.7 | 9.09 | 2.61 | 0.007 |
| miR-145 | 7.56 | 4.81 | 2.75 | 0.005 |

**Figure 1.13 MicroRNA expression profile of epiphyseal and diaphyseal cells.** CT value for each miRNA was normalised to MammU6 (dCt) and plotted as an XY scattered chart displaying the correlation of miR expression by epiphyseal and diaphyseal cells. An unpaired t-test revealed 7 miRs with significant difference in expression. MicroRNA-146b-5p, miR-138 and miR-301b were expressed at higher levels in epiphyseal cells. MicroRNA-146a, miR-34a, miR-143 and miR-145 were expressed at increased levels in diaphyseal cell populations. (n=3)

### 3.2.10 Validation of microRNA

Since many of the miRNA targets identified are expressed at relatively low levels, it was important to validate identified targets using individual miRNA TaqMan arrays. However, the miRNA array detected over 100 miRNAs with changes in expression greater than two-fold and a CT value below 35 (Signifying gene expression) rendering it impractical to revalidate all of the targets identified. Additionally, miRNAs are involved in many cellular processes such as cell cycle timing and cell maintenance as well as stem cell differentiation. Therefore, 7 miRNAs found in greater abundance in epiphyseal cells and 5 miRNAs from diaphyseal cells were selected based on their predicted targets and their level of expression for revalidation. TaqMan miRNA RT-qPCR assay was used to revalidate data generated by the miRNA. Epiphyseal and diaphyseal cell populations from three unrelated samples were used. Cells were extracted and cultured under basal conditions for 7 days before RNA extraction and subsequent TaqMan RT-qPCR assay.

Two miRNAs, miR-146a and miR-302a were validated to be highly expressed in the osteogenic diaphyseal cell populations indicating a potential role in osteogenic differentiation (Figure 3.14 and B). The roles of miR-146a and miR-302a in osteogenic differentiation have not been investigated to date in current literatures, and are therefore potential novel targets for functional analysis. MicroRNA-140 has previously been reported as a cartilage-specific miRNA expressed during chondroblast development (Miyaki et al. 2009) and was found to be expressed at a higher level in epiphyseal cells compared to diaphyseal cell populations (Figure 3.14C). In addition, miR-138, known to negatively regulate osteogenic differentiation (Eskildsen et al. 2011) was also found expressed at an increased level in epiphyseal cell populations (Figure 3.14D). The expression of the pro-chondrogenic miR-140 and the anti-osteogenic miR-138 in epiphyseal cell populations indicates epiphyseal cells are inherently chondrogenic and the novel epiphyseal – diaphyseal cell population models derived from this study can be used to identify miRNAs involved in SSC differentiation.

MicroRNA-195, miR-98 and miR-330-3p identified by the microarray were validated and found to display increased expression in epiphyseal cell populations (Figure 3.14 E-G). Their roles in SSC differentiation have, to date, not been investigated and are thus candidates for functional analysis. MicroRNA-744, miR-10b, miR-146b, miR-93 and miR-128 were previously identified by miRNA array analysis with a difference in expression between epiphyseal and diaphyseal cell populations. However, no changes in expression were detected upon revalidation using individual assays (Figure 3.15A-E). These results suggests that the data generated by microarrays may have varying reproducibility and requires additional experiments for validation.

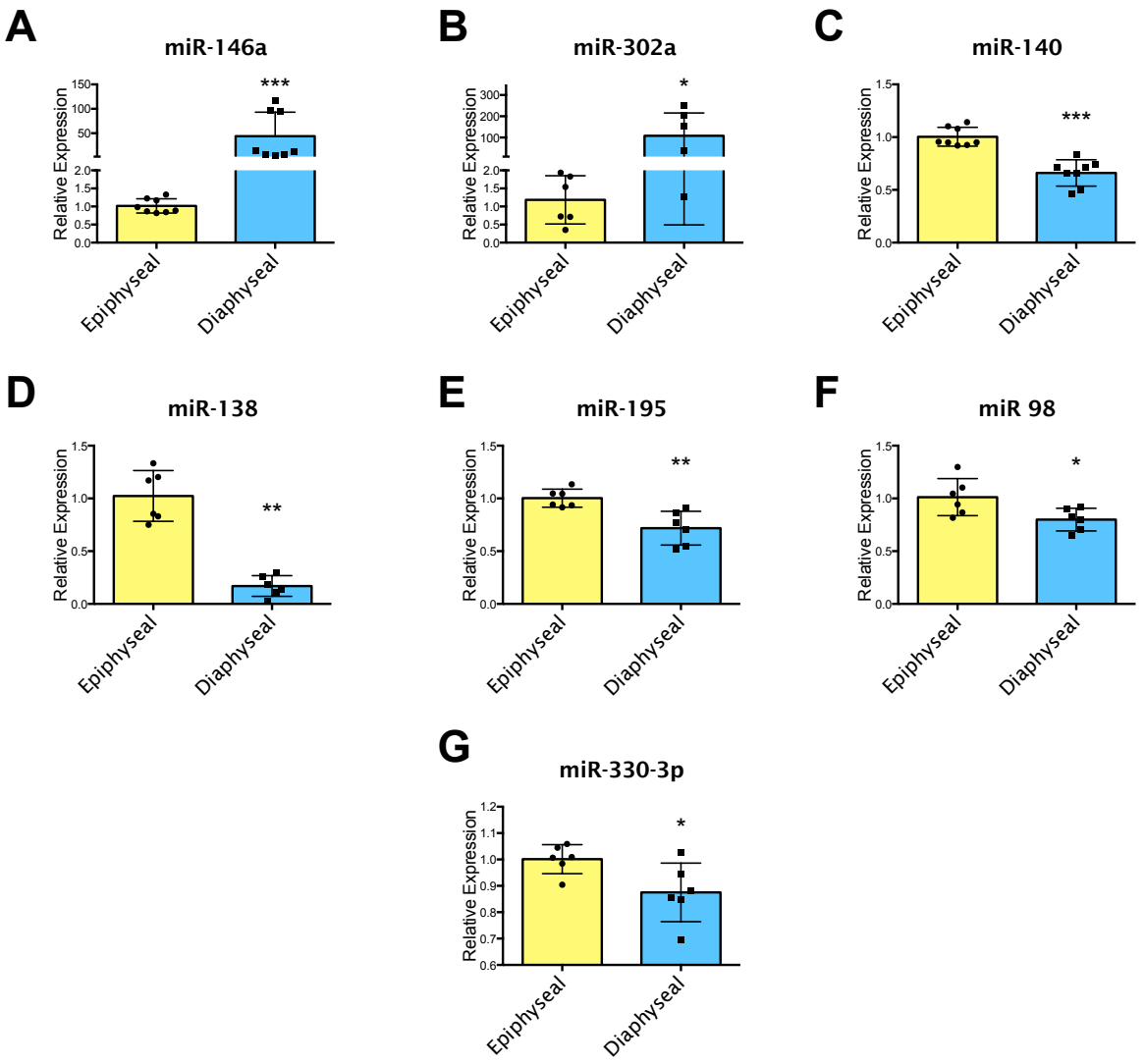


**Figure 3.14. MicroRNA expression between epiphyseal and diaphyseal cell populations**. TaqMan miRNA RT-qPCR assay result revalidating miR-146a (A) and miR-302 (B) are expressed at a higher level in diaphyseal cell populations. miR-140 (C), miR-138 (D), miR-195 (E), miR-98 (F) and miR-330-3p (G) were found to be expressed at an increased level in epiphyseal cell populations. Data represents an average of three independent patient samples, and error bars represent standard deviation. * P<0.1, ** P<0.05 and *** P<0.001 calculated using Mann-Whitney test.

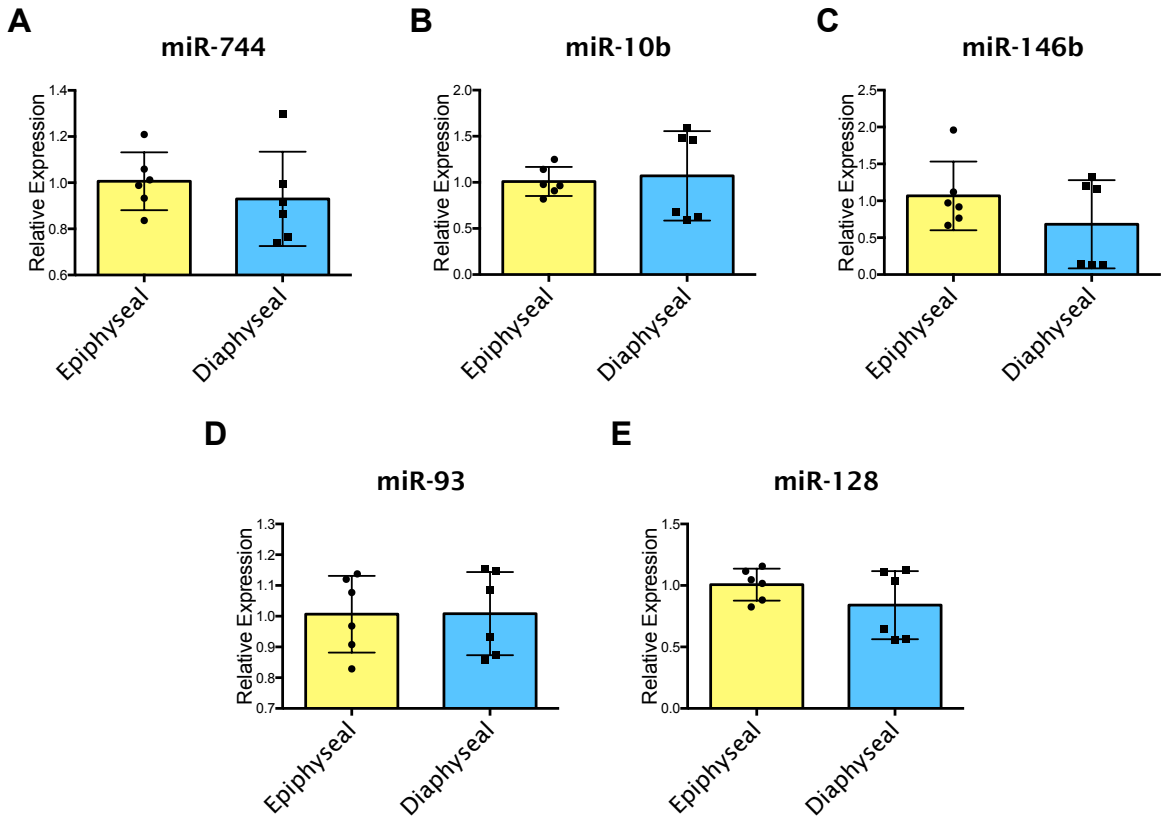


**Figure 3.15.** MicroRNA expression between epiphyseal and diaphyseal cell populations. TaqMan miRNA RT-qPCR assay result showing miR-744 (A), miR-10b (B), miR-146b (C), miR-93 (D) and miR-128 (E) previously identified using miRNA microarray had no reproducible difference in expression between epiphyseal and diaphyseal cell populations. Data represents an average of three independent patient samples, and error bars represent standard deviation.

### 3.2.11 Analysis of MicroRNAs Targets

MicroRNAs, together with the RISC, can negatively regulate gene expression by direct *mRNA* cleavage and *mRNA* decay by deadenylation through binding to the 3'-UTR of their targets (Bartel 2004). The principle of perfect/imperfect complementary binding results in numerous pair partnerships between individual miRNAs and *mRNA* targets (Bartel 2009). Using computer alorgithms such as Targetscan (Anon n.d.), *mRNA* targets can be predicted for each miRNA.

Target analysis revealed that many of the miRNAs validated with a difference in expression between epiphyseal and diaphyseal cell populations are predicted to target various components of the TGF-β superfamily (Table 3.1 – 3.3), suggesting a close interaction between miRNAs and TGF-β signalling pathways during differentiation. miR-146a and miR-302a found to be expressed in the osteogenic diaphyseal cell populations were found to target various activin receptors and *SMAD2*/*SMAD3* protein known to be involved in chondrogenic differentiation. Hence, miR-146a and miR-330 may serve to downregulate chondrogenesis to facilitate osteogenesis. Conversely, miRNAs expressed in the epiphyseal cell populations. Namely miR-140, miR-138, miR-301, miR-195 and miR-330, were predicted to target various BMP proteins and receptors along with *SMAD9* known to promote osteogenic differentiation and may serve to inhibit osteogenesis to facilitate chondrogenic differentiation. Although miRNA target prediction is a useful tool to assess the functions of expressed miRNAs, many of the identified putative targets have not been validated to be regulated by the miRNAs identified. Furthermore, due to the complexity of the interactions between miRNAs and their targets, it is difficult to draw conclusions regarding miRNA functions by using target prediction alone.

| **Expressed in Diaphyseal Cells** | | |
|---|---|---|
| **miR-146a** | 223 Conserved | 3165 Poorly Conserved |
| TGF-β Tagets | Accession Number | Gene |
| ACVR1B | NM_004302 | activin A receptor, type IB |
| ACVR1C | NM_001111031 | activin A receptor, type IC |
| ACVRL1 | NM_000020 | activin A receptor type II-like 1 |
| BAMBI | NM_012342 | BMP and activin membrane-bound inhibitor homolog |
| BMP3 | NM_001201 | bone morphogenetic protein 3 |
| BMP7 | NM_001719 | bone morphogenetic protein 7 |
| BMP8A | NM_181809 | bone morphogenetic protein 8a |
| BMPR1A | NM_004329 | bone morphogenetic protein receptor, type IA |
| BMPR2 | NM_001204 | bone morphogenetic protein receptor, type II |
| SMAD2 | NM_001003652 | SMAD family member 2 |
| SMAD3 | NM_001145102 | SMAD family member 3 |
| SMAD4 | NM_005359 | SMAD family member 4 |
| TGIF1 | NM_003244 | TGFB-induced factor homeobox 1 |
| | | |
| **miR-302a** | 996 Conserved | 2231 Poorly Conserved |
| TGF-β Tagets | Accession Number | Gene |
| ACVR1 | NM_001105 | activin A receptor, type I |
| ACVR1B | NM_004302 | activin A receptor, type IB |
| ACVR1C | NM_001111031 | activin A receptor, type IC |
| ACVR2B | NM_001106 | activin A receptor, type IIB |
| BAMBI | NM_012342 | BMP and activin membrane-bound inhibitor homolog |
| BMP6 | NM_001718 | bone morphogenetic protein 6 |
| BMP7 | NM_001719 | bone morphogenetic protein 7 |
| BMP8B | NM_001720 | bone morphogenetic protein 8b |
| BMPR1A | NM_004329 | bone morphogenetic protein receptor, type IA |
| BMPR1B | NM_001203 | bone morphogenetic protein receptor, type IB |
| BMPR2 | NM_001204 | bone morphogenetic protein receptor, type II |
| CRIM1 | NM_016441 | cysteine rich transmembrane BMP regulator 1 |
| SMAD2 | NM_001003652 | SMAD family member 2 |
| SMAD3 | NM_001145102 | SMAD family member 3 |
| SMAD5 | NM_001001419 | SMAD family member 5 |
| SMAD9 | NM_001127217 | SMAD family member 9 |
| SNIP1 | NM_024700 | Smad nuclear inter*ACTIN*g protein 1 |
| TGFA | NM_001099691 | transforming growth factor, *ALP*ha |
| TGFBR2 | NM_001024847 | transforming growth factor, beta receptor II |

**Table 3.1 Showing predicted TGF-β superfamily targets of miR-146a and miR-302a using Targetscan 6.2** (Anon n.d.).

| **Expressed in Epiphyseal Cells** | | |
|---|---|---|
| **miR-138** | 611 Conserved | 3127 Poorly Conserved |
| TGF-β Tagets | Accession Number | Gene |
| ACVR2A | NM_001616 | activin A receptor, type IIA |
| ACVR2B | NM_001106 | activin A receptor, type IIB |
| BMP1 | NM_006129 | bone morphogenetic protein 1 |
| BMP3 | NM_001201 | bone morphogenetic protein 3 |
| BMP6 | NM_001718 | bone morphogenetic protein 6 |
| BMP7 | NM_001719 | bone morphogenetic protein 7 |
| BMP8A | NM_181809 | bone morphogenetic protein 8a |
| BMPR1A | NM_004329 | bone morphogenetic protein receptor, type IA |
| BMPR2 | NM_001204 | bone morphogenetic protein receptor, type II |
| SMAD3 | NM_001145102 | SMAD family member 3 |
| SMAD4 | NM_005359 | SMAD family member 4 |
| SMURF1 | NM_001199847 | SMAD specific E3 ubiquitin protein ligase 1 |
| TGFA | NM_001099691 | transforming growth factor, *ALP*ha |
| TGFBR3 | NM_001195683 | transforming growth factor, beta receptor III |
| | | |
| **miR-140-3p** | 410 Conserved | 3802 Poorly Conserved |
| TGF-β Tagets | Accession Number | Gene |
| ACVR2B | NM_001106 | activin A receptor, type IIB |
| BMP3 | NM_001201 | bone morphogenetic protein 3 |
| BMPR1B | NM_001203 | bone morphogenetic protein receptor, type IB |
| SMAD4 | NM_005359 | SMAD family member 4 |
| SMAD5 | NM_001001419 | SMAD family member 5 |
| TGFA | NM_001099691 | transforming growth factor, *ALP*ha |

**Table 3.2. Showing predicted TGF-β superfamily targets of miR-138 and miR-140 using Targetscan 6.2** (Anon n.d.).

| **Expressed in Epiphyseal Cells** | | |
|---|---|---|
| **miR-301b** | 996 Conserved | 2231 Poorly Conserved |
| TGF-β Tagets | Accession Number | Gene |
| BMP8B | NM_001720 | bone morphogenetic protein 8b |
| BMPR1B | NM_001203 | bone morphogenetic protein receptor, type IB |
| SMAD9 | NM_001127217 | SMAD family member 9 |
| TGFA | NM_001099691 | transforming growth factor, *ALP*ha |
| TGFBR2 | NM_001024847 | transforming growth factor, beta receptor II |
| | | |
| **miR-195** | 1431 Conserved | 3651 Poorly Conserved |
| TGF-β Tagets | Accession Number | Gene |
| SMAD9 | NM_001127217 | SMAD family member 9 |
| | | |
| **miR-330-3p** | 951 Conserved | 4356 Poorly Conserved |
| TGF-β Tagets | Accession Number | Gene |
| ACVR1 | NM_001105 | activin A receptor, type I |
| ACVR1C | NM_001111031 | activin A receptor, type IC |
| ACVR2B | NM_001106 | activin A receptor, type IIB |
| BMP2K | NM_017593 | BMP2 inducible kinase |
| BMP3 | NM_001201 | bone morphogenetic protein 3 |
| BMP8A | NM_181809 | bone morphogenetic protein 8a |
| BMP8B | NM_001720 | bone morphogenetic protein 8b |
| BMPR1B | NM_001203 | bone morphogenetic protein receptor, type IB |
| BMPR2 | NM_001204 | bone morphogenetic protein receptor, type II |
| SMAD3 | NM_001145102 | SMAD family member 3 |
| SMAD4 | NM_005359 | SMAD family member 4 |
| SMAD7 | NM_001190821 | SMAD family member 7 |
| SMAD9 | NM_001127217 | SMAD family member 9 |
| SMURF2 | NM_022739 | SMAD specific E3 ubiquitin protein ligase 2 |
| TGFA | NM_001099691 | transforming growth factor, *ALP*ha |
| TGFB2 | NM_001135599 | transforming growth factor, beta 2 |
| TGFBR1 | NM_001130916 | transforming growth factor, beta receptor 1 |
| TGFBR3 | NM_001195683 | transforming growth factor, beta receptor III |

**Table 3.3. Showing predicted TGF-β superfamily targets of miR-301b and miR-195 and miR-330-3p using Targetscan 6.2** (Anon n.d.).

## 3.3 Discussion

Histological assessment showed that with increasing age, the foetal femur undergoes various developmental events such as mineralisation and marrow cavity formation, consistent with the current literature (Shapiro 2008). STRO-1, an important cell surface antigen known to reduce SSC population heterogeneity and shown to isolate SSCs with an increased osteogenic capacity (Gronthos et al. 1994), was found to be expressed in cells within the foetal femur. The expression of STRO-1 appeared to be limited to cells within distinct regions in both the epiphyseal and diaphyseal regions of the femur, suggesting the presence of distinct populations of SSCs and is shared by the two cell populations. In addition to the spatial distribution, STRO-1 expression appeared to be dynamic in a temporal fashion, suggesting STRO-1 expression might be associated with various developmental events. Interestingly, STRO-1 immuno-selected foetal SSC populations exhibited phenotype stability over prolonged passage under monolayer culture compared to their adult STRO-1-positive cell counterparts, which typically lose STRO-1 expression after a single *in vitro* passage. This observation suggests that foetal femur-derived SSC retain self-renewal and differentiation capacity better then adult derived SSCs and offer a cell source for stem cell biology, physiology and possibly, subject ot ethical consideration, tissue engineering applications.

The current study has shown that cells extracted from the epiphyseal and diaphyseal regions of a developing human foetal femur retain their progenitor cell characteristics, evidenced by the expression of *CD63*, *ALCAM* and Nucleostemin *mRNA*. However, the cells exhibit a different and distinct phenotype and display discrete affinities in differentiation along the osteogenic and chondrogenic lineages without exogenous stimulation. 2D *in vitro* characterisation revealed an osteogenic phenotype in diaphyseal cell populations evidenced by increased expression of genes associated with osteogenic differentiation, namely *RUNX2*, *ALP*, *COL1A1* and Osteonectin, while a chondrogenic phenotype was observed in epiphyseal cell populations displaying increased expression of *SOX9* and *COL2A1*. Importantly, higher *COL10A1* expression was observed in diaphyseal cell populations, signifying the presence of hypertrophic chondrocytes, important in the formation of mineralised cartilage. The differences in phenotype between epiphyseal and diaphyseal cell populations were further demonstrated by the changes in gene expression following culture under osteogenic and chondrogenic differentiation media. Osteogenic medium resulted in increased *RUNX2* expression in epiphyseal cell populations but not in diaphyseal cell populations. Furthermore, *ALP* was upregulated more than 30-fold when epiphyseal cell populations were cultured under osteogenic medium compared to only a 5-fold increase in *ALP* gene expression in the diaphyseal cell populations. These observations could be the result of diaphyseal cell populations already undergoing osteogenic differentiation; hence, additional osteogenic stimulation resulted in a reduced effect on diaphyseal cell compared to epiphyseal cell populations.

To ascertain that both epiphyseal and diaphyseal cell populations retained the capacity toward differentiation into other lineages, epiphyseal and diaphyseal cells were subjected to methods known to induce osteogenesis, adipogenesis and chondrogenesis. It was found both epiphyseal and diaphyseal cell populations were able to generate functional osteoblasts, adipocyte and chondrocytes evident in the secretion of mineralised matrix, intracellular lipid deposition and proteoglycan secretion, confirming the status of both epiphyseal and diaphyseal cell populations as skeletal stem cells.

Molecular analysis of epiphyseal and diaphyseal cell 3D pellet cultures showed similar trends in gene expression compared to monolayer cultures. However, unlike monolayer cultures, expression of mid to late osteogenic genes was not observed, indicating the absence of terminal differentiation. Expression of the chondrogenic gene *SOX9* was not significantly different between epiphyseal and diaphyseal populations, suggesting cartilaginous and pre-osteoid formation was dominant. In support, *COL10A1* expression was reduced in diaphyseal populations, highlighting the lack of hypertrophic chondrocytes important for mineralisation. Critically, the similarities and differences observed may be due to separate maturation stages within the respective populations. As such, further investigation over serial passage would be required to assess the stability of epiphyseal and diaphyseal population phenotypes. Histological analysis of 3D pellets revealed mineralisation in diaphyseal pellets and *SOX9* expression in epiphyseal pellets. Counter intuitively, type I collagen and type II collagen deposition was observed in both epiphyseal and diaphyseal cell pellets. This observation could be due to a shared sub-population resulting in both regional-derived populations exhibited expression of both osteogenic and chondrogenic markers.

Epiphyseal and diaphyseal cell populations were shown to be distinct subpopulations of SSCs with an affinity towards osteogenic and chondrogenic differentiation exhibited by molecular analysis of gene expression and by histological examination in 3D pellet culture. A miRNA microarray was used to attempt to profile miRNA expression of epiphyseal and diaphyseal cell populations in order to identify miRNAs involved in osteogenic and chondrogenic differentiation. The results showed that 67 miRNAs displayed a difference in expression of greater then 1.5 fold, indicating that epiphyseal and diaphyseal cell populations could be undergoing distinct divergence processes such as differentiation. A number of miRNAs have already been reported to play a role in osteogenic and chondrogenic differentiation (Fang et al. 2015; Lian et al. 2012). Importantly, miR-138 and miR-140, known to exhibit anti-osteogenic and pro-chondrogenic properties respectively (Eskildsen et al. 2011; Miyaki et al. 2009), have been shown to display an increased expression in the chondrogenic epiphyseal cell populations, suggesting that the epiphyseal – diaphyseal cell culture model could serve as a tool to identify miRNAs involved in osteogenesis and chondrogenesis.

MicroRNAs are involved not only in differentiation but also in regulating other cellular processes

such as cell cycle, cell proliferation and developmental timing (Ivey & Srivastava 2010). Therefore, some of the miRNAs identified may not play a role in orchestrating osteogenic and chondrogenic differentiation but, rather, other cellular processes. Therefore, it was important to look at individual putative *mRNA* targets to assess the importance of each miRNA identified. Using Targetscan 6.2 (Anon n.d.), it was found that many components of the TGF-β superfamily were predicted to be targets of the miRNAs identified. TGF-β signaling is known to be important in regulating skeletogenesis. It is generally accepted that the bone morphogenic proteins (BMPs) and their receptors induce early cartilage formation and stimulate mesenchymal cells to differentiate into osteoblasts whilst TGF-β/Activin ligands and their receptors regulate chondrocyte proliferation, differentiation and maturation (X. Yang et al. 2001). Of the miRNAs identified, miR-146a and miR-302 were expressed at a higher level in the osteogenic diaphyseal cell population and predicted to target Actvin receptors and *SMAD2*/*SMAD3,* which are known to respond to TGF-β and activins ligands, important in chondrogenic differentiation (X. Yang et al. 2001) (Roelen & Dijke 2003). MicroRNA-301b, miR-330-3p and miR-195 identified with increased expression in epiphyseal cell populations were predicted to target SMAD9 and various BMP receptors and protein, which are known to play a role in osteogenesis (Hassan et al. 2006; Yoshida et al. 2000; X. Yang et al. 2001). Although there are many other miRNAs and their targets with potential roles in regulating SSC differentiation; because of the number of potential targets, it was not possible to attempt functional analysis on all of the targets identified in this study due to cost and time constraints. Since miR-146a was found to have a 50-fold increase in expression by the osteogenic diaphyseal cell populations and predicted to target *SMAD2*/*SMAD3*, this thesis will undertake functional analysis of miR-146a on *SMAD2*/*SMAD3* function in later experiments.

## 3.4 Conclusion

The current study has characterised regional cell populations from human foetal femur. These populations offer tools for both *in vitro* and potentially *ex vivo* interrogation of biological mechanisms such as miRNAs controlling skeletal development and bone formation. Understanding these mechanisms using foetal populations as a development paradigm could inform tissue-engineering strategies to treat conditions requiring regeneration of skeletal tissue. Using micro dissection technique separating cells through the metaphysis (region between epiphysis and diaphysis) resulted in two distinct SSC populations, namely epiphyseal and diaphyseal cell populations. Although the simple dissection technique used in this study for cell isolation may lead to cross-contamination of epiphyseal and diaphyseal cell populations, it offers a quick and easy method for reducing the heterogeneity of skeletal stem cell populations isolated from foetal femur. Through gene expression and histological analysis, epiphyseal cell populations were found to have

an increased affinity for chondrogenic differentiation while diaphyseal cell populations were found to have an increased affinity for osteogenic differentiation, in the absence of any exogenous induction. MicroRNA microarray analysis of epiphyseal and diaphyseal cell populations revealed a significant difference in miRNA expression between the two cell populations and using the increased chondrogenic capacity of epiphyseal cell populations and osteogenic potentiation of diaphyseal, potential new miRNA targets involved in osteogenic and chondrogenic differentiation were identified.

# Chapter 4: Examination of a MicroRNA Delivery System Using Spermine-Pullulan Complex

## 4.1 Introduction

Skeletal stem cells respond to numerous micro-environmental cues, including mechanical signals, adhesive contexts and soluble factors. The response and subsequent modulation in function enables the cells to mount an appropriate differentiation response to produce a functioning skeletal system (Maul et al. 2011; Dado et al. 2012). The miRNAs involved in differentiation will likely exert their actions on gene expression during the process of differentiation as various genes are required to be expressed and deactivated in the process. It is therefore clear, a culture model containing differentiating skeletal cells is a prerequisite to identify and investigate miRNAs' importance in regulating bone differentiation.

A plethora of factors are known to affect the differentiation of SSC in monolayer culture (detailed in the introduction), including, for example, the use of soluble factors such as dexamethasone (Tenenbaum & Heersche 1985) and TGF-$\beta_3$ (Ravindran et al. 2011). Furthermore, cell-to-cell contact and paracrine factors have also been shown to regulate stem cell differentiation (Tang et al. 2010). This observation suggests cell confluence in monolayer culture could be an important factor in the differentiation of foetal femur-derived SSC *in vitro* and will be examined in this chapter in order to derive an appropriate culture model to investigate miRNA function.

To examine the function of a particular miRNA, investigators have typically employed the use of miRNA hairpin inhibitors and miRNA precursor mimics to knockdown or overexpress the miRNA of interest respectively (Eskildsen et al. 2011; Ng et al. 2009). This typically requires the use of transfection reagents such as viral carriers, cationic polymers, cationic lipids and dendrimers as vehicles for intra-cellular delivery of miRNA inhibitors or mimics (Kanatani et al. 2006; Jo, Ikai, Okazaki, Nagane, et al. 2007). It is generally accepted that primary cells and stem cells are difficult to transfect due to their cytotoxic sensitivity to transfection reagents and their low affinity for transfection complex uptake into the cytoplasm. Recently, Kanatani *el al* reported conjugates of pullulan with spermine displayed high transfection efficiency for plasmid DNA with lowered cytotoxicity compared to cationic lipids in several cell lines (Kanatani et al. 2006). Pullulan is a water-soluble polysaccharide with a repeat unit of maltotriose condensed through α 1,6 linkage and spermine and is a naturally occurring polyamine ($C_{10}H_{26}N_4$). Using N,N' -carbonyldiimidazole activation (CDI), spermine can be introduced to the hydroxyl group of pullulan. This process cationizes the pullulan molecule allowing the molecule to complex with oligonucleotides.

Spermine-pullulan-oligonucleotide complexes are then endocytosed by cells through an asialoglycoprotein receptor (ASGPR) dependent process (Figure 5.1) (Kanatani et al. 2006).

Interestingly, cationic polymers such as spermine-pullulan have lower immunogenicity and enhanced biological safety compared to viral carriers (Jo, Ikai, Okazaki, Yamamoto, et al. 2007). Furthermore, spermine-pullulan complexes can be incorporated into gelatin scaffolds for gene delivery in tissue engineering applications (Thakor et al. 2009; Jo, Ikai, Okazaki, Nagane, et al. 2007; Kanatani et al. 2006). The transfection efficacy of spermine-pullulan complex has been tested on murine skeletal stem cells, neurons and human bladder cancer cell line T24 (Kanatani et al. 2006) and the transfection efficacy and cytotoxicity is related to the ratio of nitrogen content of spermine to the phosphate content of the oligonucleotides, referred to as the N/P ratio. However, the efficacy of spermine-pullulan complex in transfecting miRNA mimic and inhibitors into human foetal femur-derived SSCs has not yet been confirmed and will be examined in this study.

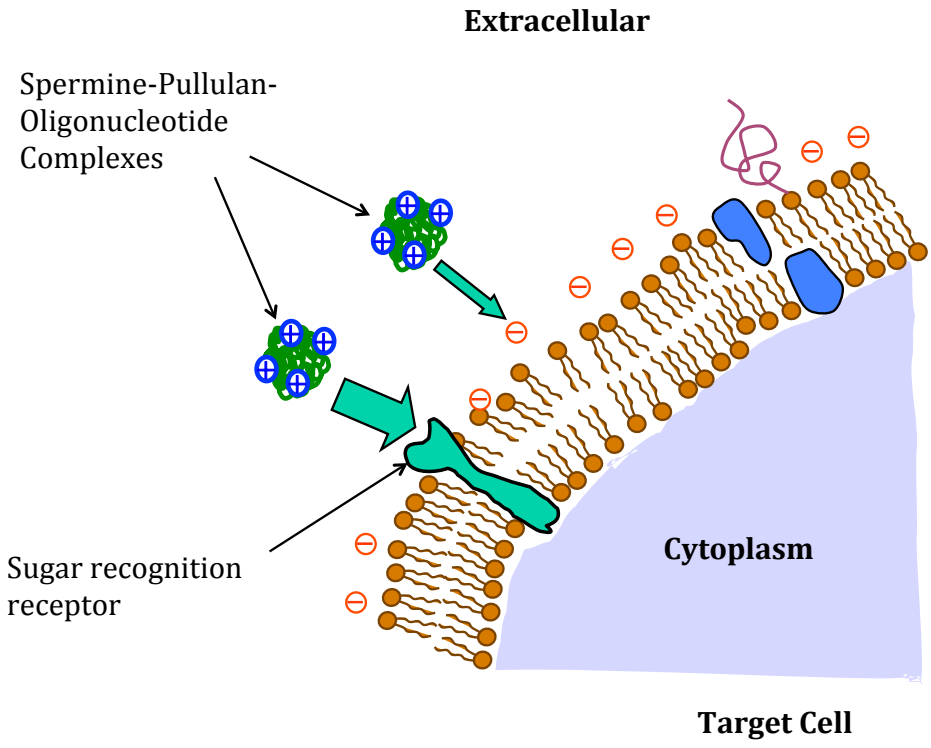


**Figure 4.1. Proposed mechanism of spermine-pullulan oligonucleotide complex transport into a target cell.** Conjugation of spermine to pullulan molecule cationized the pullulan molecule allowing binding with the negatively charged phosphate backbone of oligonucleotides and attachment to cell membranes. Spermine-pullulan complex is then actively endocytosed by cells through an asialoglycoprotein receptor into the cytoplasm where the oligonucleotide can be dissociated and exert a cellular function.

Various miRNAs have been shown to be involved in orchestrating skeletal stem cell differentiation (Ivey & Srivastava 2010) and miRNAs as are known to be essential in skeletal development. By silencing an important enzyme in miRNA synthesis, Dicer, in osteoprogenitor cells, such action was shown to compromise foetal survival and bone formation(Gaur et al. 2010). In addition, miR-138 has been found to be an inhibitor of osteogenesis through the ability to downregulate *FAK* and its down-stream target *RUNX2* and Osterix (Eskildsen et al. 2011). MiR-338-3p was shown to directly target *RUNX2* and fibroblast growth factor receptors and negatively regulate osteogenic differentiation. These actions could contribute to osteoporosis (H. Liu et al. 2014). Together with other miRNAs identified to play a role in chondrogenic and osteogenic differentiation of SSCs (Dong et al. 2012), these observations suggest that miRNAs play an essential role in SSC differentiation. It would appear multiple miRNAs are working in collaboration to orchestrate SSC differentiation. Various miRNAs have been identified through miRNA analysis as described in section 3.2.9. miR-143 and miR-145 have previously been reported to be involved in adenoma formation in colorectal cancer (Akao et al. 2010) and in the regulation of smooth muscle plasticity (Cordes et al. 2009) and thus were selected for functional analysis in this study. Furthermore, the function of miR-128, found to be upregulated following culture in osteogenic media, was also investigated in this report.

### 4.1.1 Hypothesis

A robust culture model with differentiating skeletal stem cells and an effective transfection protocol is a prerequisite for experiments designed to interrogate miRNA functions in skeletal stem cell differentiation. Since the differentiation of SSC is known to be influenced by their surrounding microenvironment, cell contact and confluence is expected to play a role in regulating bone cell differentiation in monolayer culture. A transfection protocol using a liposome base system should be effective in transfecting miRNA mimics in foetal femur-derived SSCs. A novel transfection reagent spermine-pullulan complex has been reported to effectively deliver plasmid DNA into various cell lines and might successfully transfect miRNA mimics and inhibitors into SSCs. microRNA-143, miR-145 and miR-128 have been identified to have a difference in expression between the chondrogenic epiphyseal cell populations and the osteogenic diaphyseal cell populations in chapter 3 and is hypothesize to affect osteogenic differentiation-related gene expression following experimental overexpression and inhibition

### 4.1.2 Aims and Objectives

- To develop the optimal monolayer culture with actively differentiating foetal femur-derived SSCs for miRNA functional analysis.
- To examine the effect of cell seeding density, time in culture and cell confluence on SSC differentiation and gene expression.
- To assess the effect of osteogenic and chondrogenic culture media on miRNA expression to identify miRNAs involve in osteogenic and chondrogenic differentiation of foetal femur-derived SSCs.
- To examine if spermine-pullulan complex can be used to deliver miRNA mimics and inhibitors into foetal femur-derived SSCs – specifically to inhibit and overexpress miR-143, miR-145 and mR-128 in foetal femur-derived SSCs to investigate their role during SSC differentiation.

## 4.2 Results

### 4.2.1 The Effect of Cell Confluence on Osteogenic and Chondrogenic Gene Expression

Cell contact is known to play a role in regulating stem cell differentiation (Tang et al. 2010). To assess if cell confluence in monolayer culture plays a role in regulating foetal femur-derived SSC differentiation in monolayer culture, foetal femur-derived cells from three independent patient samples were passaged (P2) and seeded at different densities into each well of a six-well plate (6250 cells/$cm^2$ to 62,500 cells/$cm^2$). After four days of monolayer culture, cells were fixed and stained for *ALP* to assess osteogenic differentiation. In addition, RT-qPCR was used to examine the change in the expression of differentiation-related genes in responce to cell confluence.

After four days in monolayer culture, wells with an initial seeding density of $12.5x10^3$ cells/$cm^2$ reached 50% confluence, while cells seeded at $37.5x10^3$ cells/$cm^2$ and $62.5x10^3$ cells/$cm^2$ reached 90% and 100% confluence respectively (Figure 4.2 A-F). With increasing cell confluence, the percentage of cells positive for ALP staining increased with 10% of cells positive for ALP staining at a cell confluence of 50% (Figure 4.2 D). At 90% confluence, 50% of cells were positive for ALP staining. Finally, 80% of cells were positive for ALP staining at 100% cell confluency (Figure 4.2 E and F). Thus, the initiation of differentiation in monolayer culture is dependent on cell confluence and cell contact, and commenced when a critical level of cell confluence was achieved.

RT-qPCR assessment of gene expression analysis was consistent with ALP staining, suggesting that cells under monolayer culture begin to differentiate when a critical level of cell confluence or cell contact is reached (Figure 4.2 D-F). *RUNX2* was the first marker to be expressed significantly when cells reached 90% confluence in monolayer culture (Figure 4.1 G). This was followed by *ALP*, attained when cells reached 100 confluence (4.2 E) and, subsequently, by *COL1A1* (Figure 4.2 I). Under basal conditions, there was no significant increase in *SOX9* expression as cell confluence increased (Figure 4.2 J). Interestingly, a surge in *COL2A1* expression was observed as cells reached 100% confluence, with a 15-fold increase in expression compared to cells at 25% confluence. This increase in expression appeared to be transient and reduced rapidly once cell confluence was reached (Figure 4.2 K).

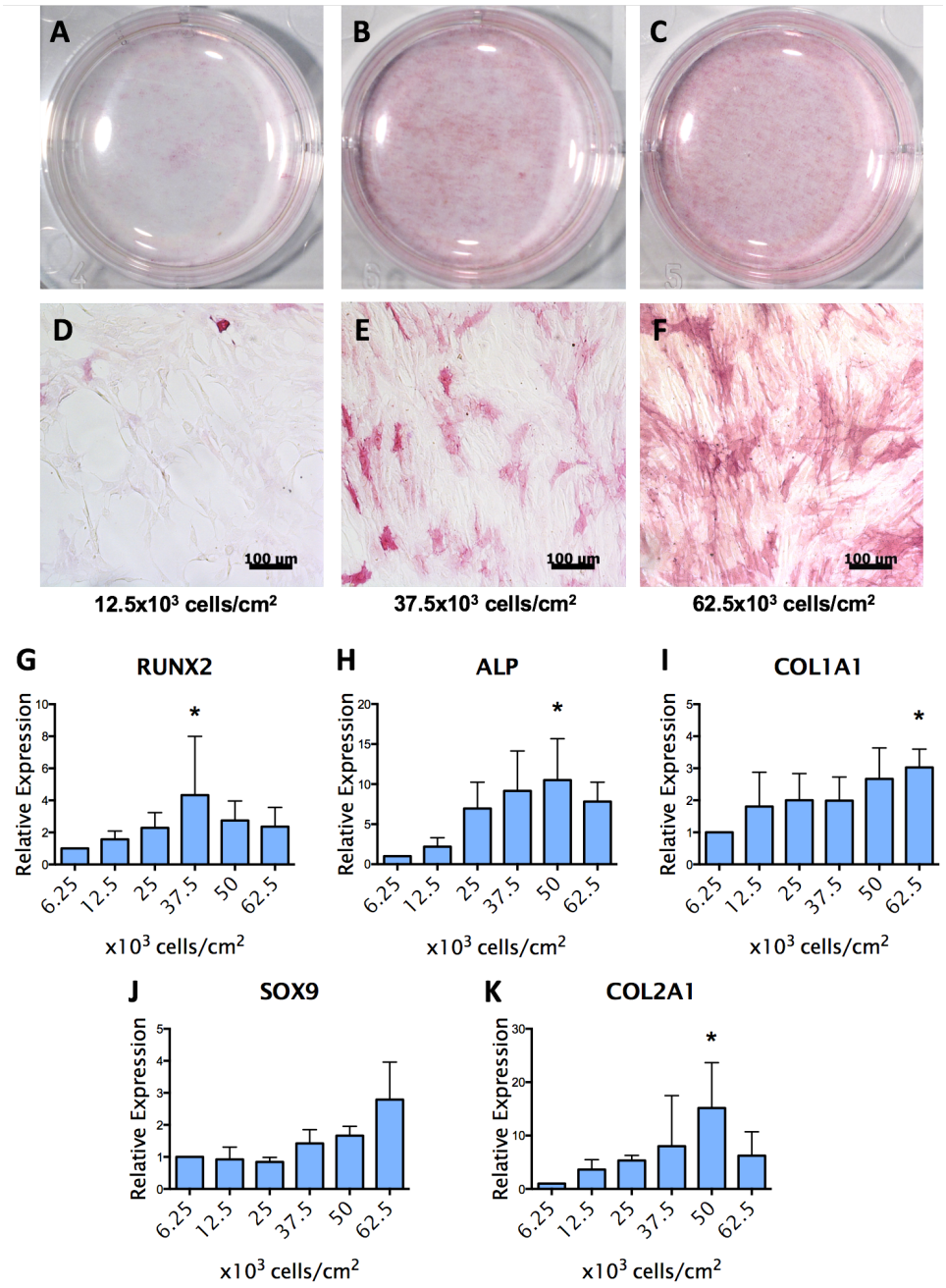


**Figure 4.2. Effects of cell confluence on SSC differentiation.** With increasing cell confluence, increased ALP staining was observed macroscopically (A-C). Microscopy examination revealed only a few cells were positive for ALP staining in culture at 50% confluence (D). 50% of cells were positive for ALP as cells reached 90% confluence within dishes, (E) and 80% of cells at 100% confluent (I). *RUNX2* expression was up regulated when cells reached 90% confluence, followed by up regulation of *ALP* (H) and *COL1A1* (I) as cells reached 100% confluence. No significant change in *SOX9* expression (J) was observed with increasing cell confluence. A 15-fold increase in *COL2A1* expression was observed when cells reached 90-100% confluence and this appeared to rapidly subside as 100% confluence was reached (K). Scale bar = 100 µm. Data represents an average of three independent patient samples, and error bars represent standard deviation. *P<0.05, calculated using ANOVA test.

### 4.2.2 The Effect of Time in Monolayer Culture on Bone Cell Differentiation

With increasing time in monolayer culture, SSC reached confluency and the rate of cell confluence was dependent on the division time of the cell type examined. To assess if increasing cell confluence by time in culture affects osteogenic gene expression in a similar way to increasing confluence, foetal femur-derived cells from three independent patient samples were used. Cells were seeded at $12.5x10^3$ cells/$cm^2$ from day 0. After 4 days in culture, cells were found to be around 50% confluence and by day 6 cells reached 100% confluence. The pattern of *RUNX2* and *ALP* expression was found to be similar to that of the cell confluence experiment. With *RUNX2* expression first to be upregulated when cells reached 90% confluence (Figure 4.3A) and *ALP* expression lagging behind *RUNX2* expression, displaying a 12-fold increase in expression when cells reached 100% confluence (Figure 4.3B). Expression of *COL1A1* was found to fluctuate 1-2 fold and no significant changes in expression were observed during the culture period examined (Figure 4.3C). The pattern for *COL2A1* expression appeared to be similar to *RUNX2* expression over time in culture (Figure 4.3D).

These observations along with the effect of cell confluence on SSC differentiation in culture is critical to the design of a culture model to examine the effects of miRNA overexpression and inhibition in subsequent experiments. Significant expression of osteogenic-related genes, namely *RUNX2*, *ALP* and *COL1A1,* can be demonstrated in four days of monolayer culture when cells are seeded at a higher density. It is also important to note that under monolayer culture, gene expression remains dynamic and follows a temporal fashion and is associated with the level of confluence of the cells in culture.

As foetal femur-derived cells appear to differentiate upon reaching 90% confluence, the monolayer culture model for miRNA functional analysis in the subsequent experiment will be as follow: Cells will be seeded at $5x10^4$ cells/$cm^2$ on day 0 and transfected with miRNA mimics after 48 hours in culture. Cells will be prepared for RNA extraction after another 48 hours following miRNA over expression or inhibition for RT-qPCR gene expression analysis to assess changes in differentiation gene expression.

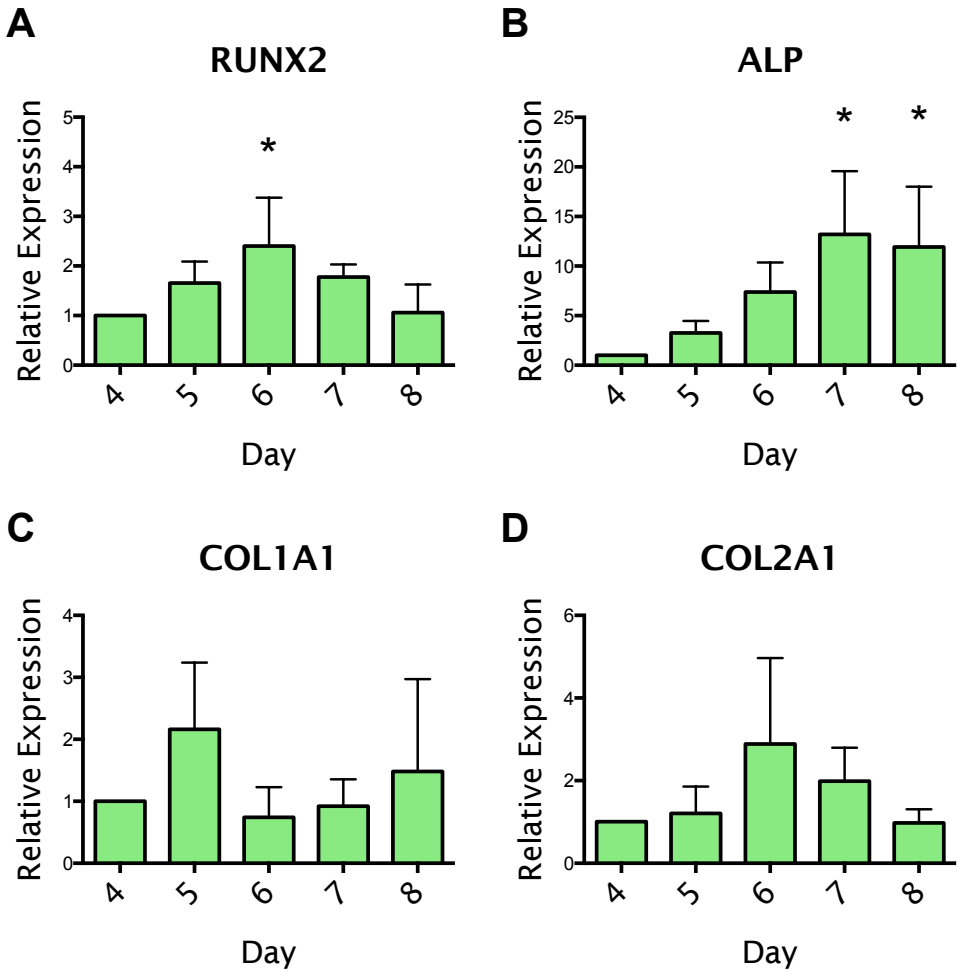


**Figure 4.3. Changes in *ALP*, *RUNX2*, *COL1A1* and *COL2A1* expression with time in culture.** *RUNX2* was observed to be upregulated following 6 days in monolayer culture (A). *ALP* was significantly expressed, although expression was observed to lag behind *RUNX2* expression after 7 days (B). No temporal expression of *COL1A1* was observed (C). *COL2A1* expression displayed a similar pattern to *RUNX2* expression (D). Data represents an average of three independent patient samples, and error bars represent mean +/- standard deviation. *P<0.05 calculated using ANOVA Test.

### 4.2.3 Factors Affecting MicroRNA Expression *in Vitro*

Osteogenic medium supplemented with dexamethasone and chondrogenic medium supplemented with TGF-$\beta_3$ have previously been shown to affect the expression of osteogenic and chondrogenic related genes in foetal femur-derived SSCs (Section 3.2.4). To examine the effects of osteogenic and chondrogenic media on miRNA expression, cells were isolated from three unrelated patient samples and seeded at 50 cells/cm$^2$ into each well of a 6-well plate. Cells were cultured under basal, osteogenic and chondrogenic conditions for 4 days prior to RNA extraction and miRNA RT-qPCR analysis. The change in expression of nine miRNAs following osteogenic and chondrogenic culture was subsequently examined.

Under osteogenic culture, miR-128, miR-98, miR-744, miR-330, miR-93 and miR-195 were found to display an increase in expression (Figure 4.4 A-F). However the increase in expression was modest (1.3-2 fold increase). Following culture under chondrogenic medium supplemented with TGF-$\beta_3$; miR-93, miR-195 and miR-140 (Figure 4.4 E-G) expression was enhanced while miR-146a and miR-146b expression were down-regulated (Figure 4.4 E-I). These results indicate that differentiation medium can simultaneously affect the expression of a various miRNAs, indicating miRNAs are typically co-expressed and may work together to exert a given cellular function.

MicroRNAs shown to be upregulated following osteogenic culture such as miR-128, miR-98, miR-744, miR-330, miR-93 and miR-195 could be involved in promoting osteogenic differentiation; in contrast, miRNAs upregulated by chondrogenic media such as miR-93, miR-195 and miR-140 could play a role in chondrogenesis. Furthermore, miR-93 and miR-195 were shown to be upregulated by both osteogenic and chondrogenic culture conditions and could be involved in regulating cell processes during differentiation such as cell cycle regulation. The role of miR-140 during chondrogenic differentiation has already been reported. MicroRNA-140 expression is upregulated in chondrogenic culture conditions and has been shown to be cartilage specific (expressed in differentiated human articular chondrocytes)(Miyaki et al. 2009); furthermore, miR-140 is known to regulate chondrogenic differentiation through regulation of *SMAD3* protein levels (Pais et al. 2010). microRNA-146a and miR-146b observed to be downregulated following culture in chondrogenic media suggests miR-146a and miR-146b could act as inhibitors of chondrogenesis. However, further experiments are needed to confirm the effects of these miRNAs and their mechanisms of action.

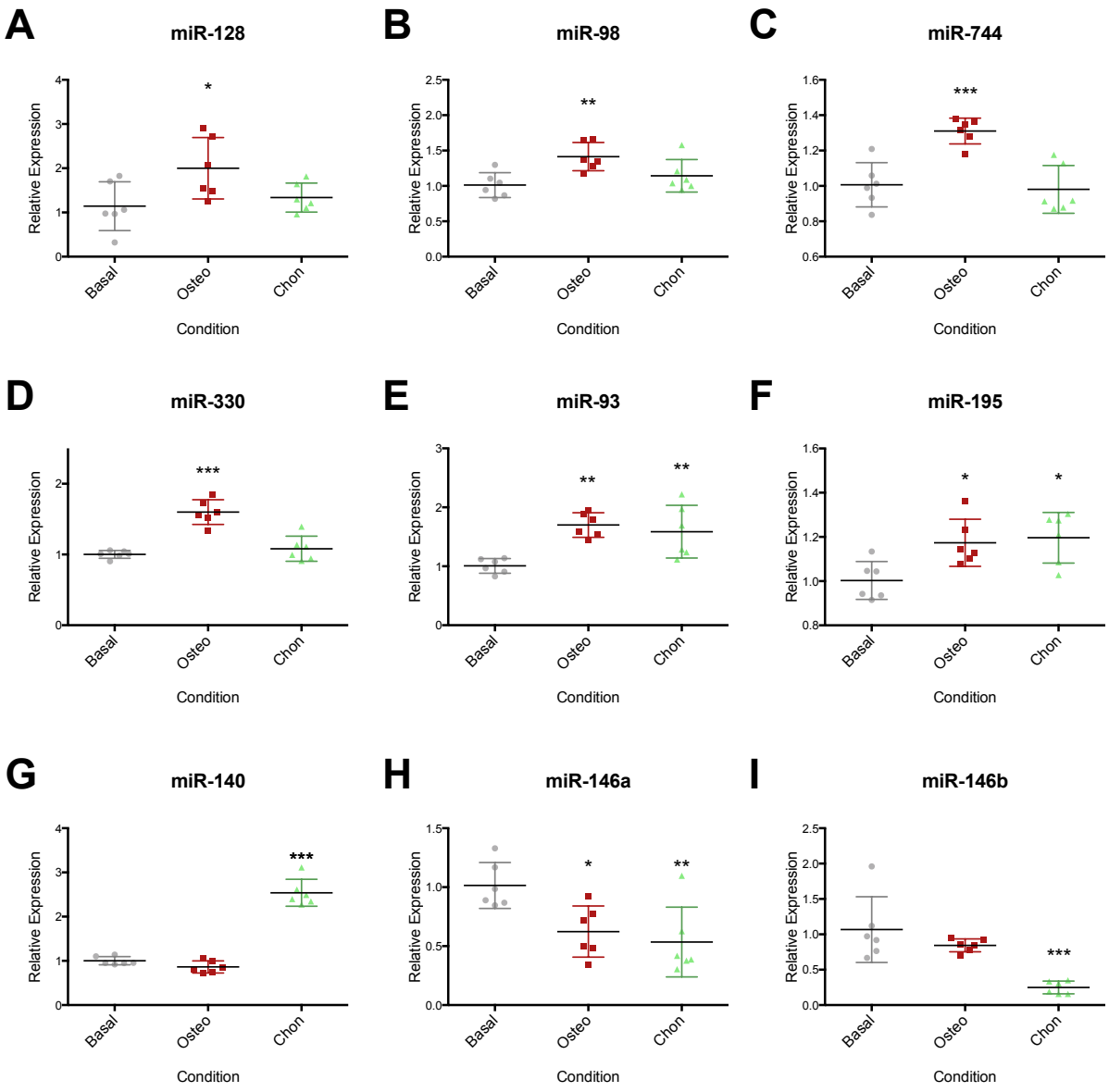


**Figure 4.4. Effects of osteogenic and chondrogenic media on microRNA expression.** miR-128 (A), miR-98 (B), miR-744 (C), miR-330 (D), miR-93 (E) and miR-195 (F) were found to be upregulated following monolayer culture under osteogenic medium. miR-93 (E) and miR-195 (F) were found to be upregulated by both osteogenic and chondrogenic media. Chondrogenic medium increased the expression of miR-140 (G) and reduced the expression of miR-146a and miR-146b. Data represents an average of three independent patient samples, and error bars represent mean and standard deviation. *P<0.05, **P<0.01, ***P<0.001 calculated using ANOVA test.

### 4.2.4 Transfection of Foetal-Derived Skeletal Stem Cells using the Dharmafect™ Transfection System

In order to examine the function of a particular miRNA, investigators typically employ the use of miRNA hairpin inhibitors and miRNA precursor mimics to knockdown or overexpress the miRNA of interest respectively (Eskildsen et al. 2011; Ng et al. 2009). Primary SSCs are known to be difficult to transfect due to their sensitivity to transfection reagents and poor uptake of transfection complexes. Several commercially available transfection protocols and reagents have been examined and tested in foetal femur-derived SSCs during the course of this study, including lipofectamine 2000 and Lonza's Amaxa Nucleofector transfection system (results not shown). However, the results showed either low transfection efficacy or high levels of cell death following transfection. Dharmacon have recently released a new commercially available transfection reagent, DharmaFECT, reported to be specifically designed to provide efficient and reliable transfection of miRNA with lower cellular toxicity. To investigate if DharmaFECT could effectively transfect foetal femur-derived SSCs with miRNA mimics, three independent patient samples were passaged and seeded at $5x10^4$ cells/$cm^2$ on day 0. After 48 hours in monolayer culture to allow cell adherence and expansion, cells were transfected with miRNA mimics labelled with DY 547 and a miRNA mimic positive control designed to target GAPDH. A scrambled miRNA mimic was used as negative control for comparison with treatment groups. 48 hours following miRNA mimic transfection, cells were fixed with 4% PFA for florescence microscopy and RNA was extracted from cells for RT-qPCR analysis.

Cell Tracker Green staining was used to examine cell viability and confirmed the majority of cells were viable. The distribution of miRNA mimics was demonstrated using a miRNA mimic labelled with the fluoresce dye DY 547 (B), and was positive in 100% of viable cells following transfection (Figure 4.5 B and C). A miRNA mimic designed to reduce the *mRNA* level of GAPDH (positive control) was used to assess the functional effect of miRNA overexpression following transfection. 48 hours post positive control miRNA expression, GAPDH expression was shown to be reduced by 80% compared to the negative control. These results indicate that DharamFect is indeed an effective reagent for transfection of miRNA mimics into foetal femur-derived SSCs with reduced cytotoxic readouts.

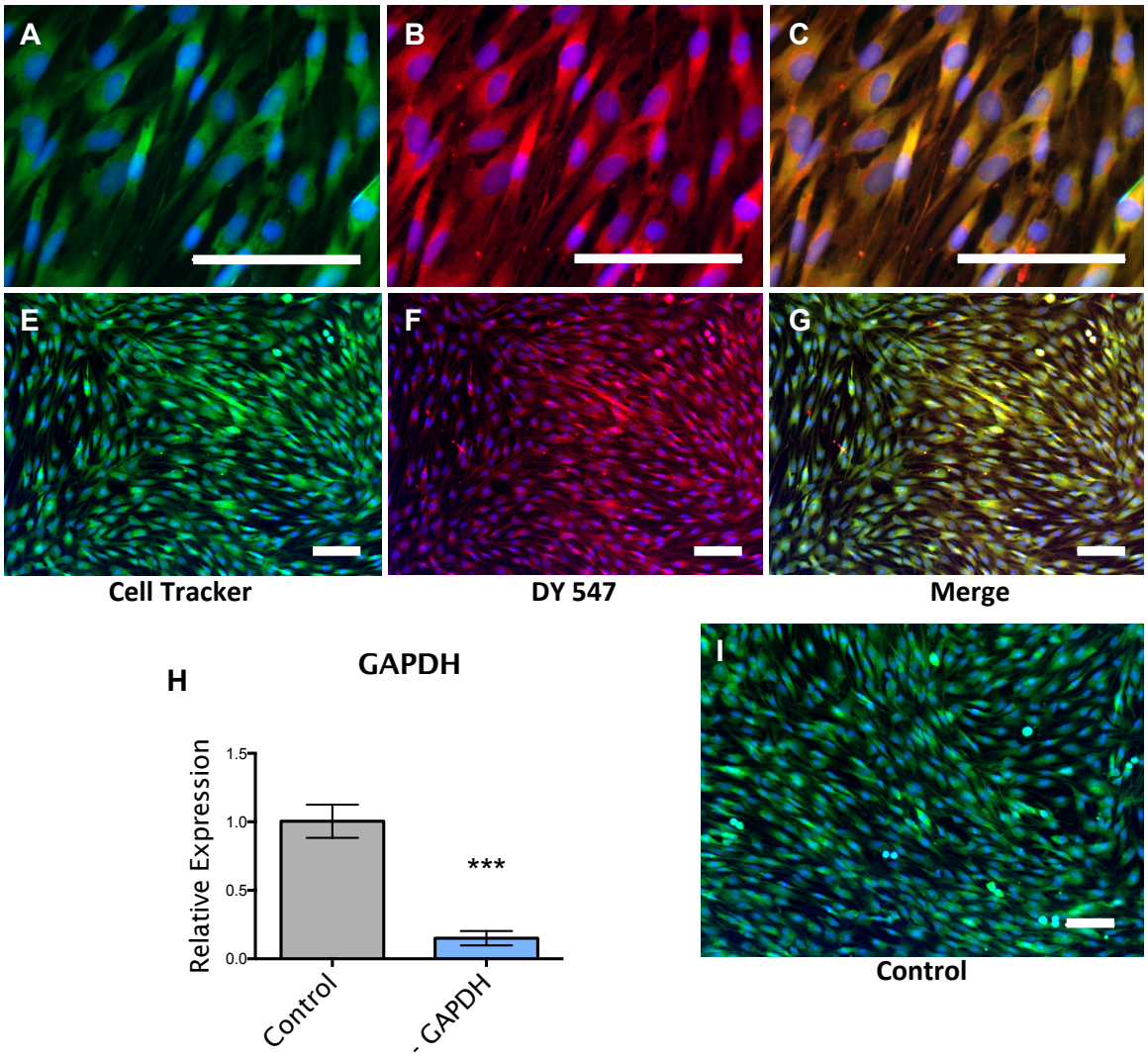


**Figure 4.5. Efficacy of the DharmaFect transfection protocol.** 48 hours post transfection with miRNA mimics, cells appeared to be viable with minimal amount of cell loss as shown by CellTracker Green (A and E) compared to control (I). Transfection of mimic labelled with DY547 revealed all cells were successfully transfected with miRNA mimic (B and F). Merged images of CellTracker green and DY547 confirms miRNA mimic transfected cells remained viable (C and G). An 80% reduction of GAPDH *mRNA* was seen following overexpression of positive control miRNA mimic designed to target GAPDH (H). Scale bar = 100 µm. Data represents an average of three independent patient samples, and error bars represent standard deviation. ***P<0.001 calculated using t-test.

### 4.2.5 Spermine-Pullulan Complex as a MicroRNA Delivery System in Foetal Femur-Derived Skeletal Stem Cells

Kanatani *el al* reported spermine-pullulan complex (S-P) to have a higher transfection efficiency with lowered cytotoxicity compared to cationic lipids such as lipofectamine 2000 in several cell lines (Kanatani et al. 2006). The S-P complex is formed by conjugation of pullulan, a polysaccharide polymer consisting of maltotriose units, with spermine ($C_{10}H_{26}N_4$) through activation of the free hydroxyl groups on the repeating maltotriose units of pullulan using 1,1 carbonyldimidazole. There are nine free hydroxyl groups available on each maltotriose repeating unit of pullulan for spermine conjugation. With different concentrations of 1,1 carbonyldimidazole, the degree of conjugation can be modified. Three different S-P complexes were formed using three different hydroxyl groups to carbonyldimidazole ratio (CDI ratio) namely; S-P CDI 1.5 (low degree of conjugation), S-P CDI 3 (intermediate degree of conjugation) and S-P CDI 4.5 (high degree of conjugation).

Using miRNA mimics labeled with DY547, distribution of S-P-miRNA complex in culture was visualized using florescence microscopy. S-P with a CDI 1.5 ratio formed small complexes with miRNA mimics and appeared to be found predominately in the cytoplasm of transfected cells (Figure 4.6 A). S-P complexes formed using CDI ratio of 3 and 4.5 formed larger complexes and observed both in the cytoplasm and attached to surfaces of transfected cells (Figure 4.6 B and C).

A miRNA mimic designed to knock down GAPDH *mRNA* was used to examine the functional efficacy of miRNA transfection using S-P complex. S-P complex with a CDI ratio of 1.5 appeared to be fast acting with maximum efficacy observed 12 hours following transfection (Figure 4.8 D). However, the effect of the miRNA mimic appeared to reduce 24 hours following transfection (figure 4.6 E–G). A S-P complex with a CDI ratio 3 appeared to maintain the effect of miRNA mimics for longer periods of time (Figure 4.6 H-K). However S-P complex with a CDI ratio of 3 only displayed a maximum reduction of 25% in GAPDH *mRNA* following transfection with miRNA mimic (Figure 4.6 H) compared to a maximum reduction of 40% in GAPDH *mRNA* when S-P with a CDI ratio of 1.5 was used (Figure 4.6 D). S-P complex with a CDI ratio of 4.5 was observed to be strongly cytotoxic (figure 4.6 C), evident by the reduction in cell number with over 70% cell loss following transfection. Therefore, functional analysis was not carried out.

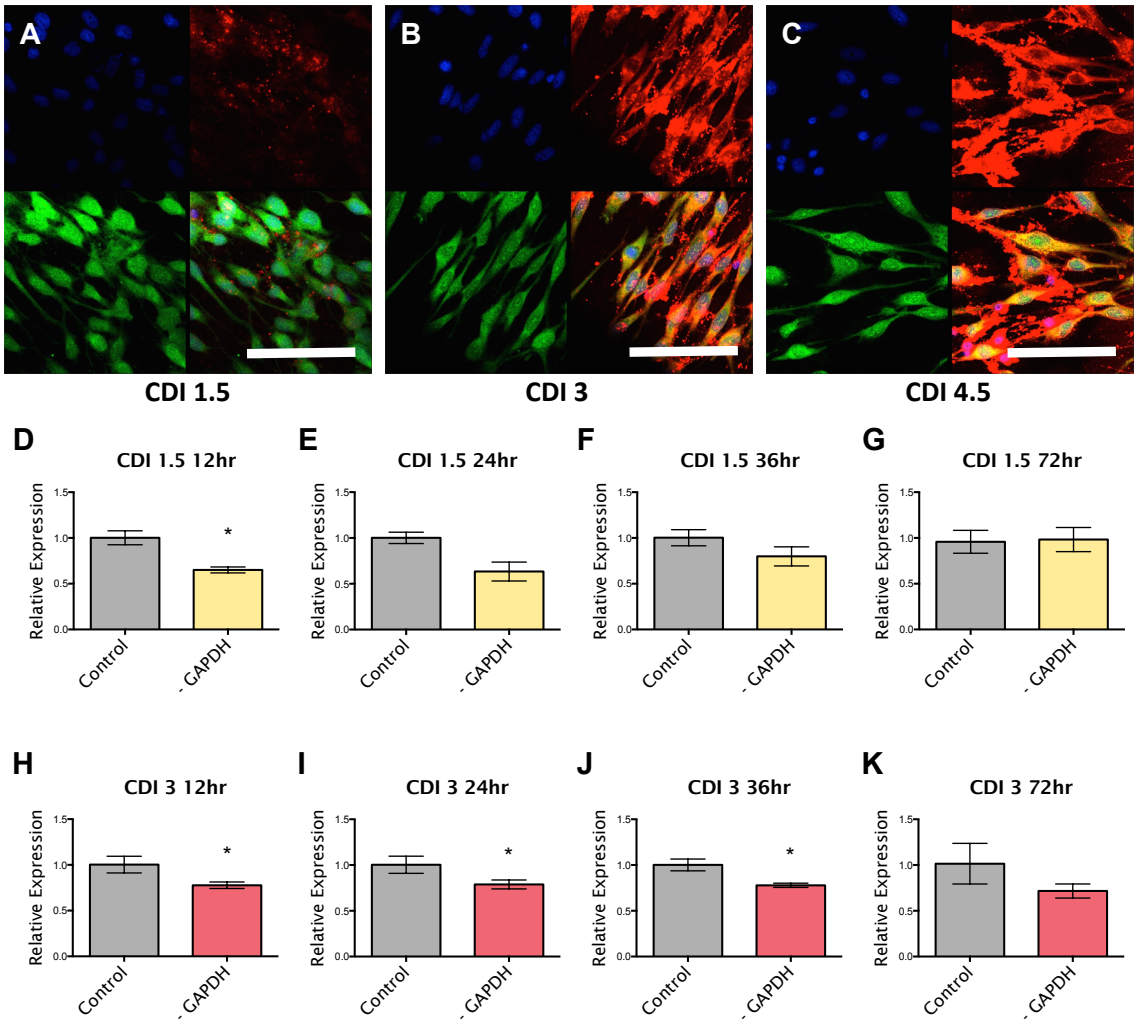


**Figure 4.6. Efficacy of transfection of Spermine-pullulan (S-P) complexes with different CDI ratios.** Nucleus stained blue (DAPI), red represents miRNA mimic labeled with DY547 and viable cells observed by CellTracker Green. S-P with a CDI ratio of 1.5 formed small complexes with miRNA mimics and were found predominately within the cytoplasm of viable transfected cells (A). S-P with a CDI ratio of 3 and 4 formed larger complexes with miRNA mimics and was observed both within the cytoplasm and attached onto the surface of transfected cells (B and C). Transfection of miRNA mimic targeting GAPDH using S-P CDI 1.5 reduced GAPDH *mRNA* by 40% (D) but the effect reduced after 24 hours (E-G). Transfection of miR mimic targeting GAPDH using S-P CDI 3 reduced expression of GAPDH by 25% (H) and was maintained for 36 hours (H-K). Scale bar = 100 µm. Data represents an average of three independent patient samples, and error bars represent standard deviation. *P<0.05 calculated using Mann-Whitney test.

### 4.2.6 Cytotoxicity of Pullulan-Spermine-MicroRNA Complexes

Conjugation of spermine and pulluan cationizes the pullulan molecule allowing it to complex with negatively charged oligonucleotides. The transfection efficacy and cytotoxicity is related to the ratio of nitrogen content of spermine to the phosphate content of the oligonucleotides being transfected (referred to as the nitrogen-phosphate (N/P) ratio). A higher N/P ratio allows more miRNA mimic or inhibitor to be bound to the S-P complex and therefore increases transfection efficacy. However, it has been shown that increasing the N/P ratio is associated with a higher degree of cell loss following transfection (Kanatani et al. 2006). To optimize the best N/P ratio for transfection of foetal femur-derived SSC populations with miRNA mimics and inhibitors, cells from three independent patient samples were passaged and seeded to each well of a six-well plate. After two days in monolayer culture, allowing cell adhesion and proliferation, cells were transfected with a complex of S-P and DY547 miRNA mimic at N/P ratios of 20, 25, 30 and 35. Two days after transfection, cells were labeled with CellTracker Green to examine for cell viability. To quantitatively measure the degree of cell loss following transfection, fluorescence-activated cell sorting (FACS) technique was used to count viable cells in each transfected sample.

Fluorescence microscopy showed cells were viable following transfection of DY547-labeled miRNA mimics (figure 4.9 A-H). S-P synthesized with a CDI ratio of 1.5 (Figure 4.7 A-D) displayed a lower cytotoxic effect on cells compared to S-P synthesized with a CDI ratio of 3 at a given N/P ratio (E-H). With increasing N/P ratio, an increased degree of cell loss was observed. For S-P CDI 1.5, a minimal degree of cell loss was observed at N/P ratios of 20 and 25 (Figure 4.7 A and B). However, cell viability significantly decreases at N/P ratios of 30 and 35 (Figure 4.7 I). For S-P CDI 3, significant cytotoxicity was seen with an N/P ratio of 25 (Figure 4.7 J) with more than 50% cell loss at an N/P ratio of 35 (Figure 4.7 J)

These results show both the N/P ratio and CDI ratio is important in determining the cytotoxicity of S-P complex. Together with the previous results in section 4.8, S-P with a CDI of 1.5 will be used with an N/P ratio of 25 to carry out functional analysis in subsequent experiments (as this combination appears to provide the highest level of miR mimic function and lowest degree of cell loss following transfection).

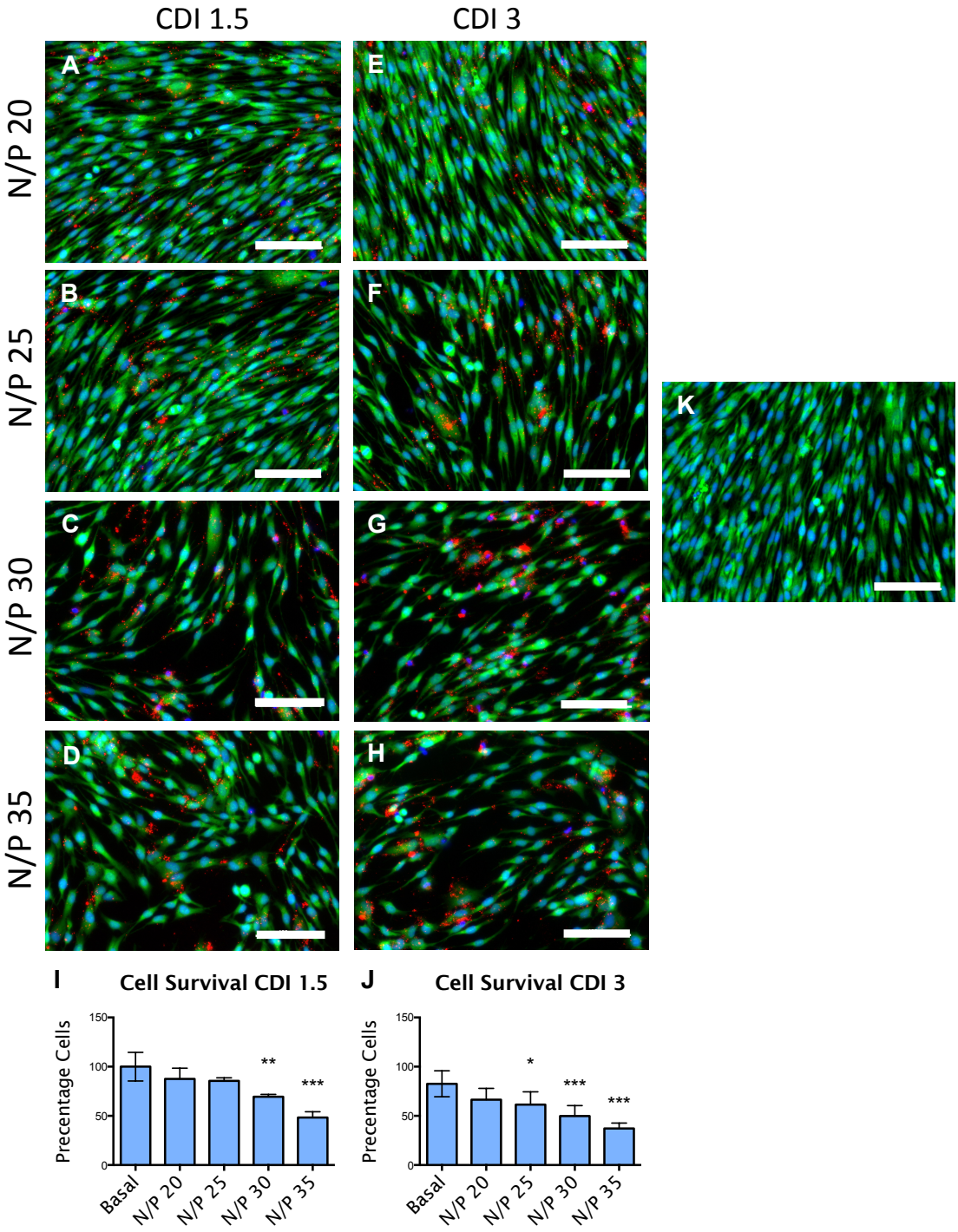


**Figure 4.7. Cell survival following transfection with S-P complex at different N/P ratios.** S-P with a CDI ratio of 1.5 (A-D) displayed less cytotoxicity compared to S-P with a CDI ratio of 3 (E-H) at a given N/P ratio. With increasing N/P ratios, an increased degree of cell loss was observed (A-H). FACS analysis revealed a significant degree of cell loss when an N/P ratio above 25 was used with S-P CDI 1.5 (I). For S-P with a CDI ratio of 3, significant cell loss was seen when an N/P ratio above 20 was used (J). Scale bar = 100 µm. Data represents an average of three independent patient samples, and error bars represent standard deviation. *P<0.05, **P<0.01 and ***P<0.001 calculated using ANOVA test.

### 4.2.7 Regulation Osterix Expression in Foetal Femur-Derived Skeletal Stem Cells Using Spermine-Pullulan and MicroRNA-138 Mimic and Inhibitor

MicroRNA-138 has been identified as an negative regulator of osteogenic differentiation through targeting focal adhesion kinase (*FAK*) and the subsequent downregulation of the function of Osterix (Eskildsen et al. 2011). To examine if osteogenesis can be enhanced or inhibited using S-P complex bound with miR-138 inhibitor and mimics, three unrelated foetal femur cell populations were used. Cells were seeded at 50,000 cells/cm$^2$ into each well of a six-well plate at day 0, and cells were cultured for 2 days prior to transfection with miR-138 inhibitor and miR-138 mimic using an S-P CDI ratio of 1.5 and an N/P ratio of 25. Cells were extracted and prepared for RNA extraction and subsequent RT-qPCR analysis to examine if a change in osteogenic-related gene expression could be observed. Following transfection with miR-138 inhibitor, Osterix was up-regulated while overexpression of miR-138 significantly reduced the expression of Osterix (Figure 4.8 A and B), consistent with previous reports identifying miR-138 as a negative regulator of osteogenesis by targeting up-stream inducers of Osterix. However, no significant change in *RUNX2* expression was observed following inhibition or overexpression of miR-138 (Figure 4.8 C and D). In addition, no significant change in *ALP mRNA* level was observed following transfection with miR-138 inhibitor (Figure 4.8 E). However, overexpression of miR-138 downregulated *ALP* expression (Figure 4.8 F). These observations suggest Spermine-Pullulan complex along with miR inhibitor and mimic can potentially be used to modify osteogenic differentiation in foetal femur-derived SSC populations.

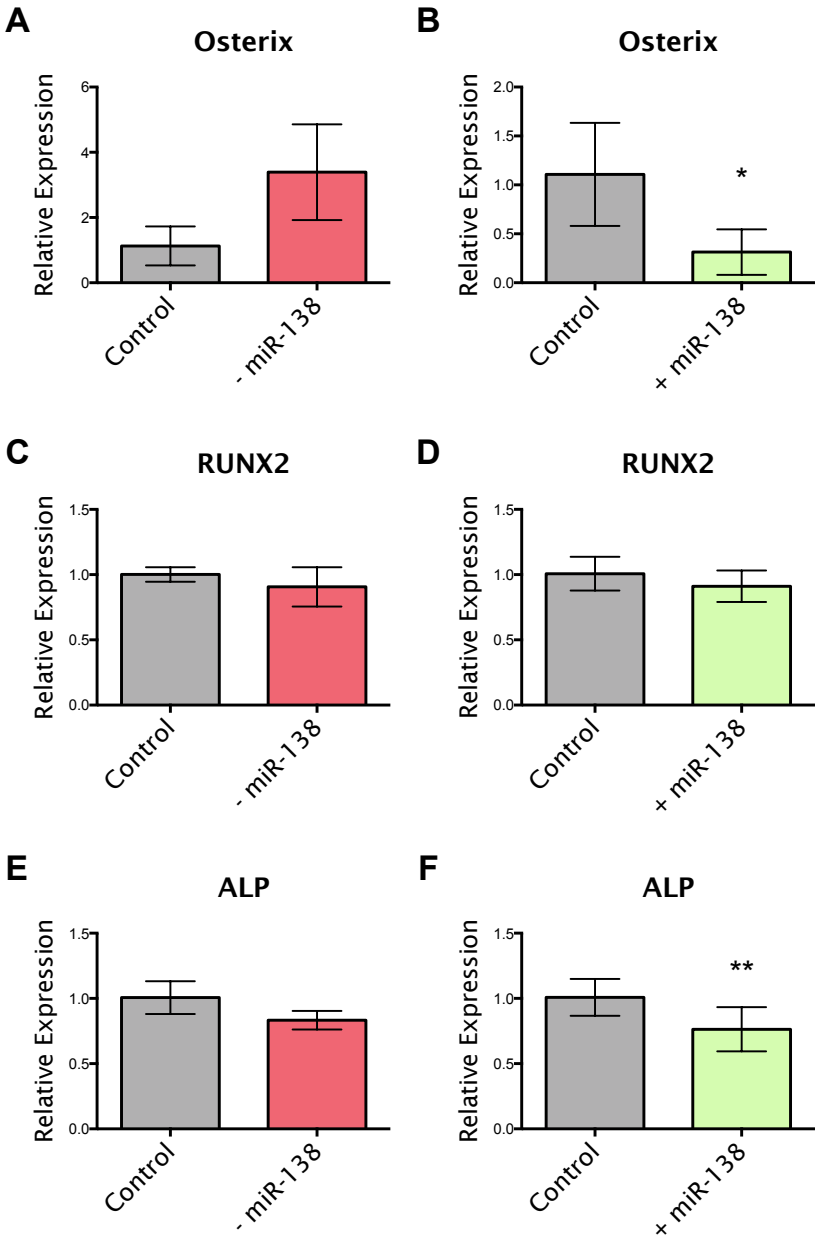


**Figure 4.8. Effects of microRNA-138 overexpression and inhibition on Osterix, *RUNX2* and *ALP* expression.** 48 hours following transfection with miR-138 inhibitor, Osterix expression appeared to be increased (A) while miR-138 mimic significantly reduced Osterix *mRNA* levels, consistent with the recent study by Eskildsen *el al*. However, no differences in *RUNX2* expression were observed following miR-138 overexpression (C) and inhibition (D). There was no significant change in *ALP* expression with miR-138 inhibitor (E). *ALP* expression appeared to be downregulated by 25% following miR-138 overexpression (F). Data represents an average of three independent patient samples, and error bars represent standard deviation. *P<0.05, **P<0.01 calculated using t-test.

### 4.2.8 MicroRNA Functional Analysis in Skeletal Stem Cells Using Spermine-Pullulan Complex

Although a number of miRNAs have been shown to either be upregulated or downregulated during osteoblast differentiation, only a few miRNAs are significantly altered and could be potential targets involved in skeletal development. In this study, miR-143, miR-145 and miR-128 were selected for functional analysis to assess if these miRNAs played a role in osteogenic differentiation. Foetal femur-derived SSCs were isolated as previously described. Using the S-P-based transfection protocol and the cell culture model derived from previous sections (4.2.5 and 4.2.6), cells were transfected with miR-143, miR-145 and miR-128 mimics and inhibitors to overexpress and or inhibit each miRNAs' function. RT-qPCR analysis was then performed to examine if a change in osteogenic-related gene expression following transfection was present.

Inhibition and overexpression of miR-143 and miR-145 had similar effects on osteogenic gene expression. Other reports have already identified miR-143 and miR-145 as functionally related and typically co-expressed and indeed to regulate smooth muscle cell fate and plasticity (Elia et al. 2009). Furthermore, miR-143 and miR-145 have been identified to be involved in the development of colorectal cancers where a downregulation of miR-143 and miR-145 was observed in adenoma formation, suggesting these miRNAs are important in maintaining the differentiated state in a cell or in regulating cell cycle (Akao et al. 2010; Sachdeva & Mo 2010).

Following inhibition of miR-143, a reduction in *RUNX2* and *ALP* was observed (Figure 4.9 A and C) and overexpression increased the expression of *RUNX2* and significantly up-regulated *ALP* (Figure 4.9 B and D) indicating miR-143 may play a role during osteogenic differentiation. However, no changes in *COL1A1* and *COL2A1* were observed following both inhibition and overexpression of miR-143 (Figure 4.9 E-H). The related miRNA, miR-145, appeared to have a similar effect to miR-143 following transfection. Inhibition of miR-145 down-regulated the expression of *RUNX2* and a significant reduction in *ALP mRNA* was observed (Figure 4.10 A and C). Overexpression of miR-145 appeared to have the reverse effect to miR-145 inhibition, increasing the expression of both *RUNX2* and *ALP* (4.10 B and D). Similar to miR-143, both inhibition and overexpression of miR-145 did not affect the expression of *COL1A1* and *COL2A1* (Figure 4.10 E-H). These observations suggest miR-143 and miR-145 are related miRNAs with a role in affecting the differentiation of foetal femur-derived SSC populations.

MicroRNA-128 has previously been shown to be highly expressed in neuronal tissue and is known to inhibit glioma proliferation and self-renewal (Cui et al. 2009). MicroRNA-128 was selected for functional analysis, given that it was one of the miRNAs found to be upregulated following culture

under osteogenic conditions. Cells transfected with miR-128 inhibitor displayed reduced Osterix expression while overexpression of miR-128 increased the expression of Osterix (Figure 4.11 A and B). Since Osterix is essential in osteoblastogenesis and bone formation (Nakashima et al. 2002), miR-128 could act to promote osteogenic differentiation. Furthermore, *RUNX2*, another important gene in osteogenic differentiation was downregulated following miR-128 inhibition and upregulated following miR-128 overexpression. These observations suggest miR-128 could be involved in SSC osteogenic differentiation. However, it is important to note that no changes in *ALP* expression were observed following transfection with the miR-128 mimic and inhibitor; indicating, possibly, that miR-128 could be involved only during early osteoblast differentiation.

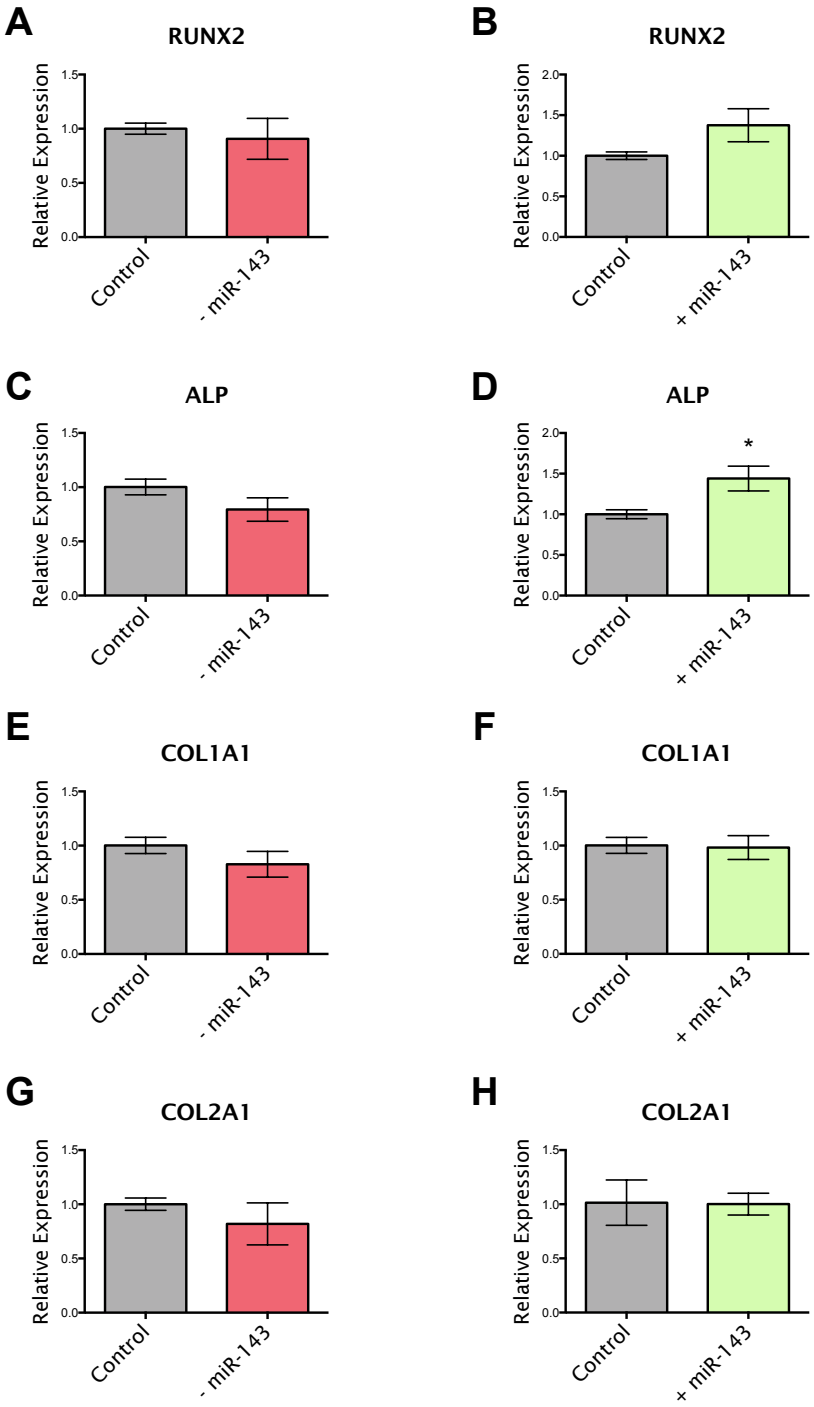


**Figure 4.9. Changes in *RUNX2*, *ALP*, *COL1A1* and *COL2A1 mRNA* level following transfection with miR-143 mimic and inhibitor.** No significant changes in expression in *RUNX2* and *ALP* were seen following transfection with miR-143 inhibitors using S-P complex (A and C). Overexpression of miR-143 appeared to increase the expression of *RUNX2* (B) and significantly up-regulate the expression of *ALP* (D). No changes in *COL1A1* and *COL2A1* were observed following miR-143 overexpression and inhibition (E-H). Data represents an average of three independent patient samples, and error bars represent standard deviation. *P<0.05 calculated using t-test.

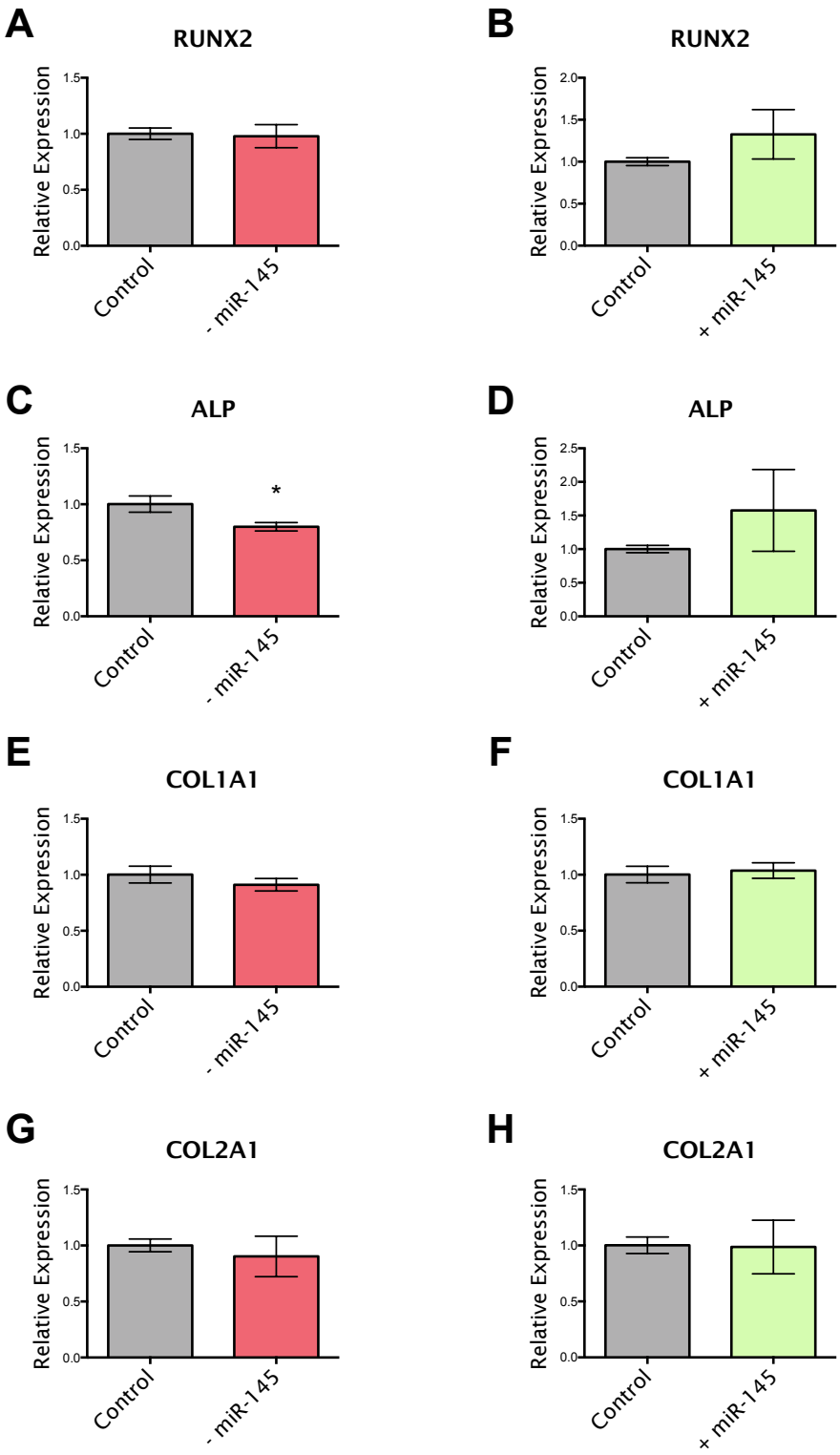


**Figure 4.10. Changes in *RUNX2*, *ALP*, *COL1A1* and *COL2A1 mRNA* level following transfection with miR-145 mimic and inhibitor.** No significant changes in *RUNX2* expression were seen following overexpression or inhibition of miR-145. Inhibition of miR-145 significantly reduced the expression of *ALP* (C) and overexpression of miR-145 appeared to increase the expression of *ALP* (D). Data represents an average of three independent patient samples, and error bars represent standard deviation. *P<0.05 calculated using t-test.

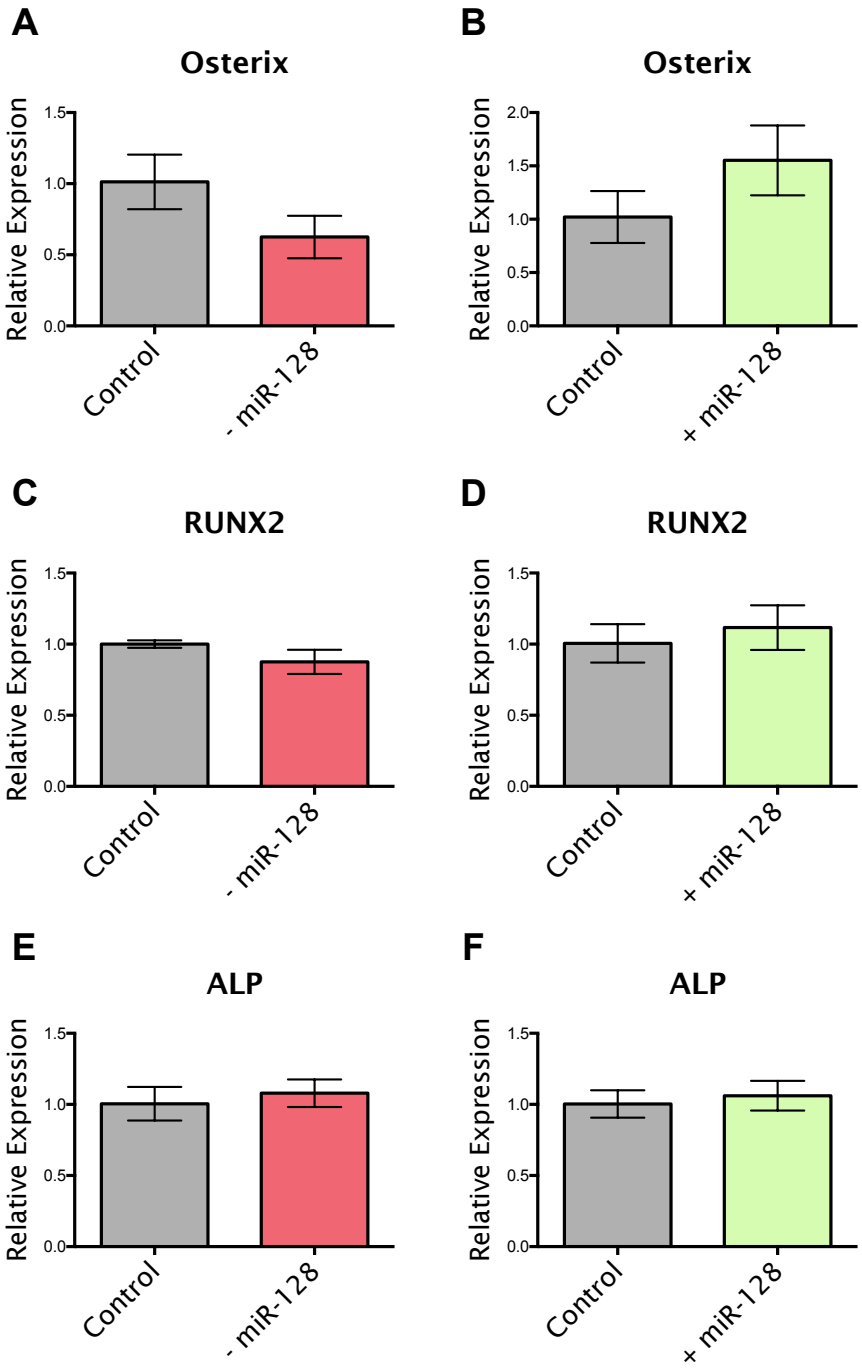


**Figure 4.11. Effect of miR-128 overexpression and inhibition on SSC osteogenic gene expression.** Inhibition of miR-128 decreased the level of Osterix (A) while overexpression appeared to upregulate Osterix expression (B). No changes in *RUNX2* expression were observed following miR-128 inhibition (C), but *RUNX2* was up-regulated following miR-128 overexpression (D). Neither miR-128 overexpression nor inhibition affected *ALP mRNA* levels (E-F). Data represents an average of three independent patient samples, and error bars represent standard deviation. *P<0.05 calculated using t-test.

## 4.3 Discussion

Stem cells differentiate in response to various factors such as soluble factors, paracrine stimulations and micro-environmental cues (Tang et al. 2010). Recently, miRNAs have been shown to be involved in orchestrating SSC differentiation and self-renewal. MicroRNA profiling methods are typically used to identify miRNAs involved in a given cellular function (Dong et al. 2012). To elucidate the function of a particular miRNA, investigators typically use miRNA inhibitors and mimics to inhibit or over-express the miRNA under investigation in order to investigate the mechanism / function. To robustly investigate the function of miRNAs in SSC differentiation *in vitro*, appropriate cell culture models are required to promote active differentiation together with a transfection protocol to enable cell transfection with miRNA inhibitors and mimics.

In this study, cells were observed to begin to differentiate once a critical level of cell confluence was reached. This observation is consistent with current literature reporting cell-to-cell contact induces SSC differentiation (Tingzhong Wang et al. 2006). For foetal femur-derived skeletal stem cell populations, cells were shown to commence the differentiation process when monolayer cultures reached 90% confluence. The cell responsible for bone formation, the osteoblast, produces bone matrix including type I collagen, Osteocalcin and high levels of membrane-bound enzyme *ALP*, which plays a role in matrix mineralization (W.-Y. Baek & J.-E. Kim 2011). The expression of *RUNX2*, *ALP* and *COL1A1* were shown to be expressed in a stepwise fashion once the cells reached 90% confluence, suggesting cells are actively undergoing differentiation. During this time, it is likely the various mechanisms promoting SSC differentiation are activated affording an opportunity to interrogate the function of miRNAs involved in differentiation. Furthermore, culture medium supplemented with dexamethasone and ascorbic-2-phosphate is known to promote osteogenic differentiation in SSC; whilst medium supplemented with TGF- $\beta_3$, ascorbic-2-phosphate, dexamethasone and Insulin-transferrin-sodium promotes chondrogenic differentiation (Ravindran et al. 2011) (Tenenbaum & Heersche 1985) and affects the expression of various miRNAs. Following culture in osteogenic and chondrogenic media, nine miRNAs displayed a change in levels of expression; miR-128, miR-98, miR-744 and miR-330 were upregulated in osteogenic media. miR-140, previously reported as a cartilage-specific miRNA (Miyaki et al. 2009), was upregulated following culture under chondrogenic media, consistent with current literature on miR-140 function (Miyaki et al. 2009). MicroRNA-146a and miR-146b were found to be downregulated following culture under chondrogenic medium and may be negative regulators of chondrogenesis. Finally, miR-93 and miR-195 were non-specifically upregulated following culture under differentiation medium, suggesting regulation of other important genes, such as housekeeping genes, during differentiation. However, the exact function of these miRNAs is still unknown and will require further experimentation to elucidate their role during SSC differentiation.

Primary SSCs are known to be difficult to transfect due their sensitivity to transfection reagents and poor uptake of the transfection complex. Through a series of transfection optimization experiments, a commercially available liposome-based transfection reagent, DharmaFect, was shown to be effective in transfecting miRNA mimics into foetal femur-derived SSCs, and a transfection protocol was developed. However, liposome-based transfection reagents typically need to be used as particles dispersed in a liquid culture medium. Such an approach limits their use as a miRNA-based gene delivery system in solid scaffolds used in bone tissue engineering applications {Bose:2012dg}. S-P incorporated into succinylated gelatin-based scaffold has been shown to successfully deliver plasmid DNA into bone marrow-derived SSCs (Kido et al. 2011). Furthermore, it has been shown that S-P can be electrostatically pre-adsorbed onto cell culture plates, allowing transfection to proceed directly from the solid culture support into subsequent seeded cells rather then using particles dispersed in culture medium (Thakor et al. 2011). The ability of S-P to be incorporated into solid materials suggests S-P could be used in tissue engineering scaffolds to deliver gene therapy to promote osteogenic differentiation.

This chapter aims to examine a *de novo* transfection system to deliver miRNA mimic and inhibitors to promote SSCs stem cell differentiation through miRNA functions. S-P has been shown to be an effective reagent for transfecting plasmid DNA into various cell lines (Kanatani et al. 2006). However, S-P complex appeared to be less efficient in delivering miRNA mimics and inhibitors compared to liposome-based transfection reagents. The S-P transfection protocol requires optimization of various parameters such as molecular weight of pullulan, the degree of conjugation of pullulan with spermine and the nitrogen-phosphate ratio between S-P complex and oligonucleotide used. Since the mimics and inhibitors used in this study were obtained commercially rather then synthesized in house, the exact chemical make up of the molecules used was unknown. Thus, only an assumed phosphate content based on the number of nucleotide of the mature miRNA sequence was used to calculate N/P ratio and this could introduce errors when calculating the exact N/P ratio. Furthermore, the different molecular weights of pullulan used to synthesize S-P complex could have an effect on transfection efficacy and were not examined due to technical limitations. Nonetheless, the S-P complex has been shown to deliver miRNA mimics and bring about a functional change as exhibited by transfection of miRNA mimic designed to target GAPDH *mRNA* in foetal femur-derived SSCs. Differently conjugated spermine and pullulan and different sized complexes were synthesized and could be tailored to modulate miRNA transfection. Since S-P with a higher CDI ratio formed larger complexes, it is possible that increased amount of miRNA mimics can be bound to the larger complex and released slowly over longer period of time. However, further experiments are needed to investigate the factors affecting the release of bio-active miRNA inhibitors or mimics and to optimize S-P as a transfection reagent for miRNA delivery.

Various miRNAs have been identified to play a role in regulating SSC differentiation and this could be used to promote osteogenesis and chondrogenesis in tissue engineering. MicroRNA-138 has been identified as a negative regulator of hMSC osteoblast differentiation through downregulation of *FAK* and, subsequently, *RUNX2* and Osterix expression (Eskildsen et al. 2011) since Osterix is known to promote osteogenic differentiation in SSCs (Nakashima et al. 2002). Cells transfected with miR-138 inhibitor were shown to secrete increased levels of bone matrix in an *in vivo* culture model (Eskildsen et al. 2011). To assess if S-P could increase osteogenic differentiation by delivering miRNA mimics into SSCs, foetal femur-derived cells were treated with S-P complex bound with miR-138 inhibitor and mimics. Transfection of miR-138 mimic using S-P resulted in decreased expression of Osterix while transfection of miR-138 inhibitor increased Osterix *mRNA* level. This suggests S-P miRNA mimic or inhibitor complex could potentially be used to attenuate osteogenic differentiation. However, the change in osteogenic expression following transfection was not as dramatic as previously reported by Eskildsen *et al* (Eskildsen et al. 2011). This could be related to the efficacy of S-P for miRNA transfection. Furthermore, the miR-138 inhibitor appeared to be less effective in modulating Osterix expression than miR-138 mimics when used with S-P complex. These observations suggest the S-P complex may be less effective in delivering miR inhibitor into cells.

MicroRNA-143 and miR-145 are thought to be related miRNAs, usually co-expressed and have been described as "anti-oncomirs" since the loss of expression of miR-143 and miR-145 results in adenoma formation in colorectal cancer (Akao et al. 2010). Furthermore, knockdown of miR-143 and miR-145 has been shown to alter smooth muscle cell maintenance and vascular homeostasis (Cordes et al. 2009), suggesting miR-143 and miR-145 play a central role in differentiation. The loss of miR-143 and miR-145 is associated with a reversion of a differentiated phenotype (Akao et al. 2010; Elia et al. 2009; Xin et al. 2009). Following inhibition of miR-143 and miR-145 in differentiating SSC populations, a modest reduction in *RUNX2* and *ALP mRNA* expression was observed. Conversely, overexpression of miR-143 and miR-145 resulted in increased expression of both *RUNX2* and *ALP*. However, only a modest change in expression was observed. MicroRNA-128 was observed to be upregulated following culture in osteogenic media and was selected for functional analysis. Following inhibition of miR-128, a reduction in Osterix was observed; while overexpression appeared to increase the expression of Osterix and *RUNX2*. However, the effect of miR-128 on Osterix and *RUNX2* expression was limited and did not reach statistical significance. Previous studies have shown that individual miRNAs are known to only exert a relatively small effect on protein translation (D. Baek et al. 2008), and miRNAs are thought to work in conjunction with other miRNAs to exert a given cellular function. Therefore, it is likely that miR-143, miR-145 and miR-128 could play a supportive role, but may not be key players in osteogenic differentiation.

## 4.4 Conclusion

A culture model with cells undergoing active differentiation and an effective transfection protocol is a prerequisite for experiments designed to interrogate miRNA functional analysis. Through examination of cell confluence, time in culture and the use of differentiation medium, this study has derived a monolayer culture model to study the effects of miRNA during SSC differentiation. Through trial and error, SSCs were successfully transfected with miRNA mimics using a liposome-based transfection reagent. An attempt was made to design a new and versatile transfection reagent: spermine – pullulan complex. The ultimate aim is to be used in solid tissue engineering scaffolds to deliver miRNA-based gene therapy to promote SSC osteogenic differentiation *in vivo*. However, the spermine – pullulan complex as a miRNA delivery system still requires considerable development and further optimisation. In addition, protocols will need to be developed to increase the transfection efficacy. MicroRNA-143, miR-145 and miR-128 functional analysis suggest these miRNAs may play a role during SSC osteogenic differentiation. However, only a small change in differentiation related gene expression was seen following inhibition and overexpression of these miRNAs, suggesting only a supportive role during SSC osteogenic differentiation. Functional analysis data for miR-143, miR-145 and miR-128 should be interpreted with caution, given a sub-optimal transfection system was used to inhibit and overexpress these miRNAs.

# Chapter 5: MicroRNA-146a Regulates Skeletal Stem Cell Differentiation Through *SMAD2* and *SMAD3*

## 5.1 Introduction

Skeletogenesis is a multistep process and is orchestrated by various factors including transcription factors and microenvironment signals (Nakashima et al. 2002; Tou et al. 2003; W.-Y. Baek & J.-E. Kim 2011). A number of growth factors, signaling molecules and transcription factors have been shown to affect skeletal stem cell and osteoprogenitor cell activity including members of the TGF-β families (Alliston 2001; Kitisin et al. 2007). Furthermore, a number of miRNAs have been reported to be involved in the regulation of osteogenesis and chondrogenesis through their ability to regulate transcription factors. For example, miR-140 has been reported as a cartilage-specific miRNA and to promote chondrogenic differentiation by increasing the expression of *RUNX2*, through downregulating HDAC4 (Miyaki et al. 2009). MicroRNA-138 was reported to be a negative regulator of osteogenic differentiation through inhibition of the expression of Osterix via targeting the up-stream target focal adhesion kinase (*FAK*) (Eskildsen et al. 2011). Thus, an understanding of the interactions of specific miRNAs with signaling pathways and growth factors that modulate bone cell function offers new strategies to manipulate SSC differentiation, enhancing our understanding of bone physiology and function critical in a reparative approach.

Work in the previous chapter showed a higher miR-146a expression in the diaphyseal cell populations, suggesting an important role of miR-146a during foetal skeletal development and, more specifically, osteogenesis. Through target analysis, miR-146a was found to target *SMAD2* and *SMAD3 mRNA* 3'-UTR, suggesting miR-146a may function through attenuation of the TGF-β pathway. This chapter aims to demonstrate the importance of miR-146a during human foetal femur development and validate the function of miR-146a in foetal femur-derived SSC populations.

### 5.1.1 Hypothesis

MicroRNA-146a was found to be highly expressed in the diaphyseal cell population and is hypothesized to display have a spatial expression in the whole foetal femur. *SMAD2* and *SMAD3* are putative targets of miR-146a, and increased expression of miR-146a is expected to reduced the expression of *SMAD2* and *SMAD3 mRNA* and protein translation. Overexpression of miR-146a is anticipated to result in a downregulation of chondrogenesis and may promote osteogenesis.

### 5.1.2 Aims and Objectives

- To assess the spatial expression of miR-146a in whole foetal femur.
- To assess the correlation between miR-146a expression with the expression levels of *SMAD2*, *SMAD3*, osteogenic and chondrogenic related genes.
- To confirm *SMAD2* and *SMAD3* as targets of miR-146a.
- To assess the effects of miR-146a overexpression on epiphyseal cell populations.
- To assess the effects of miR-146a overexpression on gene expression when epiphyseal cells were stimulated with TGF-β3.

## 5.2 Results

### 5.2.1 MicroRNA-146a Expression and Osteogenesis

To assess the spatial expression of miR-146a within human foetal femurs, whole foetal femurs were fixed and stained for miR-146a using *in-situ* hybridization. Due to the availability of foetal femur samples, only one patient sample was used.

Previous results have shown that the human foetal femur is comprised of a cartilaginous matrix rich in proteoglycan with a developing bone collar (Figure 5.1A). In-situ hybridization revealed that miR-146a was expressed at the known centers of ossification in the femur, namely the head, the greater and lesser trochanter, the body and the condyles of the femur (Figure 5.1 B). This observation suggests miR-146a may play a role in regulating osteogenesis and patterning the femur in skeletal development.

Previous results indicated that cells extracted from the epiphyseal of the foetal femur have an affinity to differentiate towards the chondrogenic lineage while cells in the diaphyseal have an affinity to differentiate along the osteogenic lineage with an increased expression of miR-146a. Target analysis revealed *SMAD2* and *SMAD3 mRNA*, important transducers of the TGF-β pathway, contain a seed region for miR-146a. The following study set out to examine whether a correlation exists between miR-146a expression and levels of *SMAD2*/ *SMAD3 mRNA*.

Epiphyseal and diaphyseal cells were isolated from three unrelated patient samples. Following 7 days in monolayer culture under basal conditions, RNA was extracted from each individual sample for gene expression analysis. MicroRNA-146a was found to be expressed at an increased level by the osteogenic diaphyseal cell populations (Figure 5.2 A). The increased expression of miR-146a was correlated with a reduced level of *SMAD3* but not *SMAD2 mRNA* (Figure 5.2 B and C). The increase in miR-146a and decrease in *SMAD3 mRNA* in diaphyseal cell populations was found to be associated with an increased expression of genes associated with osteogenesis, namely *RUNX2* and *ALP* (Figure 5.2 D and E), and a reduced expression of the chondrogenesis-related gene *SOX9* (Figure 5.2 F). This observation in gene expression suggests miR-146a may act as an inhibitor of chondrogenesis and promote osteogenic differentiation through attenuation of the TGF-β pathway by downregulating *SMAD3*.

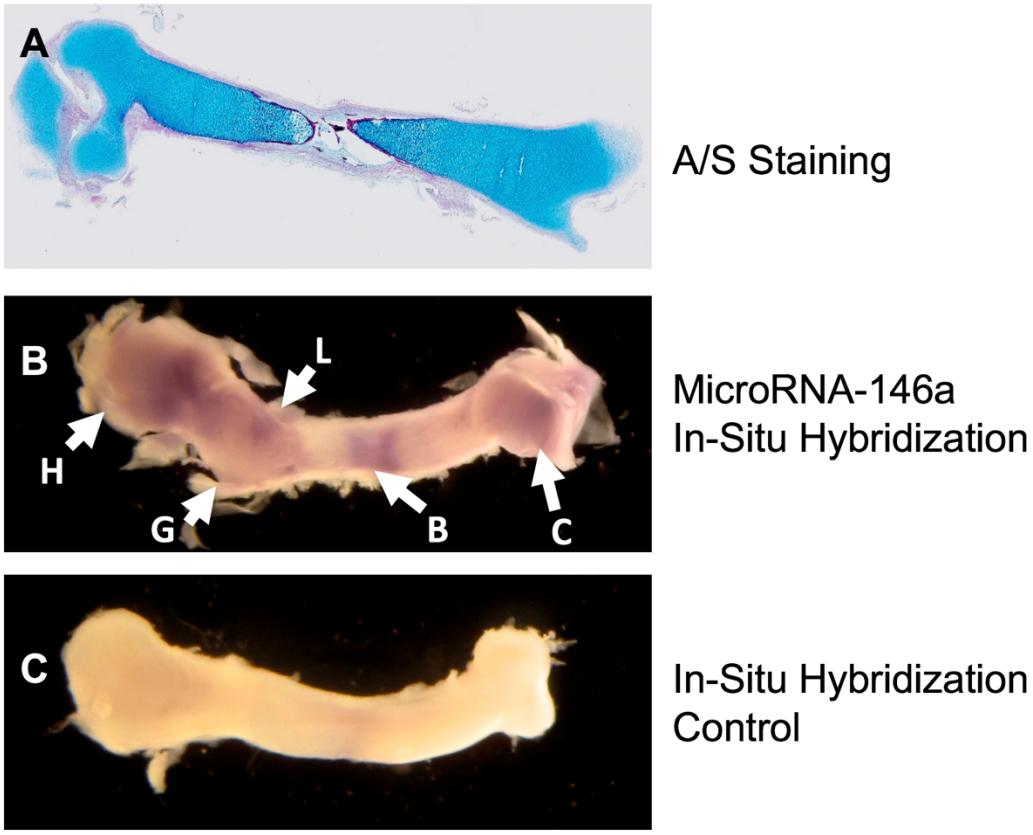


**Figure 5.1. Spatial expression of miR-146a in whole foetal femur.** Foetal femur comprised of a cartilaginous matrix rich in proteoglycan with a developing bone collar in the diaphyseal region shown by Alcian blue and Sirius red staining (A). MicroRNA-146a appeared to be expressed in centers of ossification of the femur, namely: the head (arrow H), the greater trochanter (arrow G), the lesser trochanter (arrow L), the body (arrow B) and the femoral condyles (arrow C) (B).

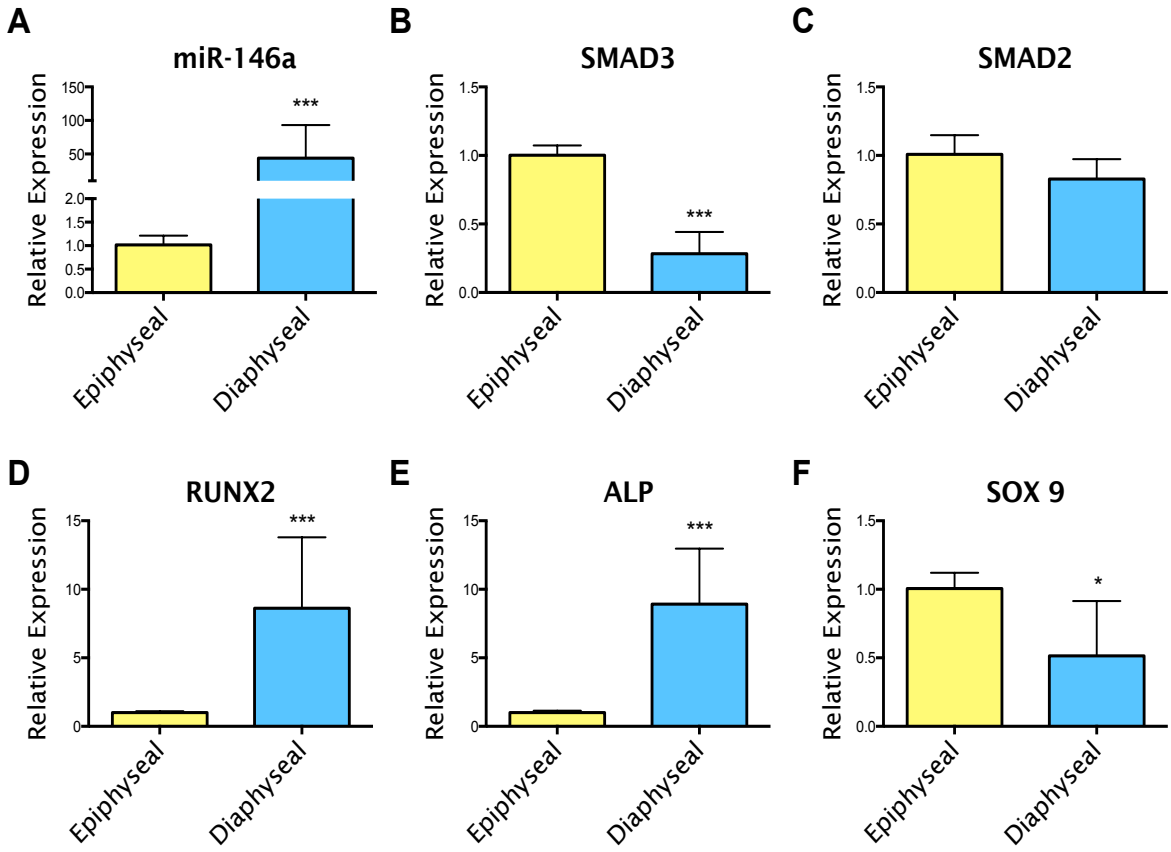


**Figure 5.2. Correlation of miR-146a expression and genes associated with differentiation.** MicroRNA-146a was expressed at an increased level in diaphyseal cell populations (A) and was found to correlate with a reduced expression of *SMAD3* (B) but not with *SMAD2* (C). Diaphyseal cells expressed a higher level of genes associated with osteogenesis, namely *RUNX2* (D) and *ALP* (E) and a reduced expression of the chondrogenesis-related gene *SOX9* (F). Data represents an average of three independent patient samples, and error bars represent standard deviation. *P<0.05, **P<0.01, ***P<0.001 calculated using Mann-Whitney Test.

### 5.2.2 MicroRNA-146a Regulate *SMAD2* and *SMAD3* Protein Expression

The seed region for miR-146a on *SMAD2* and *SMAD3* 3'-UTR are shown in figure 5.3A and 5.3B respectively. To validate the effect of miR-146a on *SMAD2* and *SMAD3* protein translation, miR-146a was transiently over-expressed in epiphyseal cells from three independent patient samples cultured under basal conditions. RNA was extracted 48 hours post transfection and protein was harvested after 72 hours.

48 hours post miR-146a overexpression, *SMAD2 mRNA* levels remained unchanged (C) but a 50% downregulation of *SMAD3 mRNA* was observed (D). Western Blot analysis showed a reduction in both *SMAD2* and *SMAD3* protein translation in the presence of miR-146a overexpression (Figure 5.3E). Densitometry techniques were used to semi-quantify the level of *SMAD2* and *SMAD3* protein level on the western blot result showing a 50% reduction in *SMAD2* protein level and a 65% decrease in *SMAD3* protein level following miR-146a overexpression. These results indicated that *SMAD2* and *SMAD3* are targets of miR-146a.

RT-qPCR was used to examine the effect of miR-146a overexpression on osteogenic and chondrogenic gene expression. MicroRNA-146a overexpression was found not to influence the expression of Osterix (Figure 5.4 A) but increased the expression of *RUNX2* (Figure 5.4B). Interestingly, there was a decrease in osteogenesis-associated genes *ALP* and *COL1A1* (Figure 5.4 C and D) and the chondrogenesis related gene *SOX9*. (Figure 5.4 E) No change in *COL2A1* (Figure 5.4 F) and *COL10A1* was observed (Figure 5.4 G).

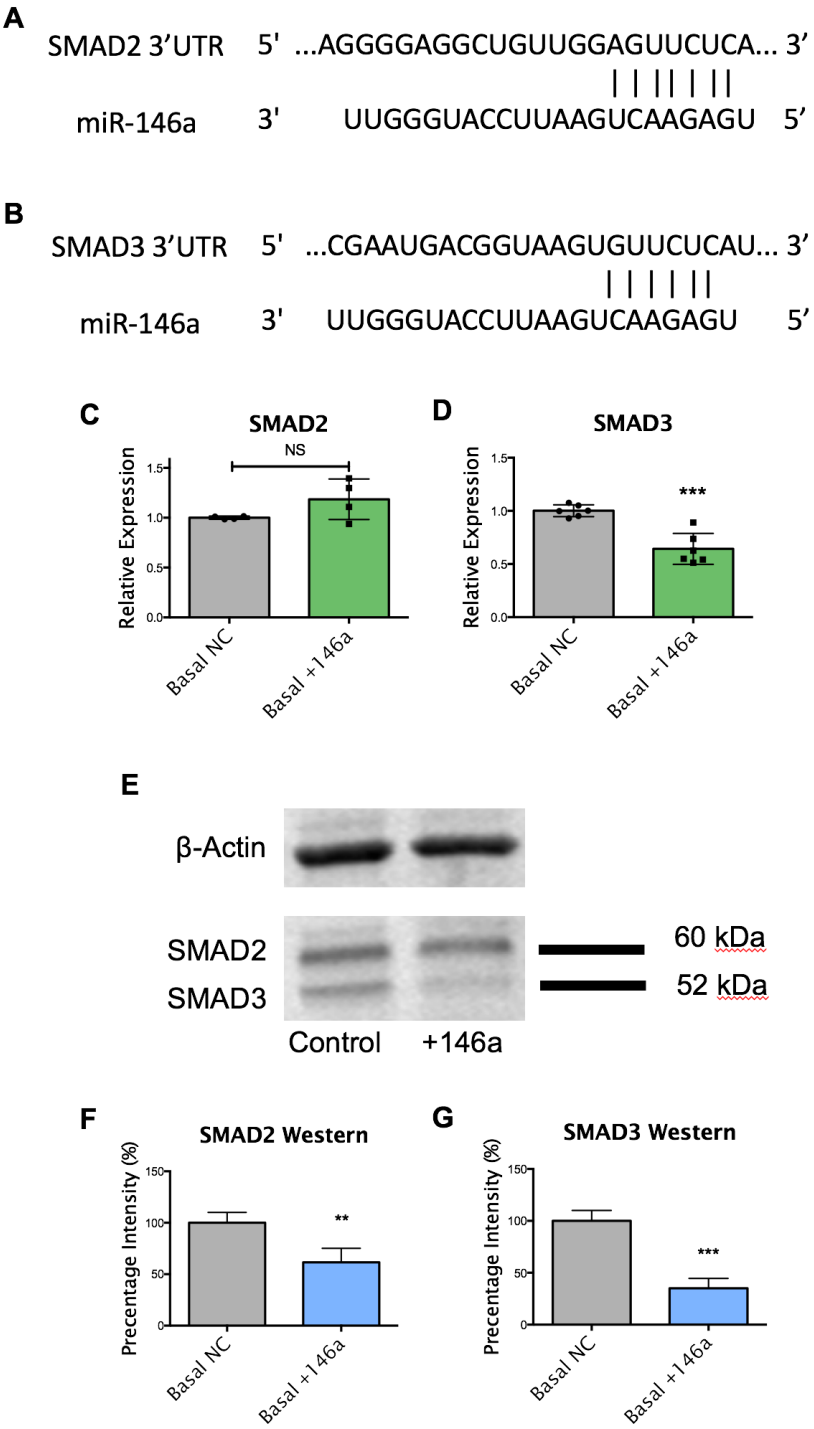


**Figure 5.3. MicroRNA-146a negatively regulates *SMAD2* and *SMAD3***. Seed region for miR-146a on *SMAD2* (A) and *SMAD3* (B) 3'-UTR. Overexpression of miR-146a did not reduce the level of *SMAD2 mRNA* significantly (C) but reduced the level of *SMAD3* by 40% (D). Overexpression of miR-146a reduced the protein level of both *SMAD2* and *SMAD3* (E). Densitometry result confirming overexpression of miR-146a reduced the protein level of *SMAD2* by 30% (F) and reduced *SMAD3* protein level by 70% compared to basal (G). Data represents an average of three independent patient samples, and error bars represent standard deviation. **P<0.01, ***P<0.001 calculated using Mann-Whitney Test.

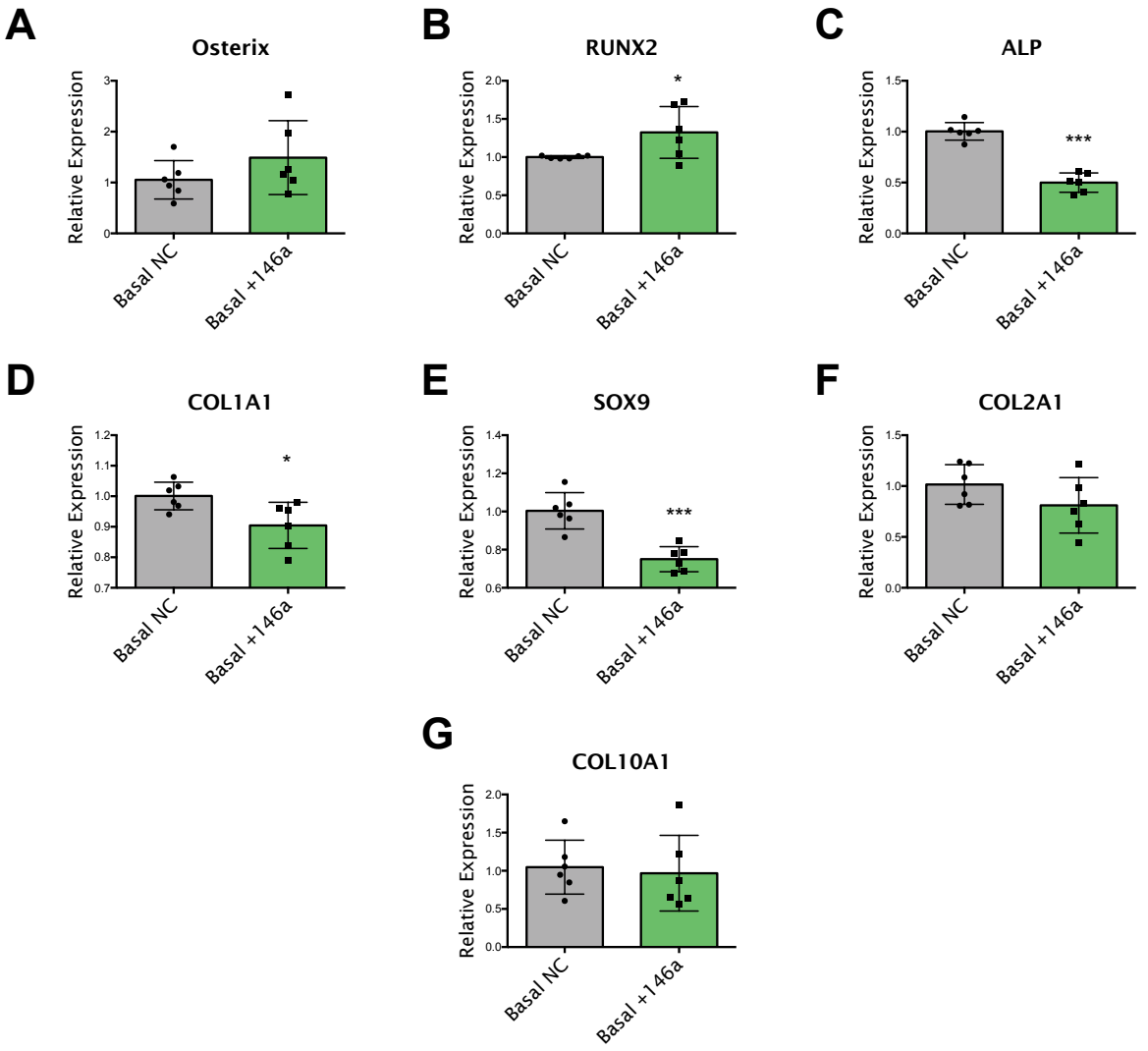


**Figure 5.4. Effect of miR-146a overexpression on expression of genes associated with osteogenic and chondrogenic differentiation.** Overexpression of miRNA increased the expression of *RUNX2* (B) but reduced the expression of *ALP* (C) and *COL1A1* (D). *SOX9* expression was reduced by over 1-fold following miR-146a expression (E). No change in the expression of *COL2A1* (F) and *COL10A1* (G) was observed following over expression of miR-146a. Data represents an average of three independent patient samples, and error bars represent standard deviation. *P<0.05, ***P<0.001 calculated using Mann-Whitney Test.

### 5.2.3 IL-1β-Induced Expression of MicroRNA-146a

IL-1β is known to result in a rapid concentration-dependent expression of miR-146a in the A549 cell line (Perry et al. 2008). To examine the effect of IL- 1β on miR-146a and differentiation-associated gene expression in foetal femur-derived SSCs, epiphyseal cell populations were cultured in medium supplemented with IL-1β. Following three days in monolayer culture, cells were prepared for RNA extraction, Taqman miRNA assay and *mRNA* RT-qPCR.

Following culture in medium supplemented with IL-1β, a 300-fold increase in miR-146a expression was observed (Figure 5.5 A). Indicating that IL-1β is a potent inducer of miR-146a expression in foetal femur epiphyseal cell populations. IL-1β supplementation did not significantly affect the expression of miR-138 and miR-140 (Figure 5.5 B and C), which are known to be involved in skeletal stem cell differentiation (Eskildsen et al. 2011; Miyaki et al. 2009). The increased expression of miR-146a induced by IL-1β reduced the level of *SMAD3 mRNA* (Figure 5.5D), further validating *SMAD3 mRNA* as a target for miR-146a. The increased expression of miR-146a and reduced expression of *SMAD3* had a similar effect on gene expression compared to the miR-146a overexpression experiment shown in Figure 5.4 with an increased expression of *RUNX2* and reduced expression of *SOX9* (Figure 5.5 E and F) but did not influence the expression of *ALP* and Osteocalcin (Figure 5.5 G and H).

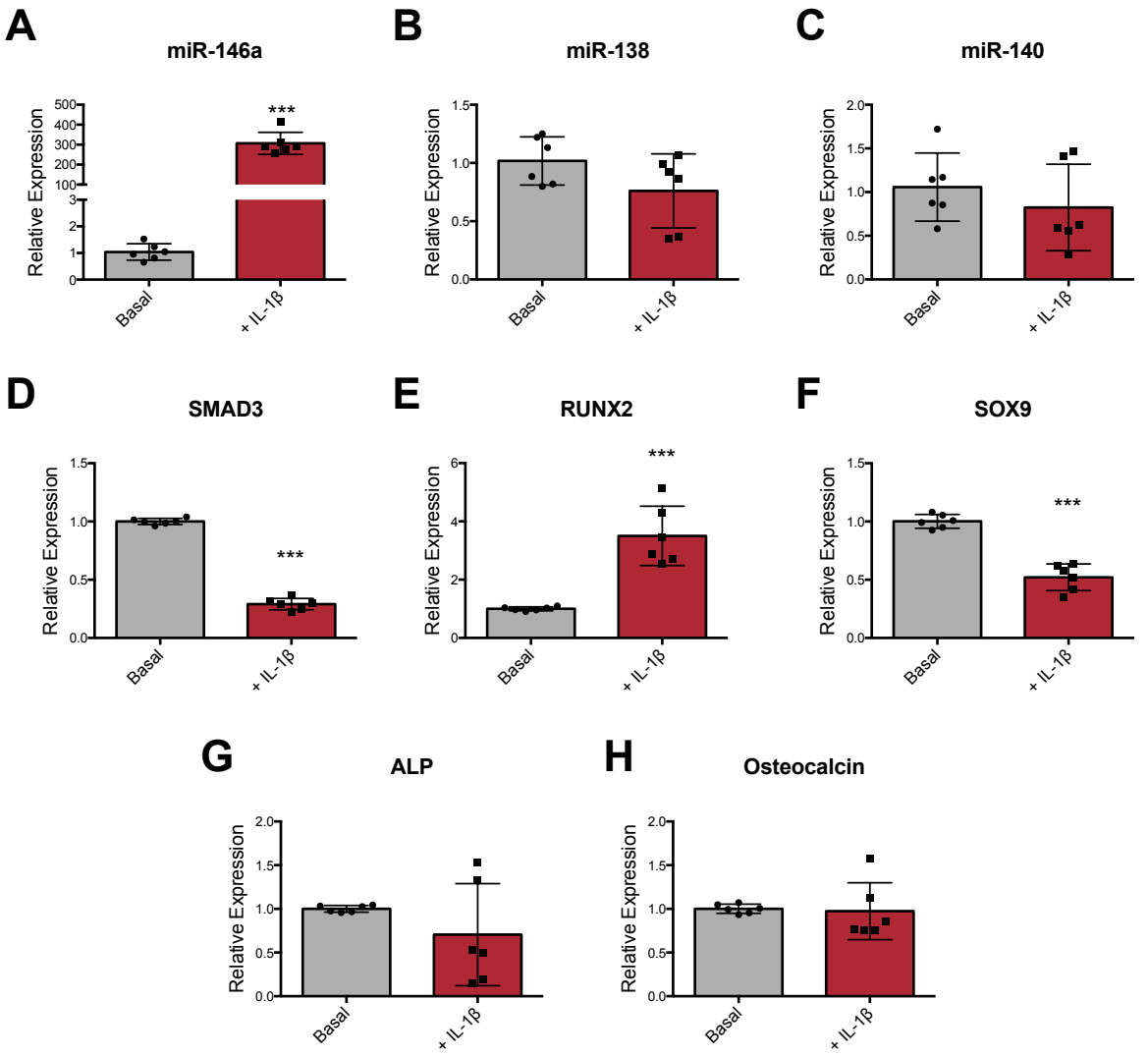


**Figure 5.5. IL-1β-induced miR-146a expression.** When epiphyseal cells were culture under medium supplemented with IL-1β, there was a 300-fold increase in expression of miR-146a (A). No change in miR-138 (B) and miR-140 (C) was seen when epiphyseal cell populations were stimulated with IL-1β. *SMAD3 mRNA* levels were significantly reduced following IL-1β-induced expression of miR-146a (D).The increase in expression of miR-146a following stimulation with IL-1β was associated with an increase in *RUNX2* expression (E) and a lowered expression of *SOX9* (F) while no change in *ALP* (E) and Osteocalcin (F) expression was observed. Data represents an average of three independent patient samples, and error bars represent standard deviation. ***P<0.001 calculated using Mann-Whitney Test.

### 5.2.4 MicroRNA-146a/TGF-$\beta_3$ Feedback Mechanism Regulates Chondrocyte Hypertrophic Differentiation

MicroRNA-146a was shown to target the *mRNA* of *SMAD3* and reduce the protein translation of *SMAD2* and *SMAD3*. Since TGF-β signaling is transduced by *SMAD2* and *SMAD3*, the effect of miRNA overexpression when cells were stimulated by TGF-$\beta_3$ in culture was examined.

Human foetal cells extracted from the epiphyseal layers undergo hypertrophic differentiation in the presence of chondrogenic medium containing TGF-$\beta_3$ (Figure 5.6A–B). *In vitro* stimulation of epiphyseal cells with chondrogenic medium containing TGF-$\beta_3$ resulted in down-regulation of miR-146a (figure 5.6C) and a substantial up-regulation of *COL10A1 mRNA* expression (Figure 5.6D). To further validate the effect of miR-146a as a negative regulator of the TGF-β ligand dependent signaling pathway through downregulating protein translation of *SMAD2* and *SMAD3*, the effect of TGF-$\beta_3$ on *COL10A1* in the presence of miR-146a overexpression in basal and chondrogenic conditions was compared. Under basal conditions, overexpression of miR-146a had no effect on the expression of *COL10A1* (Figure 5E); however, in the presence of miR-146a overexpression, upregulation of *COL10A1* by TGF-$\beta_3$ was reduced by 60%. These results suggest the effects of miR-146a on the TGF-β pathway are dependent on the presence TGF-$\beta_3$ ligands (Figure 5F).

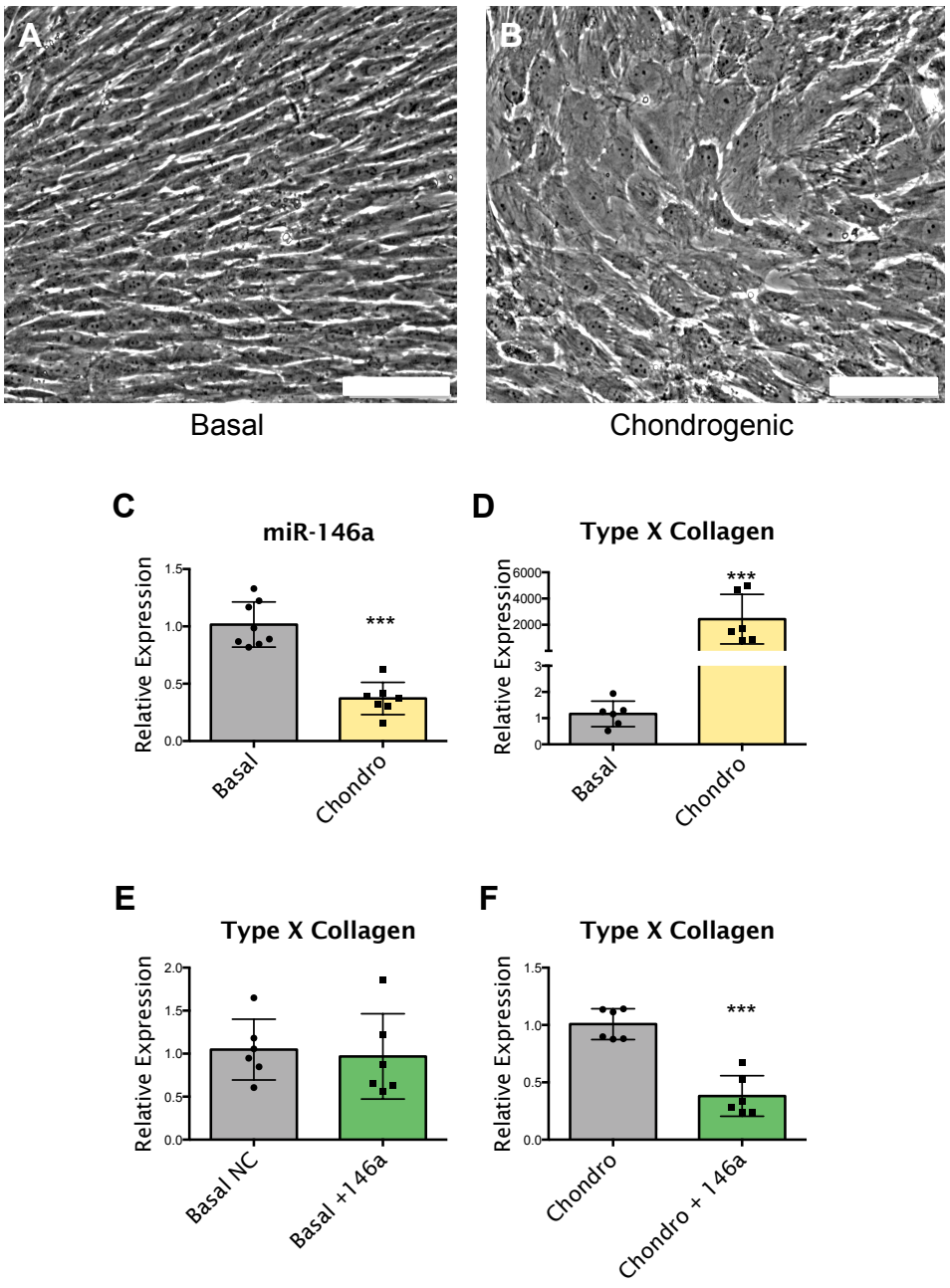


**Figure 5.6. TGF-$\beta_3$ stimulation on epiphyseal cell populations in the presence of miR-146a overexpression.** Epiphyseal cells become hypertrophic following monolayer culture with medium supplemented with TGF-$\beta_3$ (A and B). TGF-$\beta_3$ reduced the expression of miR-146a by over 1-fold (C) and increased the expression of *COL10A1* by over 2000-fold (D). Overexpression of miR-146a had no effect on *COL10A1* expression in the absence of TGF-$\beta_3$ stimulation (E). The increased expression of *COL10A1* by TGF-$\beta_3$ was reduced by 60% in the presence of miR-146a overexpression (F). Scale bar = 100µm. Data represents an average of three independent patient samples, and error bars represent standard deviation. ***P<0.001 calculated using Mann-Whitney Test.

## 5.3 Discussion

MicroRNAs have recently been demonstrated as important regulators of a variety of biological processes including stem cell differentiation (Kajimoto 2006), cell cycle regulation (Ivey & Srivastava 2010) and oncogenesis (L. Huang et al. 2010; Ng et al. 2009). MicroRNA-146 has previously been identified to modulate myofibroblast trans-differentiation during TGF-$\beta_1$ induction by targeting SMAD4 (Zhong et al. 2010), and miR-146 may also be an important regulator during the inflammatory state of osteoarthritis, as *IL-1b*-induced production of *TNF-a*, a pro- inflammatory cytokine known to play a role in osteoarthritis, was significantly reduced by miR-146 overexpression (Swingler et al. 2012). Furthermore, overexpression of miR-146a has been shown to protect the human bronchial epithelial from apoptosis and to promote cell proliferation through up-regulation of *Bcl-XL* and *STAT3* phosphorylation (X. Liu et al. 2009).

Using *in-situ* hybridization techniques, miR-146a was shown to be expressed at distinct regions within the foetal femur and to correlate to the regions of ossification during skeletal development. The femur is ossified from five centers: one for the body of the femur, one for the head of the femur, one for each trochanter, and one for the lower extremity of the femur (GIRDANY & GOLDEN 1952). Of all the long bones, except the clavicle, the femur is the first to show ossification, commencing in the middle of the body, at about the seventh week of foetal life as demonstrated by the deposition of *COL1A1* (GIRDANY & GOLDEN 1952). The other ossification centers are found later during skeletal development in the epiphyseal regions in the following order: in the lower end of the bone, at the ninth month of foetal life; in the head, at the end of the first year after birth; in the greater trochanter, during the fourth year; and in the lesser trochanter, between the thirteenth and fourteenth years(GIRDANY & GOLDEN 1952). The expression of miR-146a at the ossification centers suggests miR-146a may play a role in regulating osteogenesis during skeletal development.

Previous results demonstrated that miR-146a was expressed at higher levels in diaphyseal cells compared to epiphyseal cells, suggesting a role of miR-146a in osteogenic differentiation. Using Targetscan release 6, potential *mRNA* targets of miR-146a were identified (Anon n.d.). Various components of the TGF-β pathway; namely *SMAD2*, *SMAD3*, *SMAD4*, TGFB-induced factor homeobox 1 (*TGIF1*), BMP and activin membrane-bound inhibitor homolog (*BAMBI*) and activin A receptor type IC/I/ Type II-like 1 (*ACVR1C/ACVR1B/ACVRL1*); were highlighted as potential targets of miR-146a (Anon n.d.), suggesting the function of increased expression of miR-146a in diaphyseal cells may be mediated via attenuation of the TGF-β pathway. *SMAD2* and *SMAD3* were chosen as targets for functional interrogation of miR-146a as they are known to be important regulators of skeletal development and stem cell differentiation (B. Song et al. 2009; Roelen & Dijke 2003). MicroRNA-146a transient overexpression in epiphyseal cells (low level expression of miR-146a

compared to diaphyseal cells under normal basal culture conditions) for 48 hours resulted in a significant downregulation of *SMAD3* at the *mRNA* level and significantly reduced the protein level of *SMAD2* and *SMAD3* at the protein level after 72 hours, as shown by western blot analysis, validating miR-146a targets *SMAD2* and *SMAD3 mRNA* 3'-UTR and can effectively regulate their protein levels. Accompanying the reduction in *SMAD2* and *SMAD3* levels observed, reduced expression of the chondrogenesis-related gene *SOX9*, and upregulation of the osteogenic gene *RUNX2* was seen. These data suggest miR-146a is a negative regulator of chondrogenesis through downregulation of *SMAD2*/*SMAD3* and may indirectly promote osteogenic differentiation. To optimize transfection protocol, miR mimics against GAPDH were used and shown to reduce GAPDH expression by over 80% 48 hours post transfection (as shown in chapter 4). However, miR inhibitors were found to display a much lower efficacy. Coupled with the high expression of miR-146a in diaphyseal cells, it proved difficult to reproducibly demonstrate the effects of miR-146a inhibitor on human foetal diaphyseal cells.

TGF-β signaling is important for development (Kitisin et al. 2007; B. Song et al. 2009). It is generally accepted that the bone morphogenic proteins (BMPs) and their receptors induce early cartilage formation and stimulate mesenchymal cells to differentiate into osteoblasts whilst TGF-β ligands and their receptors regulate chondrocyte proliferation and differentiation (X. Yang et al. 2001). In the current chapter, the effect of TGF-$\beta_3$ stimulation in a monolayer culture model were consistent with current literature with TGF-$\beta_3$ -stimulated cells differentiating to give hypertrophic chondrocytes coupled with a significant up-regulation of *COL10A1 mRNA* expression (X. Yang et al. 2001; Mirmalek-Sani et al. 2006). TGF-β signals are known to be transduced to the nuclei by the intracellular mediators, SMADs (Moustakas et al. 2001). To date, eight different SMAD proteins have been identified and classified into three categories based on their functions: the receptor-activated SMADs (*SMAD- 1, 2, 3, 5 and 8*), common mediator SMAD (*SMAD4*) and the inhibitory SMADs (*SMAD6 and 7*) (Moustakas et al. 2001). The receptor-activated SMADs are further divided into two groups based on their attachment to ligand-specific receptors: *SMAD2* and *SMAD3* transduce signal by TGF-βs and Activin ligands while *SMAD1, SMAD5* and *SMAD8* respond to BMPs stimulation (B. Song et al. 2009). As *SMAD2* and *SMAD3* are known to transduce TGF-β ligand signals (Hellingman et al. 2011), the effect of miR-146a on the TGF-β pathway was examined through analysis of the effects of miR-146a transient overexpression on cells stimulated by TGF-$\beta_3$. In the absence of miR-146a overexpression, TGF-$\beta_3$ was observed to upregulate the expression of *COL10A1* by 2000 fold. However, in the presence of miR-146a overexpression, TGF-$\beta_3$-induced upregulation of *COL10A1* was reduced by over 60%. These results suggest miR-146a attenuates the TGF-$\beta_3$ ligand signal, and possibly activin signals, through downregulation of *SMAD2* and *SMAD3* protein. Interestingly, when cells were stimulated with TGF-$\beta_3$, a reduction of miR-146a expression

was observed. The current data indicate the presence of a negative feedback mechanism between TGF-$\beta_3$ stimulation and miR-146a expression, advocating the presence of an auto-regulatory mechanism (Figure 5.7). Thus miR-146a may reduce TGF-β signaling and, in turn, TGF-$\beta_3$ stimulation may suppress miR-146a expression. A similar auto-regulatory feedback mechanism has also been described for the regulation of miR-93 and downstream Osterix expression during osteoblast mineralization (L. Yang et al. 2012) as well as for miR-140 on TGF-β signaling through *SMAD3* suppression (Pais et al. 2010).

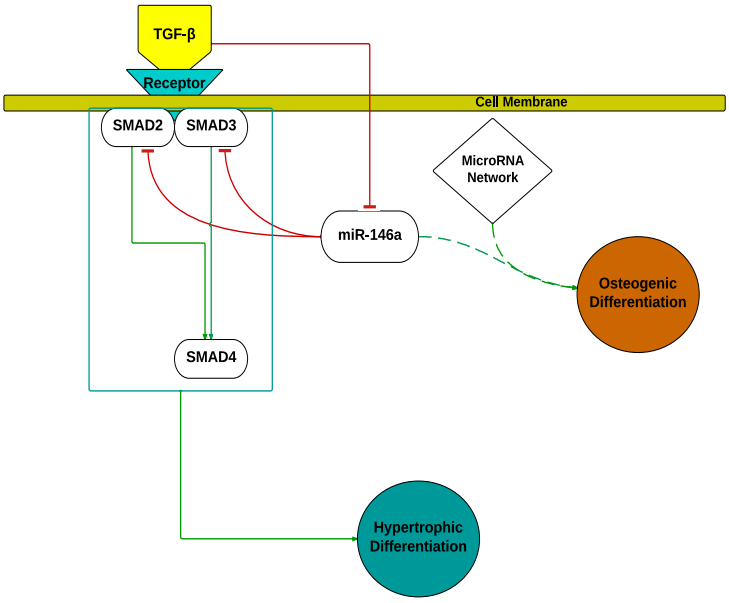


**Figure 5.7. Modulation of skeletal cell differentiation by miR-146a.** MicroRNA-146a down-regulated *SMAD2* and *SMAD3* protein levels, resulting in an attenuation of TGF-β signaling following TGF-$\beta_3$ stimulation. Stimulation by TGF-$\beta_3$ down-regulated the expression of miR-146a indicating a double negative feedback loop and thus a potential auto-regulatory mechanism. Overexpression of miR-146a under basal conditions revealed a modest but positive effect on osteogenesis-related gene expression and is likely part of a miR network involved in promoting osteogenesis. The inhibitory effect of miR-146a on SMAD4 was previously reported by Zhong *et al* (Zhong et al. 2010) and was not reevaluated in this study.

Various reports have already demonstrated the importance of miRs during SSC differentiation; miR-140, a cartilage-specific miRNA (Swingler et al. 2012), was reported as a positive effector of chondrogenesis through PDGF signaling in zebra fish (Eberhart et al. 2008). In addition, miR-140 has been linked to the regulation of *SMAD3*-dependent TGF-β pathways through down regulation of *SMAD3* protein levels and thus to play a role in chondrocyte development (Pais et al. 2010). microRNA-138 has been shown to inhibit osteogenic differentiation in telomerase-immortalized bone marrow derived hMSC through down-regulation of *FAK* and subsequently downregulation of the *FAK* downstream targets *RUNX2* and Osterix (Eskildsen et al. 2011). These studies demonstrate various miRNAs may work in concert to regulate the complex mechanisms orchestrating SSC differentiation.

Together with the distinct spatial expression of miR-146a within foetal femur, the increased expression of miR-146a observed in the osteogenic diaphyseal cell populations, the data in this chapter suggests miR-146a is an important regulator of skeletal development and is involved in orchestrating skeletal stem cell differentiation through attenuation of the TGF-β pathway.

# Chapter 6: Discussion

This thesis set out to 1) identify an appropriate cell source for tissue engineering, 2) undertake miRNA functional analysis to identify miRNAs involved in the regulation of skeletal stem cell differentiation and 3) to design a system allowing delivery of miRNA-based gene therapy for incorporation into engineered scaffolds for bone tissue regeneration strategies. In recent years, induced pluripotent stem cells (iPSC) discovered by Yamanaka *et al* {Yamanaka:2006wd} have been in the spotlight as the new potential cell source for tissue engineering applications. Ectopic expression of *Oct4*, *Sox2*, *Klf4* and *c-Myc* in adult somatic cells has shown the potential for reprogramming to resemble ESCs in a broad spectrum of features including the capacity to differentiate into all three primary germ layers with totipotency features (Abad et al. 2013). Therefore, iPSCs could potentially be used in tissue engineering applications to regenerate all tissues. However, the genes used in the synthesis of iPSC are also known to be oncogenic. The expression of *Oct4* has been shown to be involved in the development of human non-small cell lung cancer (Karoubi et al. 2009) and the expression of *Klf4* is associated with breast cancer cell migration and invasion (Yu et al. 2011). Additionally, aberrant expression of Sox2 has been shown to result in the development of colon carcinomas (Neumann et al. 2011). Furthermore, c-Myc is an oncogene involved in the development of around 70% of human cancers (Dang 2012). The oncogenic properties of genes used to synthesize iPSC along with the various technical problems surrounding gene delivery for reprogramming have limited, to date, the use of iPSC in clinical applications (Medvedev et al. 2010). Skeletal tissue engineering typically only requires cells with osteo-chondral differentiation capacity. Therefore, the ability of human SSCs to differentiate into bone, adipose tissue and cartilage makes them a promising cell source for skeletal tissue engineering applications and, at present, remain preferential over iPSC due to the current accepted safety profile.

Human bone marrow stromal cells (HBMSCs) contain a diminutive SSC populations which exhibit osteochondral differentiation capacity and have been extensively investigated over many decades as a potential cell source for bone tissue engineering applications (Friedenstein et al. 1966). In addition, foetal femur-derived skeletal stem cells have been shown to display enhanced self-renewal and differentiation capacity compared to HBMSCs (Mirmalek-Sani et al. 2006). Importantly, foetal tissue has been shown to be less immunogenic than adult tissue (Tuch 1988), making foetal-derived SSC an attractive cell source for regenerative medicine strategies. Previous reports have indeed acknowledged that foetal-derived cell populations are heterogeneous yet capable of differentiating into osteoblasts, chondroblasts and adipocytes. The current study has examined methods to reduce the heterogeneity of SSC populations by histological examination, immunocytochemistry and gene expression analysis. Histological and immunocytochemistry

examination revealed cells found in the epiphyseal and diaphyseal region of the developing foetal femur possess distinct phenotypes. Cells within the epiphyseal region display a small, densely packed cell population surrounded by a proteoglycan-rich matrix, while cells within the diaphyseal region display a hypertrophic phenotype associated with a developing bone collar, rich in type I collagen. This observation prompted me to investigate if one could reduce the heterogeneity of foetal femur cell populations by simply separating the two populations using micro dissection prior to cell isolation for monolayer culture. An initial approach examined osteogenic and chondrogenic differentiation-associated genes expressed in epiphyseal and diaphyseal cell populations following expansion in monolayer culture. Epiphyseal cells were found to display higher expression of genes associated with chondrogenesis: *SOX9* and *COL2A1*. In contrast, diaphyseal cell populations expressed genes associated with osteogenic differentiation, namely; Osterix, *RUNX2*, *ALP*, *COL1A1* and Osteocalcin. This suggests epiphyseal cells are chondrogenic by nature while diaphyseal cell populations have an increased capacity for osteogenic differentiation. These observations suggest epiphyseal and diaphyseal cell populations could be used as a potential cell source for bone and cartilage tissue engineering strategies, as well as a tool for both *in vitro* and *ex vivo* interrogation of the biological mechanism controlling skeletal development.

Currently, no single marker exists to identify “skeletal stem cell”. Instead, an array of markers are employed in the attempt to identify SSCs from heterogeneous cell populations isolated from the bone marrow. Markers include *CD105*, *CD73*, *CD44*, *CD90*, *CD71* and STRO-1 antigen, as well as the adhesion molecules *CD106*, *CD166*, *ICAM-1* and *CD29* (Tare et al. 2008). The STRO-1 antigen has been shown to be expressed by SSC populations with an increased osteogenic capacity and was found to be expressed in cells within distinct regions of the epiphyseal and diaphyseal femur, indicating the presence of yet another sub population of SSCs are shared by the epiphyseal and diaphyseal cell populations. Using magnetic activated cell sorting (MACS) method, STRO-1-positive cell populations were successfully isolated from foetal femurs and expanded by monolayer culture. Interestingly, STRO-1 immuno-selected foetal SSC populations exhibited phenotype stability over multiple passages under monolayer culture compared to their adult STRO-1-positive counterparts. Adult-derived SSCs typically lose STRO-1 expression within 13-19 days or at first passage (Gothard et al. 2015). The ability for foetal femur-derived SSCs to maintain STRO-1 expression indicates a subpopulation of foetal SSCs with self-renewal and differentiation capacity.

The current studies have also used molecular approaches to characterize the skeletal populations of interest. RT-qPCR was used to assess the expression of *CD63*, *ALCAM* and Nucleostemin to determine the mesenchymal progenitor characteristics of chondrogenic epiphyseal and osteogenic

diaphyseal cells. In addition, it was important to ascertain that both epiphyseal and diaphyseal cell populations retained the capacity for differentiation into other lineages. By subjecting epiphyseal and diaphyseal cell populations to methods known to induce chondrogenesis, adipogenesis and osteogenesis, both epiphyseal and diaphyseal cells were shown to be able to generate osteoblasts, adipocyte and chondrocyte linages, as evident by the secretion of proteoglycan, intracellular lipid deposition and mineralized matrix formation respectively. Collectively, the data suggest distinct chondrogenic and osteogenic sub-populations of SSC with a reduced heterogeneity and enhanced self-renewal capacity from within the foetal femur using a simple micro-dissection method. Most importantly, epiphyseal and diaphyseal cell populations provided a tool to interrogate mechanisms such as miRNA functions involved in SSC differentiation from a skeletal developmental standpoint.

MicroRNAs are endogenous non protein-coding RNA molecules of around 22 nucleotide in length capable of regulating various cellular processes such as cell differentiation and cell cycle regulation (Ivey & Srivastava 2010). Various studies have already determined miRNAs play a critical role in bone development and skeletogenesis (Dong et al. 2012) (Fang et al. 2015). A recent review by Lian *et al* summarised the effects of 42 miRNAs reported to be involved in osteogenic differentiation (Lian et al. 2012). For example, miR-338-3p was shown to directly target *RUNX2* and fibroblast growth factors, serve as a negative regulator of osteogenic differentiation and possibly contribute to the development of osteoporosis (H. Liu et al. 2014). *FAK* has been shown to be targeted by miR-138, and overexpression of miR-138 in osteoprogenitor cells was shown to down regulate the downstream target of *FAK*; Osterix, which is a gene essential for osteoblast development, resulted in a reduced bone matrix production *in vivo* (Nakashima et al. 2002; Eskildsen et al. 2011). It has previously been reported that overexpression of a single miRNA can result in the down regulation of hundreds of proteins but only to a modest degree (D. Baek et al. 2008). This observation suggests miRNAs act as rheostats, providing fine adjustments to protein output (D. Baek et al. 2008). Given that multiple miRNAs have been shown to be involved in osteogenic differentiation by targeting various pathways and transcription factors (Lian et al. 2012; Fang et al. 2015), it is likely that multiple miRNAs work in concert to exert a given cellular function such as differentiation. In addition to the potential of miRNAs to be used to augment stem cell differentiation along a specific a lineage, miRNAs could potentially be used as a marker to identify SSCs, as suggested by a study identifying a unique set of miRNAs expressed by human embryonic stem cells (Suh et al. 2004). Furthermore, urinary miR-126 and miR-182 ratios have been suggested as a method to aid in the diagnosis of bladder cancer, advocating miRNA as a diagnostic tool in clinical practice (Hanke et al. 2010).

MicroRNA expression profiling by microarray analysis can be used to identify miRNAs whose levels alter during osteoblast differentiation (a commonly used technique for genome-wide miRNA

expression analysis). Many investigators have already performed miRNA array analysis in various cell lines undergoing induced osteogenesis (Fang et al. 2015). A recent study by Baglio *et al* demonstrated that 17 miRNAs are up-regulated and 12 miRNAs are down-regulated during osteogenic differentiation of HBMSCs through microarray analysis (Baglìo et al. 2013). By expression and target analysis, miR-31 was found to down-regulate Osterix, suggesting miR-31 in the regulation of osteogenic differentiation (Baglìo et al. 2013). Another study by Li *et al* observed that HBMSCs osteogenic and chondrogenic differentiation capacity decreases with age. Through micro-array analysis, miR-196a, miR-378, miR-486-5p and miR-664 were found to display an increased expression in HBMSCs isolated from older subjects (ranging from 65-80 years old) while younger patient samples (from 17-30 years old) displayed an increased expression of miR-10a, miR-708, and miR-3197 (J. Li et al. 2013). Further analysis showed that miR-10a can act to increase differentiation capacity and reduce cell senescence by repressing KLF4 (J. Li et al. 2013). In this study, by using miRNA RT-qPCR microarray, the miRNAs expressed in the chondrogenic epiphyseal cell and the osteogenic diaphyseal cell populations were profiled. It was shown that 67 miRNAs displayed a difference in expression greater then 1.5 fold. Of these, 7 miRNAs were identified with a significant difference between epiphyseal and diaphyseal cell populations, namely miR-146b-5p, miR-301b, and miR-138 with an increased expression in epiphyseal cell population and miR-143, mR-145, miR-146a and miR-34a with an increased expression of diaphyseal cell populations. However, since miRNAs are involved in regulating various cellular processes, it is likely that many of the miRNAs found to have a difference in expression are involved in regulating other cellular processes other then osteogenic and chondrogenic differentiation. Nonetheless, miRNA expression profiling of epiphyseal and diaphyseal cell populations in this report has detected miRNAs that had previously been reported to change during osteoblast differentiation and chondrogenic differentiation. microRNA-138 expressed in the epiphyseal cell populations have previously been reported to be a negative regulator of osteogenesis (Eskildsen et al. 2011). miR-140, a cartilage specific miRNA previously reported to be important in chondrogenesis, was found to have an increased expression in the epiphyseal cell populations (Pais et al. 2010; Tuddenham et al. 2006; Swingler et al. 2012). microRNA-34a, previously reported to be highly expressed by osteoblast during differentiation, was found to be expressed at an elevated level in diaphyseal cells (L. Chen et al. 2014). The miRNA microarray data suggests epiphyseal and diaphyseal cell populations can be used as a model to identify new miRNAs involved in chondrogenesis and osteogenesis.

To elucidate the function of a particular miRNA, investigators typically use miRNA inhibitors and mimic to inhibit or over-express the miRNA of interest to examine the effects on *mRNA* expression and protein expressions of predicted targets following transfection. In order to accurately investigate miRNA functions in SSCs differentiation, this study attempted to develop a clear culture

model containing differentiating SSCs and an effective transfection protocol to deliver miRNA mimics and inhibitors into foetal-derived skeletal stem cells. It was found that foetal femur cells begin to differentiate once a critical level of cell confluence is reached. By increasing initial seeding density in monolayer culture, foetal femur cells were shown to display *ALP* activity after only four days in monolayer culture, and could provide a method to obtain actively differentiating SSCs in a relatively short period of time for use in miRNA functional analysis experiments. Various methods to transfect miRNA mimics and inhibitors into foetal femur-derived SSCs have been pursued throughout this study, and foetal femur-derived SSCs were deemed to be extremely difficult to transfect due to the increased sensitivity to the cytotoxic effects of various transfection reagent and poor uptake of transfection complex compared to other cell lines such as MG63 and SaOS2. Nonetheless, an effective transfection protocol for primary SSCs derived from human foetal femur was achieved by using a liposome-based transfection reagent and is sufficient for use in miRNA functional analysis *in vitro*. Bone tissue engineering aims to replace lost bone tissue via the synergistic combination of biomaterial, cells and osteogenic factors (Amini et al. 2012). In order to use miRNA-based gene therapy in tissue engineering application, miRNA mimics or inhibitors have to be combined with solid scaffolds and effectively deliver osteogenic miRNAs into pre-seeded or surrounding cells. Viral vectors allow efficient gene delivery but present a limited payload capacity and might be associated with *in vivo* adverse effect such as gene insertion-related oncogenesis and severe immune reactions (Escriou et al. 2003). Liposome-based gene delivery systems are relatively safer but typically require reagents to be used as particles dispersed in a liquid medium, which limits their role in solid scaffolds used in bone tissue engineering (Kanatani et al. 2006). Recently, it has been shown that the conjugation of naturally derived polysaccharide and polyamine, spermine-pullulan complex, can be used to deliver plasmid DNA effectively into various cell lines (Thakor et al. 2009; Kanatani et al. 2006). Importantly, cationic polymers such as spermine-pullulan have lower immunogenicity and enhanced biological safety compared to viral carriers (Jo, Ikai, Okazaki, Yamamoto, et al. 2007), Furthermore, S-P can be electrostatically pre-adsorbed onto solid surfaces such as tissue culture plates and incorporated into succinylated gelatin-based scaffolds (Kido et al. 2011) (Thakor et al. 2011), making S-P a potential gene delivery system for miRNA-based therapy. This thesis investigated the efficacy of S-P complex in delivering miRNA mimic and inhibitors into foetal femur-derived SSCs. Attempts have been made to increase the transfection efficacy of S-P in transfecting miRNAs into foetal femur-derived SSCs by changing conditions such as the degree of spermine introduced to pullulan and different nitrogen to phosphate ratios between S-P complex and oligonucleotide used. However, only an intermediate level of transfection was achieved. Nonetheless, miRNA mimic was shown to be successfully transfected into foetal femur-derived SSCs and produced a functional change as displayed by the reduction in GAPDH *mRNA* level by the positive control miRNA mimic and reduction in Osterix expression following miR-138 mimic

overexpression using S-P complex as the transfection agent. However, it was concluded that S-P complex transfection still requires considerable development and further optimization to be used as a transfection reagent to deliver miRNA into primary SSCs.

Through target analysis, it was found that many miRNAs identified with a significant change in expression between epiphyseal and diaphyseal cell populations target various components of the TGF-β superfamily, which implies interplay between miRNAs and the TGF-β pathway might be involved in the regulation of skeletogenesis and SSCs differentiation. Members of the TGF-β superfamily are known to be involved in regulating osteogenic and chondrogenic differentiation (X. Yang et al. 2001; Kitisin et al. 2007; S. Zhou 2011). It has been shown that TGF-β and activin ligands can provide competence for early stages of chondroblastic and osteoblastic differentiation, but inhibits myogenesis, adipogenesis and late-stage osteoblast differentiation (S. Zhou 2011; X. Yang et al. 2001) while BMPs inhibit adipogenesis and myogenesis but strongly promote osteoblast differentiation (Roelen & Dijke 2003). The TGF-β superfamily members signal via serine/threonine kinase receptors and their nuclear effectors, known as SMAD proteins (Roelen & Dijke 2003). There are eight SMAD isoforms and they fall into three sub-families. In SSC differentiation, the chondrogenic TGF-β isoform signaling depends on *SMAD2* and *SMAD3*, while the osteogenic BMP signaling depends on *SMAD1, SMAD5 and SMAD8* (Moustakas et al. 2001). MicroRNA-146a, was identified to be expressed at tremendously elevated levels in the osteogenic diaphyseal cell populations compared to the epiphyseal cell populations, suggesting miR-146 might play a role in osteogenic differentiation. Through target analysis, miR-146a was found to target various components of the TGF-β pathway, namely *SMAD2*, *SMAD3*, *SMAD4*, TGFB-induced factor homeobox 1 (*TGIF1*), BMPs and activin membrane-bound inhibitor homolog (*BAMBI*) as well as activin A receptor type IC/I/ Type II-like 1 (*ACVR1C/ACVR1B/ACVRL1*) (Anon n.d.). Since miR-146a was predicted to target *SMAD2* and *SMAD3* simultaneously, it was hypothesized that miR-146a might be involved in SSC osteogenic differentiation by down regulating chondrogenesis. Interestingly, *in situ* hybridization of miR-146a displayed a spatial expression of miR-146 within the developing foetal femur, particularly in sites known to be centers for ossification during skeletal development.

By examining the effect of miR-146a overexpression on *SMAD2* and *SMAD3 mRNA* and protein levels, *SMAD2* and *SMAD3* were confirmed to be targets of miR-146a. Under basal conditions, miR-146a overexpression was shown to increase the expression of *RUNX2* while down-regulating *SOX9,* suggesting miR-146a could play a role in directing SSC differentiation down osteogenic pathways while inhibiting chondrogenesis. To demonstrate the functional effect of miR-146a on TGF-β by down regulating *SMAD2* and *SMAD3*, the effects of miR-146a transient overexpression on cells stimulated by TGF-$\beta_3$ were examined. Without miR-146a overexpression, TGF-$\beta_3$ stimulation in

monolayer culture results in an increased expression of *COL10A1* and cells displaying a hypertrophic phenotype suggesting TGF-$\beta_3$ direct SSCs to differentiate into hypertrophic chondrocytes. Indeeded, the increased expression of *COL10A1* by TGF-$\beta_3$ was reduced by 60% in the presence of miR-146a overexpression. This observation consolidates the notion that miR-146a inhibits chondrogenesis by down regulating the TGF-β and activin ligand signal through reducing *SMAD2* and *SMAD3* protein.

## 6.1 Conclusion

This study has identified and characterized distinct populations of skeletal stem cells found within the foetal femur. Harvesting the increased chondrogenic properties of epiphyseal cells and the augmented osteogenic potential of diaphyseal cell populations, microRNA targets involved in skeletal stem cell differentiation were identified. A clear culture method delivering differentiating SSCs was derived experimentally and an effective miRNA transfection protocol for primary SSCs was devised. In addition, attempts have been made to design a transfection system to allow miRNA functional analysis *ex vivo* and *in vivo.* By combining the data found throughout this report, miR-146a was identified as an important regulator of TGF-β signaling during chondrocyte development and, by extension, foetal skeletogenesis. It is hoped that this thesis will further inform bone tissue engineering strategies to provide novel treatments for patients requiring reparation of the skeletal system.

# Bibliography

Abad, M. et al., 2013. Reprogramming in vivo produces teratomas and iPS cells with totipotency features. *Nature*, 502(7471), pp.340–345.

Acampora, D. et al., 1999. Craniofacial, vestibular and bone defects in mice lacking the Distal-less-related gene Dlx5. *Development*, 126(17), pp.3795–3809.

Adams, B.D., Furneaux, H. & White, B.A., 2007. The Micro-Ribonucleic Acid (miRNA) miR-206 Targets the Human Estrogen Receptor- (ER ) and Represses ER Messenger RNA and Protein Expression in Breast Cancer Cell Lines. *Molecular Endocrinology*, 21(5), pp.1132–1147.

Akao, Y. et al., 2010. Role of anti-oncomirs miR-143 and -145 in human colorectal tumors. *Cancer Gene Therapy*, 17(6), pp.398–408.

Alford, A.I. & Hankenson, K.D., 2006. Matricellular proteins: Extracellular modulators of bone development, remodeling, and regeneration. *Bone*, 38(6), pp.749–757.

Alliston, T., 2001. TGF-beta-induced repression of CBFA1 by Smad3 decreases cbfa1 and osteocalcin expression and inhibits osteoblast differentiation. *The EMBO journal*, 20(9), pp.2254–2272.

Amini, A.R., Laurencin, C.T. & Nukavarapu, S.P., 2012. Bone tissue engineering: recent advances and challenges. *Critical reviews in biomedical engineering*, 40(5), pp.363–408.

Anon, TargetScanHuman 6.2. *targetscan.org*. Available at: http://www.targetscan.org [Accessed March 25, 2013].

Augello, A. & De Bari, C., 2010. The regulation of differentiation in mesenchymal stem cells. *Human gene therapy*, 21(10), pp.1226–1238.

Baek, D. et al., 2008. The impact of microRNAs on protein output. *Nature*, 455(7209), pp.64–71.

Baek, W.-Y. & Kim, J.-E., 2011. Transcriptional regulation of bone formation. *Frontiers in bioscience (Scholar edition)*, 3, pp.126–135.

Baglìo, S.R. et al., 2013. MicroRNA expression profiling of human bone marrow mesenchymal stem cells during osteogenic differentiation reveals Osterix regulation by miR-31. *Gene*, 527(1), pp.321–331.

Banerjee, C. et al., 2001. Differential regulation of the two principal Runx2/Cbfa1 n-terminal isoforms in response to bone morphogenetic protein-2 during development of the osteoblast phenotype. *Endocrinology*, 142(9), pp.4026–4039.

Bartel, D.P., 2004. MicroRNAs: genomics, biogenesis, mechanism, and function. *Cell*, 116(2), pp.281–297.

Bartel, D.P., 2009. MicroRNAs: target recognition and regulatory functions. *Cell*, 136(2), pp.215–233.

Beresford, J.N., Gallagher, J.A. & Russell, R.G., 1986. 1,25-Dihydroxyvitamin D3 and human bone-derived cells in vitro: effects on alkaline phosphatase, type I collagen and proliferation. *Endocrinology*, 119(4), pp.1776–1785.

Bernstein, E. et al., 2003. Dicer is essential for mouse development. *Nature genetics*, 35(3), pp.215–217.

Bhatt, R.A. & Rozental, T.D., 2012. Bone graft substitutes. *Hand clinics*, 28(4), pp.457–468.

Bialek, P. et al., 2004. A Twist Code Determines the Onset of Osteoblast Differentiation. *Dev Cell*, 6(3), pp.423–435.

Bianco, P., Robey, P.G. & Simmons, P.J., 2008. Mesenchymal Stem Cells: Revisiting History, Concepts, and Assays. *Cell Stem Cell*, 2(4), pp.313–319.

Bilezikian, J.P., Raisz, L.G. & Rodan, G.A., 2008. *Principles of Bone Biology*,

Boyce, T., Edwards, J. & Scarborough, N., 1999. Allograft bone. The influence of processing on safety and performance. *The Orthopedic clinics of North America*, 30(4), pp.571–581.

Bruder, S.P., Fink, D.J. & Caplan, A.I., 1994. Mesenchymal stem cells in bone development, bone repair, and skeletal regenaration therapy. *Journal of cellular biochemistry*, 56(3), pp.283–294.

Busse, B. et al., 2010. Decrease in the osteocyte lacunar density accompanied by hypermineralized lacunar occlusion reveals failure and delay of remodeling in aged human bone. *Aging cell*, 9(6), pp.1065–1075.

Chen, G., Deng, C. & Li, Y.-P., 2012. TGF-β and BMP signaling in osteoblast differentiation and bone formation. *International journal of biological sciences*, 8(2), pp.272–288.

Chen, J.-F. et al., 2005. The role of microRNA-1 and microRNA-133 in skeletal muscle proliferation and differentiation. *Nature genetics*, 38(2), pp.228–233.

Chen, L. et al., 2014. MicroRNA-34a inhibits osteoblast differentiation and in vivo bone formation of human stromal stem cells. *Stem cells*, 32(4), pp.902–912.

Cheung, K.S.C. et al., 2014. MicroRNA-146a Regulates Human Foetal Femur Derived Skeletal Stem Cell Differentiation by Down-Regulating SMAD2 and SMAD3. *PloS one*, 9(6), p.e98063.

Cimmino, A., 2005. miR-15 and miR-16 induce apoptosis by targeting BCL2. *Proceedings of the National Academy of Sciences*, 102(39), pp.13944–13949.

Cordes, K.R. et al., 2009. miR-145 and miR-143 regulate smooth muscle cell fate and plasticity. *Nature*.

Cui, J.G. et al., 2009. Micro-RNA-128 (miRNA-128) down-regulation in glioblastoma targets ARP5 (ANGPTL6), Bmi-1 and E2F-3a, key regulators of brain cell proliferation. *Journal of Neuro-Oncology*, 98(3), pp.297–304.

Dado, D. et al., 2012. Mechanical control of stem cell differentiation. *Regenerative Medicine*, 7(1), pp.101–116.

Damien, C.J. & Parsons, J.R., 1991. Bone graft and bone graft substitutes: a review of current technology and applications. *Journal of applied biomaterials : an official journal of the Society for Biomaterials*, 2(3), pp.187–208.

Dang, C.V., 2012. MYC on the path to cancer. *Cell*, 149(1), pp.22–35.

DAY, T. et al., 2005. Wnt/β-Catenin Signaling in Mesenchymal Progenitors Controls Osteoblast and Chondrocyte Differentiation during Vertebrate Skeletogenesis. *Developmental Cell*, 8(5),

pp.739–750.

Denhardt, D.T. & Noda, M., 1998. Osteopontin expression and function: role in bone remodeling. *Journal of cellular biochemistry. Supplement*, 30-31, pp.92–102.

Diefenderfer, D.L. et al., 2003. BMP responsiveness in human mesenchymal stem cells. *Connective tissue research*, 44 Suppl 1, pp.305–311.

Dobreva, G. et al., 2006. SATB2 Is a Multifunctional Determinant of Craniofacial Patterning and Osteoblast Differentiation. *Cell*, 125(5), pp.971–986.

Dong, S. et al., 2012. MicroRNAs regulate osteogenesis and chondrogenesis. *Biochemical and biophysical research communications*, 418(4), pp.587–591.

Eberhart, J.K. et al., 2008. MicroRNA Mirn140 modulates Pdgf signaling during palatogenesis. *Nature genetics*, 40(3), pp.290–298.

Elia, L. et al., 2009. The knockout of miR-143 and -145 alters smooth muscle cell maintenance and vascular homeostasis in mice: correlates with human disease. *Cell Death Differ*, 16(12), pp.1590–1598.

Escriou, V. et al., 2003. NLS bioconjugates for targeting therapeutic genes to the nucleus. *Advanced drug delivery reviews*, 55(2), pp.295–306.

Eskildsen, T. et al., 2011. MicroRNA-138 regulates osteogenic differentiation of human stromal (mesenchymal) stem cells in vivo. *Proceedings of the National Academy of Sciences*, 108(15), pp.6139–6144.

Fang, S. et al., 2015. MicroRNAs regulate bone development and regeneration. *International journal of molecular sciences*, 16(4), pp.8227–8253.

Fiore, R. & Schratt, G., 2007. MicroRNAs in synapse development: tiny molecules to remember. *Expert Opinion on Biological Therapy*, 7(12), pp.1823–1831.

Firth J, P.G., 2008. Transcription Control of Mesenchymal Stem Cell Differentiation. *Transfusion Medicine and Hemotherapy*, (35), pp.216–227.

Fogelman, I., Gnanasegaran, G. & van der Wall, H., 2013. *Radionuclide and Hybrid Bone Imaging* I. Fogelman, G. Gnanasegaran, & H. van der Wall, eds., Berlin, Heidelberg: Springer.

Friedenstein, A.J., Piatetzky, S.I. & Petrakova, K.V., 1966. Osteogenesis in transplants of bone marrow cells. *J Embryol Exp Morphol*, 16(3), pp.381–390.

Fu, H.-J. et al., 2006. A Novel Method to Monitor the Expression of microRNAs. *Molecular biotechnology*, 32(3), pp.197–204.

Furumatsu, T. et al., 2005. Smad3 induces chondrogenesis through the activation of SOX9 via CREB-binding protein/p300 recruitment. *The Journal of biological chemistry*, 280(9), pp.8343–8350.

Gaur, T. et al., 2010. Dicer inactivation in osteoprogenitor cells compromises fetal survival and bone formation, while excision in differentiated osteoblasts increases bone mass in the adult mouse. *Developmental biology*, 340(1), pp.10–21.

GIRDANY, B.R. & GOLDEN, R., 1952. Centers of ossification of the skeleton. *The American journal*

*of roentgenology, radium therapy, and nuclear medicine*, 68(6), pp.922–924.

Gothard, D. et al., 2015. Regionally-derived cell populations and skeletal stem cells from human foetal femora exhibit specific osteochondral and multi-lineage differentiation capacity in vitro and ex vivo. *Stem cell research & therapy*, 6(1), p.251.

Gronthos, S. et al., 1994. The STRO-1+ fraction of adult human bone marrow contains the osteogenic precursors. *Blood*, 84(12), pp.4164–4173.

Großhans, H. & Filipowicz, W., 2008. Proteomics Joins the Search for MicroRNA Targets. *Cell*, 134(4), pp.560–562.

Hanke, M. et al., 2010. A robust methodology to study urine microRNA as tumor marker: microRNA-126 and microRNA-182 are related to urinary bladder cancer. *Urologic oncology*, 28(6), pp.655–661.

Hartmann, C., 2009. Transcriptional networks controlling skeletal development. *Current Opinion in Genetics & Development*, 19(5), pp.437–443.

Hassan, M.Q. et al., 2006. BMP2 Commitment to the Osteogenic Lineage Involves Activation of Runx2 by DLX3 and a Homeodomain Transcriptional Network. *Journal of Biological Chemistry*, 281(52), pp.40515–40526.

Hassan, M.Q. et al., 2004. Dlx3 Transcriptional Regulation of Osteoblast Differentiation: Temporal Recruitment of Msx2, Dlx3, and Dlx5 Homeodomain Proteins to Chromatin of the Osteocalcin Gene. *Molecular and Cellular Biology*, 24(20), pp.9248–9261.

Hellingman, C.A. et al., 2011. Smad Signaling Determines Chondrogenic Differentiation of Bone-Marrow-Derived Mesenchymal Stem Cells: Inhibition of Smad1/5/8P Prevents Terminal Differentiation and Calcification. *Tissue engineering. Part A*, 17(7-8), pp.1157–1167.

Huang, J. et al., 2009. MicroRNA-204 Regulates Runx2 Protein Expression and Mesenchymal Progenitor Cell Differentiation. *Stem cells*, pp.N/A–N/A.

Huang, L. et al., 2010. MicroRNA-125b suppresses the development of bladder cancer by targeting E2F3. *Int J Cancer*, 128(8), pp.1758–1769.

Inada, M. et al., 1999. Maturational disturbance of chondrocytes in Cbfa1-deficient mice. *Developmental dynamics : an official publication of the American Association of Anatomists*, 214(4), pp.279–290.

Iorio, M.V., Piovan, C. & Croce, C.M., 2010. Interplay between microRNAs and the epigenetic machinery: An intricate network. *Biochimica et Biophysica Acta (BBA) - Gene Regulatory Mechanisms*, 1799(10-12), pp.694–701.

Ivanovska, I. & Cleary, M.A., 2008. Combinatorial microRNAs: working together to make a difference. *Cell Cycle*, 7(20), pp.3137–3142.

Ivey, K.N. & Srivastava, D., 2010. MicroRNAs as regulators of differentiation and cell fate decisions. *Cell Stem Cell*, 7(1), pp.36–41.

Jo, J.-I., Ikai, T., Okazaki, A., Nagane, K., et al., 2007. Expression profile of plasmid DNA obtained using spermine derivatives of pullulan with different molecular weights. *Journal of Biomaterials Science, Polymer Edition*, 18(7), pp.883–899.

Jo, J.-I., Ikai, T., Okazaki, A., Yamamoto, M., et al., 2007. Expression profile of plasmid DNA by spermine derivatives of pullulan with different extents of spermine introduced. *Journal of Controlled Release*, 118(3), pp.389–398.

Johnell, O. & Kanis, J.A., 2006. An estimate of the worldwide prevalence and disability associated with osteoporotic fractures. *Osteoporosis International*, 17(12), pp.1726–1733.

Jones, D.C., 2006. Regulation of Adult Bone Mass by the Zinc Finger Adapter Protein Schnurri-3. *Science*, 312(5777), pp.1223–1227.

Judson, R.L. et al., 2009. Embryonic stem cell–specific microRNAs promote induced pluripotency. *Nat Biotechnol*, 27(5), pp.459–461.

Kajimoto, K., 2006. MicroRNA and 3T3-L1 pre-adipocyte differentiation. *RNA*, 12(9), pp.1626–1632.

Kanatani, I. et al., 2006. Efficient gene transfer by pullulan–spermine occurs through both clathrin- and raft/caveolae-dependent mechanisms. *Journal of Controlled Release*, 116(1), pp.75–82.

Karoubi, G. et al., 2009. OCT4 expression in human non-small cell lung cancer: implications for therapeutic intervention. *Interactive cardiovascular and thoracic surgery*, 8(4), pp.393–397.

Karsenty, G., 1998. Genetics of skeletogenesis. *Developmental Genetics*, 22(4), pp.301–313.

Khraiwesh, B. et al., 2010. Transcriptional Control of Gene Expression by MicroRNAs. *Cell*, 140(1), pp.111–122. Available at: http://www.ncbi.nlm.nih.gov/entrez/query.fcgi?cmd=Retrieve&db=PubMed&dopt=Citation&list_uids=20085706.

Kido, Y., Jo, J.-I. & Tabata, Y., 2011. A gene transfection for rat mesenchymal stromal cells in biodegradable gelatin scaffolds containing cationized polysaccharides. *Biomaterials*, 32(3), pp.919–925.

Kim, V.N., 2005. MicroRNA biogenesis: coordinated cropping and dicing. *Nature reviews. Molecular cell biology*, 6(5), pp.376–385.

Kim, V.N., Han, J. & Siomi, M.C., 2009. Biogenesis of small RNAs in animals. *Nature reviews. Molecular cell biology*, 10(2), pp.126–139.

Kirste, G., Wilms, H. & Freudenberg, N., 1989. Investigations of the viability and immunogenicity of fetal pancreas islet tissue. *Transplantation proceedings*, 21(1 Pt 3), p.2673.

Kitisin, K. et al., 2007. TGF-beta Signaling in Development. *Science's STKE*, 2007(399), pp.cm1–cm1.

Kode, J.A. et al., 2009. Mesenchymal stem cells: immunobiology and role in immunomodulation and tissue regeneration. *Cytotherapy*, 11(4), pp.377–391.

Komori, T. et al., 1997. Targeted disruption of Cbfa1 results in a complete lack of bone formation owing to maturational arrest of osteoblasts. *Cell*, 89(5), pp.755–764.

Kundu, M. et al., 2002. Cbfbeta interacts with Runx2 and has a critical role in bone development. *Nature genetics*, 32(4), pp.639–644.

Lakshmipathy, U. & Hart, R.P., 2008. Concise Review: MicroRNA Expression in Multipotent

Mesenchymal Stromal Cells. *Stem cells*, 26(2), pp.356–363.

Lallemand, Y., 2005. Analysis of Msx1; Msx2 double mutants reveals multiple roles for Msx genes in limb development. *Development*, 132(13), pp.3003–3014.

Langenbach, F. & Handschel, J., 2013. Effects of dexamethasone, ascorbic acid and β-glycerophosphate on the osteogenic differentiation of stem cells in vitro. *Stem cell research & therapy*, 4(5), p.117.

LEE, P. et al., 2006. A WNT of things to come: Evolution of Wnt signaling and polarity in cnidarians. *Seminars in Cell & Developmental Biology*, 17(2), pp.157–167.

Lee, R.C., Feinbaum, R.L. & Ambros, V., 1993. The C. elegans heterochronic gene lin-4 encodes small RNAs with antisense complementarity to lin-14. *Cell*, 75(5), pp.843–854.

Lee, Y.S. & Dutta, A., 2006. MicroRNAs: small but potent oncogenes or tumor suppressors. *Curr Opin Investig Drugs*, 7(6), pp.560–564.

Lewis, B.P., Burge, C.B. & Bartel, D.P., 2005. Conserved Seed Pairing, Often Flanked by Adenosines, Indicates that Thousands of Human Genes are MicroRNA Targets. *Cell*, 120(1), pp.15–20.

Li, J. et al., 2013. miR-10a restores human mesenchymal stem cell differentiation by repressing KLF4. *Journal of cellular physiology*, 228(12), pp.2324–2336.

Li, Z. et al., 2008. A microRNA signature for a BMP2-induced osteoblast lineage commitment program. *Proceedings of the National Academy of Sciences*, 105(37), pp.13906–13911.

Li, Z. et al., 2009. Biological Functions of miR-29b Contribute to Positive Regulation of Osteoblast Differentiation. *Journal of Biological Chemistry*, 284(23), pp.15676–15684.

Lian, J.B. et al., 2012. MicroRNA control of bone formation and homeostasis. *Nature Reviews Endocrinology*, 8(4), pp.212–227.

Liang, R., Bates, D. & Wang, E., 2009. Epigenetic Control of MicroRNA Expression and Aging. *Current Genomics*, 10(3), pp.184–193.

Ling, L., Nurcombe, V. & Cool, S.M., 2009. Wnt signaling controls the fate of mesenchymal stem cells. *Gene*, 433(1-2), pp.1–7.

Liu, C.-G. et al., 2008. MicroRNA expression profiling using microarrays. *Nature protocols*, 3(4), pp.563–578.

Liu, H. et al., 2014. MicroRNA-338-3p regulates osteogenic differentiation of mouse bone marrow stromal stem cells by targeting Runx2 and Fgfr2. *Journal of cellular physiology*, 229(10), pp.1494–1502.

Liu, X. et al., 2009. MicroRNA-146a modulates human bronchial epithelial cell survival in response to the cytokine-induced apoptosis. *Biochemical and biophysical research communications*, 380(1), pp.177–182.

Liu, Z. et al., 2011. MicroRNA-146a modulates TGF-β1-induced phenotypic differentiation in human dermal fibroblasts by targeting SMAD4. *Archives of Dermatological Research*, 304(3), pp.195–202.

Lujambio, A. et al., 2008. A microRNA DNA methylation signature for human cancer metastasis. *Proceedings of the National Academy of Sciences*, 105(36), pp.13556–13561.

Malaval, L. et al., 2008. Bone sialoprotein plays a functional role in bone formation and osteoclastogenesis. *Journal of Experimental Medicine*, 205(5), pp.1145–1153.

Maul, T.M. et al., 2011. Mechanical stimuli differentially control stem cell behavior: morphology, proliferation, and differentiation. *Biomechanics and Modeling in Mechanobiology*, 10(6), pp.939–953.

Medvedev, S.P., Shevchenko, A.I. & Zakian, S.M., 2010. Induced Pluripotent Stem Cells: Problems and Advantages when Applying them in Regenerative Medicine. *Acta naturae*, 2(2), pp.18–28.

Min, H. & Yoon, S., 2010. Got target? Computational methods for microRNA target prediction and their extension. *Experimental & molecular medicine*, 42(4), pp.233–244.

Mirmalek-Sani, S.-H. et al., 2006. Characterization and Multipotentiality of Human Fetal Femur-Derived Cells: Implications for Skeletal Tissue Regeneration. *Stem cells*, 24(4), pp.1042–1053.

Mirmalek-Sani, S.-H. et al., 2009. Derivation of a novel undifferentiated human foetal phenotype in serum-free cultures with BMP-2. *Journal of Cellular and Molecular Medicine*, 13(9b), pp.3541–3555.

Miyaki, S. et al., 2009. MicroRNA-140 is expressed in differentiated human articular chondrocytes and modulates interleukin-1 responses. *Arthritis and rheumatism*, 60(9), pp.2723–2730.

Mizuno, Y. et al., 2009. miR-210 promotes osteoblastic differentiation through inhibition of AcvR1b. *FEBS letters*, 583(13), pp.2263–2268.

Moustakas, A., Souchelnytskyi, S. & Heldin, C.H., 2001. Smad regulation in TGF-beta signal transduction. *Journal of cell science*, 114(Pt 24), pp.4359–4369.

Nakashima, K. et al., 2002. The novel zinc finger-containing transcription factor osterix is required for osteoblast differentiation and bone formation. *Cell*, 108(1), pp.17–29.

Neumann, J. et al., 2011. SOX2 expression correlates with lymph-node metastases and distant spread in right-sided colon cancer. *BMC Cancer*, 11(1), p.518.

Ng, E.K.O. et al., 2009. MicroRNA-143 targets DNA methyltransferases 3A in colorectal cancer. *Br J Cancer*, 101(4), pp.699–706.

Nieden, zur, N.I., Kempka, G. & Ahr, H.J., 2003. In vitro differentiation of embryonic stem cells into mineralized osteoblasts. *Differentiation*, 71(1), pp.18–27.

Ono, M. et al., 2011. WISP-1/CCN4 regulates osteogenesis by enhancing BMP-2 activity. *J Bone Miner Res*, 26(1), pp.193–208.

Orriss, I.R. et al., 2014. Optimisation of the differing conditions required for bone formation in vitro by primary osteoblasts from mice and rats. *International Journal of Molecular Medicine*, 34(5), pp.1201–1208.

Pais, H. et al., 2010. Analyzing mRNA expression identifies Smad3 as a microRNA-140 target regulated only at protein level. *RNA*, 16(3), pp.489–494.

Palmer, W., Crawford-Sykes, A. & Rose, R.E.C., 2008. Donor site morbidity following iliac crest

bone graft. *The West Indian medical journal*, 57(5), pp.490–492.

Pepper, A.S.R., 2004. The C. elegans heterochronic gene lin-46 affects developmental timing at two larval stages and encodes a relative of the scaffolding protein gephyrin. *Development*, 131(9), pp.2049–2059.

Perry, M.M. et al., 2008. Rapid changes in microRNA-146a expression negatively regulate the IL-1beta-induced inflammatory response in human lung alveolar epithelial cells. *J Immunol*, 180(8), pp.5689–5698.

Peto, L. & Allaby, M., Screening for Osteoporosis in Postmenopausal Women. Available at: http://www.google.co.uk/webhp?client=safari&rls=10_7_4&ie=UTF-8&oe=UTF-8&redir_esc=&ei=OIhKUa-QO9LB0gWqlYG4Dw [Accessed March 25, 2013].

Petrie Aronin, C.E. & Tuan, R.S., 2010. Therapeutic potential of the immunomodulatory activities of adult mesenchymal stem cells. *Birth Defects Research Part C: Embryo Today: Reviews*, 90(1), pp.67–74.

Pillai, R.S., 2005. MicroRNA function: Multiple mechanisms for a tiny RNA? *RNA*, 11(12), pp.1753–1761.

Pratap, J. et al., 2003. Cell growth regulatory role of Runx2 during proliferative expansion of preosteoblasts. *Cancer research*, 63(17), pp.5357–5362.

Raggatt, L.J. & Partridge, N.C., 2010. Cellular and Molecular Mechanisms of Bone Remodeling. *Journal of Biological Chemistry*, 285(33), pp.25103–25108.

Ravindran, S. et al., 2011. Changes of chondrocyte expression profiles in human MSC aggregates in the presence of PEG microspheres and TGF-β3. *Biomaterials*, 32(33), pp.8436–8445.

Rho, J.Y., Kuhn-Spearing, L. & Zioupos, P., 1998. Mechanical properties and the hierarchical structure of bone. *Medical engineering & physics*, 20(2), pp.92–102.

Roelen, B.A.J. & Dijke, P.T., 2003. Controlling mesenchymal stem cell differentiation by TGF? family members. *Journal of Orthopaedic Science*, 8(5), pp.740–748.

Rose, F.R.A.J. & Oreffo, R.O.C., 2002. Bone Tissue Engineering: Hope vs Hype. *Biochemical and biophysical research communications*, 292(1), pp.1–7.

Ryoo, H.-M., Lee, M.-H. & Kim, Y.-J., 2006. Critical molecular switches involved in BMP-2-induced osteogenic differentiation of mesenchymal cells. *Gene*, 366(1), pp.51–57.

Sachdeva, M. & Mo, Y.Y., 2010. miR-145-mediated suppression of cell growth, invasion and metastasis. *Am J Transl Res*, 2(2), pp.170–180.

Saito, Y. et al., 2006. Specific activation of microRNA-127 with downregulation of the proto-oncogene BCL6 by chromatin-modifying drugs in human cancer cells. *Cancer Cell*, 9(6), pp.435–443.

Satokata, I. & Maas, R., 1994. Msx1 deficient mice exhibit cleft palate and abnormalities of craniofacial and tooth development. *Nature genetics*, 6(4), pp.348–356.

Scott, M.A. et al., 2011. Current methods of adipogenic differentiation of mesenchymal stem cells. *Stem cells and development*, 20(10), pp.1793–1804.

Shapiro, F., 2008. Bone development and its relation to fracture repair. The role of mesenchymal osteoblasts and surface osteoblasts. *European cells & materials*, 15, pp.53–76.

Skjødt, H. et al., 1985. Vitamin D metabolites regulate osteocalcin synthesis and proliferation of human bone cells in vitro. *The Journal of endocrinology*, 105(3), pp.391–396.

Song, B., Estrada, K.D. & Lyons, K.M., 2009. Smad signaling in skeletal development and regeneration. *Cytokine & Growth Factor Reviews*, 20(5-6), pp.379–388.

Song, S.J. et al., 2007. Effects of culture conditions on osteogenic differentiation in human mesenchymal stem cells. *Journal of microbiology and biotechnology*, 17(7), pp.1113–1119.

St-Jacques, B., Hammerschmidt, M. & McMahon, A.P., 1999. Indian hedgehog signaling regulates proliferation and differentiation of chondrocytes and is essential for bone formation. *Genes Dev*, 13(16), pp.2072–2086.

Suh, M.-R. et al., 2004. Human embryonic stem cells express a unique set of microRNAs. *Developmental biology*, 270(2), pp.488–498.

Suomi, S. et al., 2008. MicroRNAs regulate osteogenesis and chondrogenesis of mouse bone marrow stromal cells. *Gene regulation and systems biology*, 2, pp.177–191.

Swingler, T.E. et al., 2012. The expression and function of microRNAs in chondrogenesis and osteoarthritis. *Arthritis and rheumatism*, 64(6), pp.1909–1919.

Takamizawa, S. et al., 2004. Effects of ascorbic acid and ascorbic acid 2-phosphate, a long-acting vitamin C derivative, on the proliferation and differentiation of human osteoblast-like cells. *Cell Biology International*, 28(4), pp.255–265.

Tang, J., Peng, R. & Ding, J., 2010. The regulation of stem cell differentiation by cell-cell contact on micropatterned material surfaces. *Biomaterials*, 31(9), pp.2470–2476.

Tare, R.S. et al., 2008. Skeletal stem cells: Phenotype, biology and environmental niches informing tissue regeneration. *Molecular and Cellular Endocrinology*, 288(1-2), pp.11–21.

Tare, R.S. et al., 2005. Tissue engineering strategies for cartilage generation--micromass and three dimensional cultures using human chondrocytes and a continuous cell line. *Biochemical and biophysical research communications*, 333(2), pp.609–621.

Tenenbaum, H.C. & Heersche, J.N., 1985. Dexamethasone stimulates osteogenesis in chick periosteum in vitro. *Endocrinology*, 117(5), pp.2211–2217.

Teti, A., 2011. Bone Development: Overview of Bone Cells and Signaling. *Current Osteoporosis Reports*, 9(4), pp.264–273.

Thakor, D.K. et al., 2011. Nontoxic Genetic Engineering of Mesenchymal Stem Cells Using Serum-Compatible Pullulan-Spermine/DNA Anioplexes. *Tissue Engineering Part C: Methods*, 17(2), pp.131–144.

Thakor, D.K., Teng, Y.D. & Tabata, Y., 2009. Neuronal gene delivery by negatively charged pullulan–spermine/DNA anioplexes. *Biomaterials*, 30(9), pp.1815–1826.

Tou, L., Quibria, N. & Alexander, J.M., 2003. Transcriptional regulation of the human Runx2/Cbfa1 gene promoter by bone morphogenetic protein-7. *Molecular and Cellular Endocrinology*, 205(1-2), pp.121–129.

Tuch, B., 1988. Immunogenicity of fetal tissue. *The Hastings Center report*, 18(4), p.44.

Tuddenham, L. et al., 2006. The cartilage specific microRNA-140 targets histone deacetylase 4 in mouse cells. *FEBS letters*, 580(17), pp.4214–4217.

Vanderpuye, O.A., Labarrere, C.A. & McIntyre, J.A., 1992. The complement system in human reproduction. *Am J Reprod Immunol*, 27(3-4), pp.145–155.

Várallyay, E., Burgyán, J. & Havelda, Z., 2008. MicroRNA detection by northern blotting using locked nucleic acid probes. *Nature protocols*, 3(2), pp.190–196.

Wang, Qing et al., 2013. miR-346 regulates osteogenic differentiation of human bone marrow-derived mesenchymal stem cells by targeting the Wnt/β-catenin pathway. X.-M. Shi, ed. *PloS one*, 8(9), p.e72266.

Wang, Tao & Xu, Z., 2010. miR-27 promotes osteoblast differentiation by modulating Wnt signaling. *Biochemical and biophysical research communications*, 402(2), pp.186–189.

Wang, Tingzhong et al., 2006. Cell-to-cell contact induces mesenchymal stem cell to differentiate into cardiomyocyte and smooth muscle cell. *International journal of cardiology*, 109(1), pp.74–81.

Weber, B. et al., 2007. Methylation of human microRNA genes in normal and neoplastic cells. *Cell Cycle*, 6(9), pp.1001–1005.

Wienholds, E. et al., 2003. The microRNA-producing enzyme Dicer1 is essential for zebrafish development. *Nature genetics*, 35(3), pp.217–218.

Wightman, B., Ha, I. & Ruvkun, G., 1993. Posttranscriptional regulation of the heterochronic gene lin-14 by lin-4 mediates temporal pattern formation in C. elegans. *Cell*, 75(5), pp.855–862.

Wright, E.M., Snopek, B. & Koopman, P., 1993. Seven new members of the Sox gene family expressed during mouse development. *Nucleic acids research*, 21(3), p.744.

Xin, M. et al., 2009. MicroRNAs miR-143 and miR-145 modulate cytoskeletal dynamics and responsiveness of smooth muscle cells to injury. *Genes & Development*, 23(18), pp.2166–2178.

Xu, N. et al., 2009. MicroRNA-145 Regulates OCT4, SOX2, and KLF4 and Represses Pluripotency in Human Embryonic Stem Cells. *Cell*, 137(4), pp.647–658.

Xu, P. et al., 2003. The Drosophila microRNA Mir-14 suppresses cell death and is required for normal fat metabolism. *Curr Biol*, 13(9), pp.790–795.

Yamashita, S. et al., 2009. Sox9 directly promotes Bapx1 gene expression to repress Runx2 in chondrocytes. *Experimental Cell Research*, 315(13), pp.2231–2240.

Yang, L. et al., 2012. miR-93/Sp7 function loop mediates osteoblast mineralization. *J Bone Miner Res*, 27(7), pp.1598–1606.

Yang, X. et al., 2004. ATF4 is a substrate of RSK2 and an essential regulator of osteoblast biology; implication for Coffin-Lowry Syndrome. *Cell*, 117(3), pp.387–398.

Yang, X. et al., 2001. TGF-beta/Smad3 signals repress chondrocyte hypertrophic differentiation and are required for maintaining articular cartilage. *The Journal of cell biology*, 153(1), pp.35–

46.

Yoshida, Y. et al., 2000. Negative regulation of BMP/Smad signaling by Tob in osteoblasts. *Cell*, 103(7), pp.1085–1097.

Yu, F. et al., 2011. Kruppel-like factor 4 (KLF4) is required for maintenance of breast cancer stem cells and for cell migration and invasion. *Oncogene*, 30(18), pp.2161–2172.

Zhang, C., 2010. Transcriptional regulation of bone formation by the osteoblast-specific transcription factor Osx. *Journal of Orthopaedic Surgery and Research*, 5(1), p.37.

Zhang, Y. et al., 2011. A program of microRNAs controls osteogenic lineage progression by targeting transcription factor Runx2. *Proceedings of the National Academy of Sciences*, 108(24), pp.9863–9868.

Zhang, Y. et al., 2012. Control of mesenchymal lineage progression by microRNAs targeting skeletal gene regulators Trps1 and Runx2. *Journal of Biological Chemistry*, 287(26), pp.21926–21935.

Zhong, H. et al., 2010. Targeting Smad4 links microRNA-146a to the TGF-β pathway during retinoid acid induction in acute promyelocytic leukemia cell line. *International journal of hematology*, 92(1), pp.129–135.

Zhou, S., 2011. TGF-β regulates β-catenin signaling and osteoblast differentiation in human mesenchymal stem cells. *Journal of cellular biochemistry*, 112(6), pp.1651–1660.

Zhou, X. et al., 2010. Multiple functions of Osterix are required for bone growth and homeostasis in postnatal mice. *Proceedings of the National Academy of Sciences*, 107(29), pp.12919–12924.